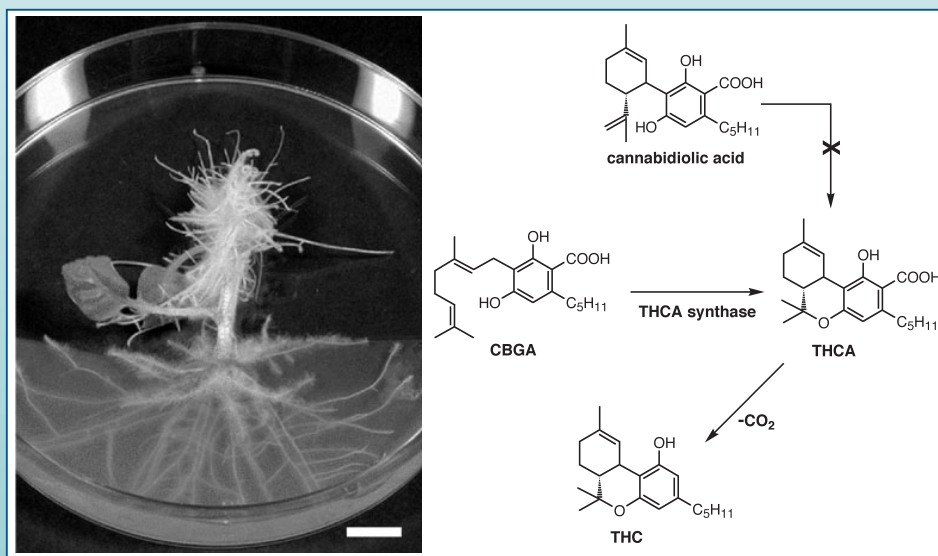


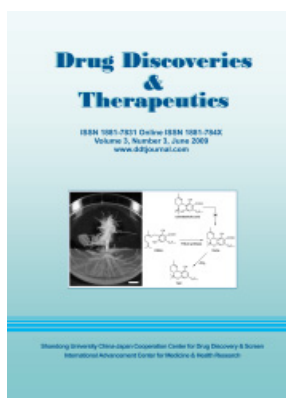
Drug Discoveries & Therapeutics

ISSN 1881-7831 Online ISSN 1881-784X
Volume 3, Number 3, June 2009
www.ddtjournal.com



Shandong University China-Japan Cooperation Center for Drug Discovery & Screen
International Advancement Center for Medicine & Health Research

Drug Discoveries & Therapeutics



Editor-in-Chief:

Kazuhisa SEKIMIZU
(The University of Tokyo, Tokyo, Japan)

Associate Editor:

Norihiro KOKUDO
(The University of Tokyo, Tokyo, Japan)

Drug Discoveries & Therapeutics is a peer-reviewed international journal published bimonthly by *Shandong University China-Japan Cooperation Center for Drug Discovery & Screen (SDU-DDSC)* and *International Advancement Center for Medicine & Health Research Co., Ltd. (IACMHR Co., Ltd.)*.

Drug Discoveries & Therapeutics mainly publishes articles related to basic and clinical pharmaceutical research such as pharmaceutical and therapeutical chemistry, pharmacology, pharmacy, pharmacokinetics, industrial pharmacy, pharmaceutical manufacturing, pharmaceutical technology, drug delivery, toxicology, and traditional herb medicine. Studies on drug-related fields such as biology, biochemistry, physiology, microbiology, and immunology are also within the scope of this journal.

Subject Coverage: Basic and clinical pharmaceutical research including Pharmaceutical and therapeutical chemistry, Pharmacology, Pharmacy, Pharmacokinetics, Industrial pharmacy, Pharmaceutical manufacturing, Pharmaceutical technology, Drug delivery, Toxicology, and Traditional herb medicine.

Language: English

Issues/Year: 6

Published by: IACMHR and SDU-DDSC

ISSN: 1881-7831 (Online ISSN 1881-784X)

Editorial and Head Office

Wei TANG, MD PhD
Executive Editor
Drug Discoveries & Therapeutics

TSUIN-IKIZAKA 410,
2-17-5 Hongo, Bunkyo-ku,
Tokyo 113-0033, Japan.
Tel: 03-5840-9697
Fax: 03-5840-9698
E-mail: office@ddtjournal.com
URL: www.ddtjournal.com



Drug Discoveries & Therapeutics

Editorial Board

Editor-in-Chief:

Kazuhiisa SEKIMIZU (*The University of Tokyo, Tokyo, Japan*)

Associate Editor:

Norihiro KOKUDO (*The University of Tokyo, Tokyo, Japan*)

Executive Editor:

Wei TANG (*The University of Tokyo, Tokyo, Japan*)

Managing Editor:

Munehiro NAKATA (*Tokai University, Kanagawa, Japan*)

Web Editor:

Yu CHEN (*The University of Tokyo, Tokyo, Japan*)

English Editor:

Curtis BENTLEY (*Roswell, GA, USA*)

Thomas R. LeBon (*Los Angeles Trade Technical College, Los Angeles, CA, USA*)

China Office:

Wenfang XU (*Shandong University, Shandong, China*)

Editorial Board Members:

Yoshihiro ARAKAWA (<i>Tokyo, Japan</i>)	Jikai LIU (<i>Kunming, China</i>)
Santad CHANPRAPAPH (<i>Bangkok, Thailand</i>)	Hongxiang LOU (<i>Jinan, China</i>)
Fen-Er CHEN (<i>Shanghai, China</i>)	Ken-ichi MAFUNE (<i>Tokyo, Japan</i>)
Zilin CHEN (<i>Wuhan, China</i>)	Norio MATSUKI (<i>Tokyo, Japan</i>)
Guanhua DU (<i>Beijing, China</i>)	Tohru MIZUSHIMA (<i>Kumamoto, Japan</i>)
Chandradhar DWIVEDI (<i>Brookings, SD, USA</i>)	Abdulla M. MOLOKHIA (<i>Alexandria, Egypt</i>)
Mohamed F. EL-MILIGI (<i>Cairo, Egypt</i>)	Masahiro MURAKAMI (<i>Osaka, Japan</i>)
Harald HAMACHER (<i>Tuebingen, Germany</i>)	Yoshinobu NAKANISHI (<i>Ishikawa, Japan</i>)
Hiroshi HAMAMOTO (<i>Tokyo, Japan</i>)	Yutaka ORIHARA (<i>Tokyo, Japan</i>)
Xiaojiang HAO (<i>Kunming, China</i>)	Xiao-Ming OU (<i>Jackson, MS, USA</i>)
Langchong HE (<i>Xi'an, China</i>)	Weisan PAN (<i>Shenyang, China</i>)
David A. HORNE (<i>Duarte, CA, USA</i>)	Shafiqur RAHMAN (<i>Brookings, SD, USA</i>)
Yongzhou HU (<i>Hangzhou, China</i>)	Adel SAKR (<i>Cincinnati, OH, USA</i>)
Wei HUANG (<i>Shanghai, China</i>)	Abdel Aziz M. SALEH (<i>Cairo, Egypt</i>)
Yu HUANG (<i>Hong Kong, China</i>)	Tomofumi SANTA (<i>Tokyo, Japan</i>)
Hans E. JUNGINGER (<i>Phitsanulok, Thailand</i>)	Yasufumi SAWADA (<i>Tokyo, Japan</i>)
Toshiaki KATADA (<i>Tokyo, Japan</i>)	Brahma N. SINGH (<i>Commack, NY, USA</i>)
Ibrahim S. KHATTAB (<i>Safat, Kuwait</i>)	Hongbin SUN (<i>Nanjing, China</i>)
Hirromichi KIMURA (<i>Tokyo, Japan</i>)	Benny K. H. TAN (<i>Singapore, Singapore</i>)
Shiroh KISHIOKA (<i>Wakayama, Japan</i>)	Renxiang TAN (<i>Nanjing, China</i>)
Kam Ming KO (<i>Hong Kong, China</i>)	Murat TURKOGLU (<i>Istanbul, Turkey</i>)
Nobuyuki KOBAYASHI (<i>Nagasaki, Japan</i>)	Stephen G. WARD (<i>Bath, UK</i>)
Toshiro KONISHI (<i>Tokyo, Japan</i>)	Takako YOKOZAWA (<i>Toyama, Japan</i>)
Masahiro KUROYANAGI (<i>Hiroshima, Japan</i>)	Liangren ZHANG (<i>Beijing, China</i>)
Chun Guang LI (<i>Victoria, Australia</i>)	Jianping ZUO (<i>Shanghai, China</i>)
Hongmin LIU (<i>Zhengzhou, China</i>)	

(as of April 20, 2009)

Review

- 83 - 87** **Studies on tetrahydrocannabinolic acid synthase that produces the acidic precursor of tetrahydrocannabinol, the pharmacologically active cannabinoid in marijuana.**

Futoshi Taura

Original Articles

- 88 - 92** **Antidiabetic activity of standardized extract of *Picrorhiza kurroa* in rat model of NIDDM.**

Gulam Mohammed Husain, Paras Nath Singh, Vikas Kumar

- 93 - 96** **Synthesis and reaction mechanism of 3-(4-methoxyphenylazo)acrylic acid.**

Bing Liu, Runling Wang, Weiren Xu, Guilong Zhao, Lida Tang, Xianchao Cheng, Hui Zhou

- 97 - 103** **A validated stability-indicating HPLC method for analysis of glabridin prodrugs in hydrolysis studies.**

Warunee Jirawattanapong, Ekarin Saifah, Chamnan Patarapanich

- 104 - 113** **Correlation of *in vitro* dissolution rate and apparent solubility in buffered media using a miniaturized rotating disk equipment: Part I. Comparison with a traditional USP rotating disk apparatus.**

Anita M. Persson, Anders Sokolowski, Curt Pettersson

- 114 - 122** **Correlation of *in vitro* dissolution rate and apparent solubility in buffered media using a miniaturized rotating disk equipment: Part II. Comparing different buffer media.**

Anita M. Persson, Curt Pettersson, Anders Sokolowski

CONTENTS

(Continued)

- 123 - 135** **Formulation and optimization of sustained release terbutaline sulfate microspheres using response surface methodology.**

Ibrahim Khattab, Farzana Bandarkar, Ahmed Lila

- 136 - 142** **Stability studies of the effect of crosslinking on hydrochlorothiazide release.**

Aliaa N. Elmeshad, Manal K. Darwish

Guide for Authors

Copyright

Review

Studies on tetrahydrocannabinolic acid synthase that produces the acidic precursor of tetrahydrocannabinol, the pharmacologically active cannabinoid in marijuana

Futoshi Taura*

Graduate School of Pharmaceutical Sciences, Kyushu University, Fukuoka, Japan.

ABSTRACT: Tetrahydrocannabinol (THC), the psychoactive component of marijuana, is now regarded as a promising medicine because this cannabinoid has been shown to exert a variety of therapeutic activities. It has been demonstrated that THC is generated from the acidic precursor, tetrahydrocannabinolic acid (THCA) by non-enzymatic decarboxylation, and that THCA is biosynthesized by THCA synthase, which catalyzes a unique biosynthetic reaction, the stereospecific oxidative cyclization of the geranyl group of the substrate cannabigerolic acid. Molecular characterization of THCA synthase has revealed its structural characteristics and reaction mechanism. THCA synthase is the first cannabinoid synthase to be studied and is potentially attractive target for various biotechnological applications as it produces the direct precursor of THC. This review describes the research history of this enzyme, *i.e.*, purification, molecular cloning, biochemical characterization, and possible biotechnological application of THCA synthase.

Keywords: Cannabinoid, *Cannabis sativa*, marijuana, tetrahydrocannabinol, tetrahydrocannabinolic acid synthase

1. Introduction

To date, more than 60 cannabinoids have been isolated from marijuana or fresh *Cannabis sativa* (*C. sativa*) plants (1). Among them, tetrahydrocannabinol (THC) is the well-known psychoactive cannabinoid (2). Recent studies have demonstrated that this cannabinoid exerts a variety of therapeutic activities, and therefore, THC has attracted a great deal of attention as a promising medicine

for treating various diseases (3). In some countries, THC has been approved as a medicine for suppressing nausea and vomiting caused by cancer chemotherapy, and more recently, Sativex, a *Cannabis*-based preparation containing THC, was licensed in Canada as a neuropathic pain reliever for adult patients with multiple sclerosis (4). The demand for THC has been increasing; however, asymmetric synthesis of this cannabinoid requires very intricate procedures (5). In addition, it is not easy to isolate THC because marijuana contains a complicated mixture of various cannabinoids.

Cannabinoids are classified into two types, neutral cannabinoids and cannabinoid acids, based on whether they contain a carboxyl group or not. In fresh *Cannabis* plants, cannabinoids are biosynthesized and accumulated as cannabinoid acids, and non-enzymatically decarboxylated into their neutral forms during storage and smoking (6,7). Likewise, THC is generated from an acidic precursor, tetrahydrocannabinolic acid (THCA) (Figure 1). With respect to the biosynthesis of THCA,

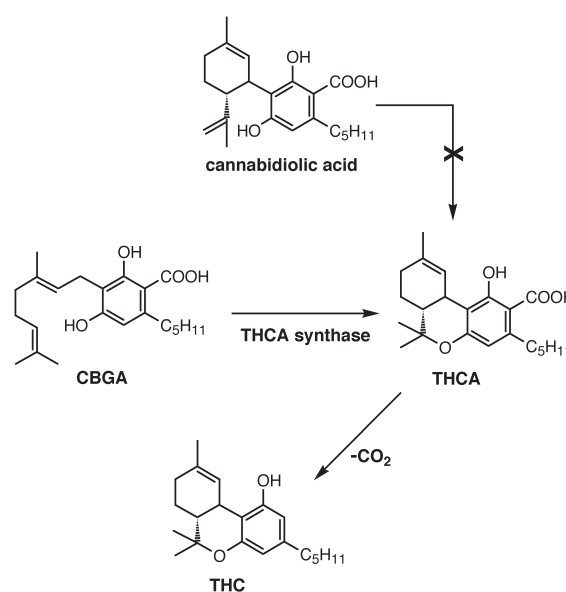


Figure 1. Biogenesis of THC. THCA synthase catalyzes the oxidative cyclization of CBGA to form THCA. THC is generated from THCA by non-enzymatic decarboxylation.

*Address correspondence to:

Dr. Futoshi Taura, Graduate School of Pharmaceutical Sciences, Kyushu University, 3-1-1 Maidashi, Higashi-ku, Fukuoka 812-8582, Japan.
e-mail: taura@phar.kyushu-u.ac.jp

it has been demonstrated that THCA is biosynthesized by an oxidoreductase named THCA synthase, which converts cannabigerolic acid (CBGA) into THCA, contrary to the generally postulated scheme that THCA is derived from cannabidiolic acid (8) (Figure 1).

THCA synthase was identified in the young leaves of *C. sativa*, and then purified and characterized (8). However, the molecular structure and detailed reaction mechanism could not be determined by the studies on the native enzyme. Thus, the cDNA encoding THCA synthase was cloned, and the structural and biochemical characterization was conducted in detail subsequently (9). In addition, cost- and fermentation-friendly expression systems for recombinant THCA synthase were established as a first step to develop a novel biotechnological production system of THC (9,10).

2. Purification and characterization of THCA synthase from *C. sativa*

THCA, the acidic precursor of THC, is one of the major constituents of *C. sativa*. With regard to the biosynthesis of THCA, it had long been postulated that THCA is formed by ring closure of cannabidiolic acid, an isomer of THCA. However, the isomerase activity, which converts cannabidiolic acid into THCA, could not be detected in any enzyme assays using crude enzyme extracts prepared from various parts of *C. sativa*. In contrast, a potent THCA producing activity was confirmed in the soluble fraction from young leaves when CBGA was included as a substrate. Therefore, it appeared evident that THCA is actually biosynthesized from CBGA *via* oxidative cyclization of the geranyl group by the action of a novel enzyme named THCA synthase (8) (Figure 1).

To evaluate its biochemical properties, THCA synthase was purified to homogeneity by various column chromatography steps using DE-52, phenyl Sepharose CL-4B, and hydroxylapatite. The purified THCA synthase was detected as a single band with a molecular mass of ~75 kDa on SDS-PAGE analysis (Figure 2). The native molecular mass was estimated to be ~76 kDa by gel filtration chromatography, indicating that THCA synthase is a monomeric protein. Concerning the stereoselectivity of the enzyme reaction, the CD spectrum of THCA produced by the purified enzyme was identical to that of authentic (-)-THCA, confirming that THCA synthase stereoselectively produces (-)-THCA.

THCA synthase catalyzes a unique monoterpene cyclase-like reaction coupled with a two-electron oxidation. As most monoterpene cyclases require divalent ions such as Mg^{2+} or Mn^{2+} for their activity (11), the effects of metal ions on THCA synthase activity were tested. In addition, to obtain information on the enzymatic oxidation mechanism, the effects of a variety of cofactors and coenzymes, including NAD, NADP,

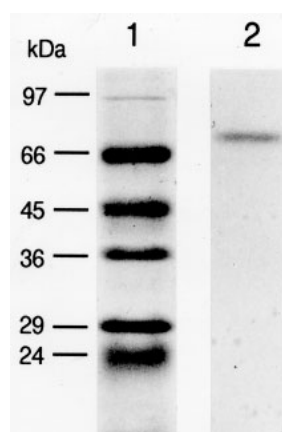


Figure 2. SDS-PAGE analysis of THCA synthase purified from *C. sativa*. Lane 1, molecular mass standards; Lane 2, purified THCA synthase.

FAD, and FMN, were also investigated. As a result, purified THCA synthase was found not to require any metal ions, cofactors, or coenzymes. These properties indicated that this enzyme can complete the oxidative cyclization reaction by itself. As described above, THCA synthase is the first cannabinoid synthase to be purified and characterized.

3. Molecular cloning and heterologous expression

Because characterization of the native enzyme did not provide detailed functional and structural information, cDNA cloning and molecular characterization of THCA synthase was attempted (9). The molecular cloning was carried out by reverse transcription and polymerase chain reaction techniques using degenerate and gene specific primers. The THCA synthase cDNA consisted of a 1,635-nucleotide open reading frame, encoding a 545-amino acid polypeptide, of which the first 28 amino acids constituted the signal peptide. THCA synthase was the first enzyme involved in cannabinoid biosynthesis to be cloned.

Surprisingly, the primary structure deduced from the cDNA exhibited high homology to berberine bridge enzyme from *Eschscholtzia californica*, which is involved in alkaloid biosynthesis (12). It is of great interest that homologous enzymes work in apparently distinct secondary pathways, namely the cannabinoid and alkaloid biosynthetic pathways. Berberine bridge enzyme is a well characterized covalently flavinylated oxidase that catalyzes FAD dependent oxidation of (*S*)-reticuline to form (*S*)-scoulerine (13). The structural similarity implied the possibility that THCA synthase is also a FAD dependent oxidase type enzyme.

For detailed characterization, recombinant THCA synthase was overexpressed using a baculovirus-insect expression system. The purified recombinant enzyme obtained from the insect culture medium gave yellow coloration suggesting flavin binding.

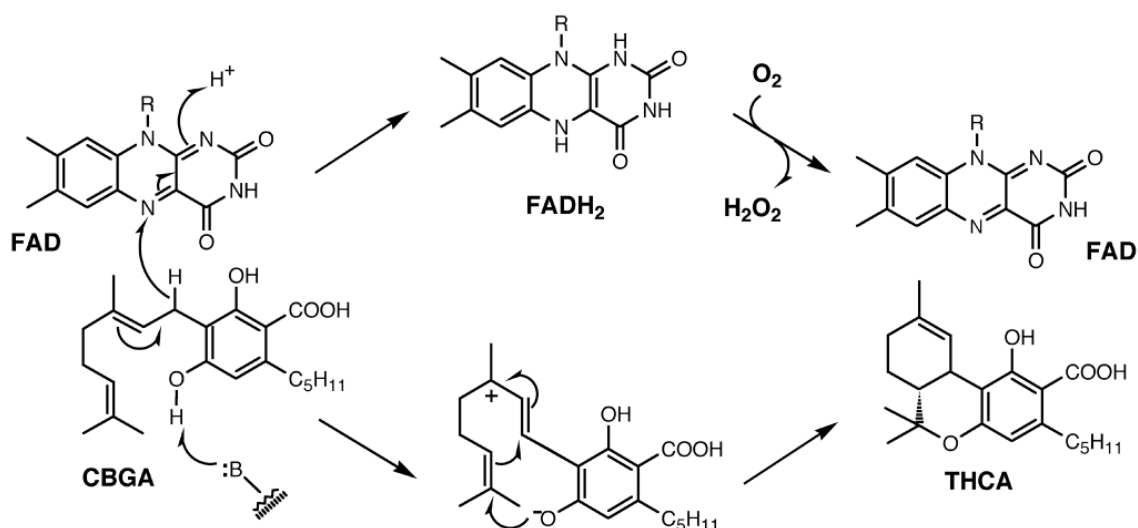


Figure 3. The reaction mechanism of THCA synthase. R is the rest of FAD molecule and B is the proposed basic residue of the enzyme.

Furthermore, various spectroscopic analyses of the enzyme demonstrated that THCA synthase contains covalently attached FAD cofactor at a molar ratio of FAD to protein of 1:1. The FAD binding residue was determined to be His-114 because the site-directed mutant enzyme at this position exhibited neither absorption characteristics of flavoproteins nor THCA synthase activity. In addition, it was also confirmed that THCA synthase requires molecular oxygen and releases hydrogen peroxide stoichiometrically with THCA. Based on the biochemical properties of THCA synthase, the reaction mechanism was proposed as shown in Figure 3. Subsequent studies, such as X-ray crystallographic analysis (14), may demonstrate the structure-function relationship of the enzyme active site and may provide rational strategies for controlling the oxidative cyclization reaction.

4. Production of THCA by recombinant THCA synthase

As described above, THCA synthase stereoselectively synthesizes THCA from CBGA. Because CBGA is easy to synthesize (9), and THCA is readily decarboxylized into THC by heating (6), it was considered that THCA synthase could contribute to the biotechnological production of THC once a suitable expression system was developed. The insect cell system expression afforded a large amount of enzyme (~1 mg/L culture); however, the system required an expensive complex medium as well as elaborate viral infection and amplification procedures. Therefore, two different cost- and fermentation-friendly expression systems have been established, *i.e.*, THCA synthase was expressed in transgenic tobacco hairy roots (9) and methylotrophic yeast *Pichia pastoris* (10). The bioconversion of CBGA into THCA by recombinant THCA synthase was

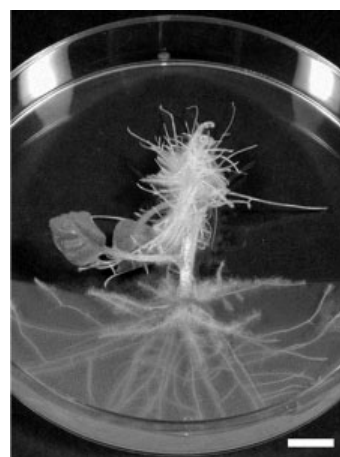


Figure 4. Transgenic tobacco hairy roots harboring THCA synthase. Bar, 1 cm.

attempted as a first step toward the biotechnological production of THC (9,10).

4.1. THCA production by THCA synthase in transgenic tobacco hairy roots

For expression in plants, the THCA synthase cDNA was cloned into a pBI121 vector with a cauliflower mosaic virus 35S promoter (15). The resulting construct was introduced into the tobacco (*Nicotiana tabacum* cv Xanthi) genome using *Agrobacterium rhizogenes* (16). The transformants appeared as rapidly growing hairy roots from tobacco stems infected by *Agrobacterium* (Figure 4). The transgenic hairy roots could produce THCA upon feeding of CBGA. When the hairy roots were cultured in liquid medium (30 mL) supplemented with 1 mg of CBGA, the maximum level of THCA (82 µg, 8.2% conversion from CBGA) was produced 2 days after the addition of CBGA. Although the

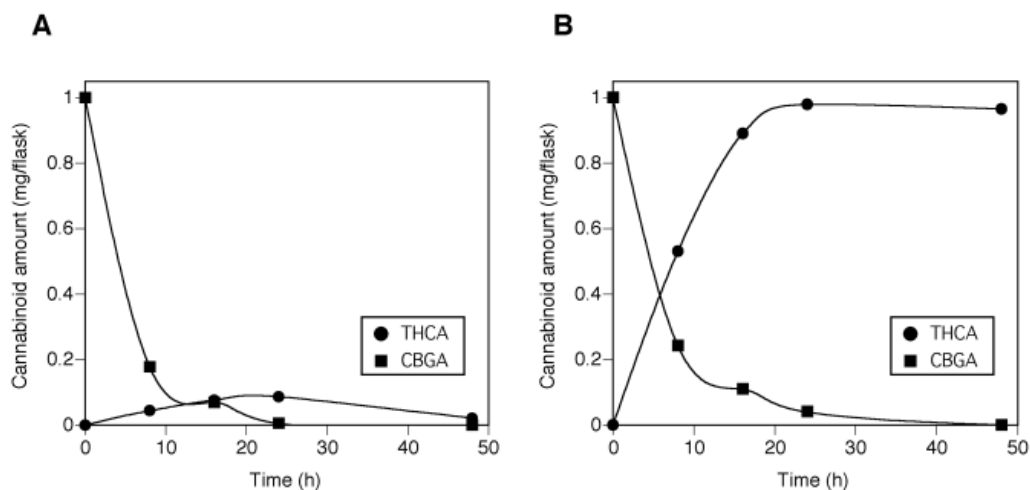


Figure 5. Conversion of CBGA into THCA by recombinant THCA synthase. A, Bioconversion by *P. pastoris* cultures. CBGA (1 mg) was added to the cultures (30 mL), and the amounts of CBGA and THCA were monitored by HPLC as described (10). B, Enzymatic conversion by the culture supernatant. CBGA (1 mg) was added to the culture supernatant (30 mL), and the cannabinoid amounts were measured.

conversion rate was limited, this result provided direct evidence for the *in vivo* functionality of the recombinant THCA synthase, and suggested a possibility that the THCA synthase gene can control THCA production not only in *C. sativa* but also in other plants such as tobacco.

4.2. THCA production by THCA synthase secreted from transgenic *P. pastoris*

The coding region of the THCA synthase cDNA was introduced into the genome of SMD1168h, a proteinase-deficient *P. pastoris*. The transformed cells cultured in liquid medium could secrete a catalytically active THCA synthase. Under optimized culture conditions, the bioconversion of CBGA into THCA was attempted. When CBGA (1 mg) was added directly to the culture (30 mL), THCA production was not more than 10% in 24 h, and prolonged incubation metabolized the THCA (Figure 5A). Although the level of production was very low, the CBGA concentration decreased quickly and was almost fully removed after 24 h incubation (Figure 5A). These results implied that enzymes other than THCA synthase metabolized both the substrate and the product. On the other hand, the culture supernatant, from which the cells were removed, could effectively convert CBGA into THCA with a maximum conversion rate of ~98% in 24 h (Figure 5B). The yield of THCA was 0.98 mg/flask, equal to 32.6 mg per liter of medium, which was much more than that obtained by bioconversion using transgenic tobacco root cultures. The THCA produced was stable in the solution as it was not metabolized at a significant rate by a further 24 h of incubation (Figure 5B). Therefore, cannabinoid-metabolizing enzymes produced by *Pichia* cells were not secreted into the medium. This was the first effective production of THCA using a recombinant biosynthetic enzyme.

However, it was not possible to further improve the yield of THCA by added larger amounts of CBGA because of the low solubility of this substrate in the culture medium. Therefore, to obtain more THCA, a feeding method of the substrate should be investigated. For example, an immobilized-enzyme-based method may be a possible way to produce THCA more efficiently. In the near future, recombinant THCA synthase may contribute to the development of a practical system for producing THC with the combined application of a previously established procedure for heat decarboxylation of THCA (6).

5. Conclusion and Perspective

THCA synthase, the key enzyme in the biogenesis of THC, was identified, cloned, and characterized. The culture medium of transgenic *P. pastoris* harboring THCA synthase gene could produce THCA upon feeding the substrate CBGA, suggesting a potential biotechnological production system for THC. Further molecular studies on cannabinoid biosynthesis may develop a biomimetic de novo production system without the need for feeding precursors. In addition, THCA synthase gene could also contribute to the artificial control of THCA production in *C. sativa*. For example, the overexpression of THCA synthase could produce THCA-rich plants with increased therapeutic potential. Conversely, THCA-free plants without abuse potential may be produced by silencing of the gene. THCA synthase is an attractive target for various biotechnological applications.

References

1. Turner CE, Elsohly MA, Boeren EG. Constituents of *Cannabis sativa* L. XVII. A review of the natural

- constituents. *J Nat Prod.* 1980; 43:169-234.
2. Gaoni R, Mechoulam R. Isolation, structure and partial synthesis of an active constituent of hashish. *J Am Chem Soc.* 1964; 86:1946-1947.
 3. Pertwee RG. Cannabinoid pharmacology: the first 66 years. *Br J Pharmacol.* 2006; 147:S163-S171.
 4. Robson P. Human studies of cannabinoids and medicinal cannabis. In: *Handbook of Experimental Pharmacology: Vol. 168 Cannabinoids* (Pertwee RG, ed.). Springer-Verlag, Heidelberg, Germany, 2005; pp. 719-756.
 5. Mechoulam R. Marijuana chemistry. *Science.* 1970; 168:1159-1166.
 6. Yamauchi T, Shoyama Y, Aramaki H, Azuma T, Nishioka I. Tetrahydrocannabinolic acid, a genuine substance of tetrahydrocannabinol. *Chem Pharm Bull.* 1967; 15:1075-1076.
 7. Kimura M, Okamoto K. Distribution of tetrahydrocannabinolic acid in fresh wild Cannabis. *Experientia.* 1970; 26:819-820.
 8. Taura F, Morimoto S, Shoyama Y, Mechoulam R. First direct evidence for the mechanism of Δ^1 -tetrahydrocannabinolic acid biosynthesis. *J Am Chem Soc.* 1995; 117:9766-9767.
 9. Sirikantaramas S, Morimoto S, Shoyama Y, Ishikawa Y, Wada Y, Shoyama Y, Taura F. The gene controlling marijuana psychoactivity. *J Biol Chem.* 2004; 279:39767-39774.
 10. Taura F, Dono E, Sirikantaramas S, Yoshimura K, Shoyama Y, Morimoto S. Production of Δ^1 -tetrahydrocannabinolic-acid by the biosynthetic enzyme secreted from transgenic *Pichia pastoris*. *Biochem Biophys Res Commun.* 2007; 361:675-680.
 11. Croteau R. Biosynthesis and catabolism of monoterpenes. *Chem Rev.* 1987; 87:929-954.
 12. Dittrich H, Kutchan TM. Molecular cloning, expression and induction of berberine bridge enzyme, an enzyme essential to the formation of benzophenanthridine alkaloids in the response of plants to pathogenic attack. *Proc Natl Acad Sci U S A.* 1991; 88:9969-9973.
 13. Kutchan TM, Dittrich H. Characterization and mechanism of the berberine bridge enzyme, a covalently flavinylated oxidase of benzophenanthridine alkaloid biosynthesis in plants. *J Biol Chem.* 1995; 270:24475-24481.
 14. Shoyama Y, Takeuchi A, Taura F, Tamada T, Adachi M, Kuroki R, Shoyama Y, Morimoto S. Crystallization of Δ^1 -tetrahydrocannabinolic acid (THCA) synthase from *Cannabis sativa*. *Acta Cryst F.* 2005; 61:799-801.
 15. Jefferson RA, Kavanagh TA, Bevan MW. GUS fusion: β -glucuronidase as a sensitive and versatile gene fusion marker in higher plants. *EMBO J.* 1987; 6:3901-3907.
 16. White FF, Nester EW. Hairy root: plasmid encodes virulence traits in *Agrobacterium rhizogenes*. *J Bacteriol.* 1980; 141:1134-1141.

(Received April 28, 2009; Accepted May 14, 2009)

Original Article

Antidiabetic activity of standardized extract of *Picrorhiza kurroa* in rat model of NIDDM

Gulam Mohammed Husain, Paras Nath Singh, Vikas Kumar*

Pharmacology Research Laboratory, Department of Pharmaceutics, Institute of Technology, Banaras Hindu University, Varanasi, India.

ABSTRACT: The present study was undertaken to investigate the effect of standardized aqueous extract of *Picrorhiza kurroa* Royle ex Benth. on diabetes. Diabetes mellitus was induced with streptozotocin-nicotinamide and rats found diabetic were orally administered standardized aqueous extract of *Picrorhiza kurroa* (100 and 200 mg/kg, *p.o.*) or glibenclamide (10 mg/kg, *p.o.*) or vehicle (0.3% carboxy methyl cellulose suspension) for 14 days. Fasting blood glucose levels and lipid profiles were measured in control as well as diabetic rats after two week treatment. In addition, liver glycogen level of *Picrorhiza kurroa* extract (PKE) treated diabetic rats were compared to that of control and diabetic control rats. Oral glucose tolerance test was also performed on nondiabetic normal rats. Statistical analyses were performed by one way analysis of variance followed by Tukey-Kramer multiple comparisons test. PKE treatment induced significant reduction ($p < 0.001$) in elevated fasting blood glucose level in streptozotocin-nicotinamide induced type-2 diabetic rats. In oral glucose tolerance test, oral administration of PKE increased the glucose tolerance. PKE treatment also significantly ($p < 0.001$) reversed the weight loss associated with streptozotocin treatment. These findings provide *in vivo* evidence that standardized extract of *Picrorhiza kurroa* possess significant antidiabetic activity in streptozotocin-nicotinamide induced type-2 diabetes mellitus in rats.

Keywords: *Picrorhiza kurroa*, antidiabetic, streptozotocin, nicotinamide, diabetes mellitus

1. Introduction

Diabetes mellitus (DM) refers to a group of common metabolic disorders that share the phenotype of

hyperglycemia. It is characterized by elevated blood glucose concentration caused by insulin deficiency, often combined with insulin resistance. Type-2 DM is more prevalent and account for about 90% to 95% of all diagnosed cases of diabetes. With an increasing incidence worldwide, DM will be a leading cause of morbidity and mortality in the near future (1).

The drugs currently available for treatment of diabetes have a number of serious adverse effects. As the knowledge of the heterogeneity of this disorder increases, there is a need to look for more effective agents with fewer side effects. This has led to the search for alternative therapies that may have a similar efficacy without potential adverse effects associated with conventional drug treatment. Ethnobotanical knowledge played a particularly important role in historical diabetes therapies, with over 1,200 species of medicinal plants recognized throughout the world for their ability to treat diabetic indications (2).

Picrorhiza kurroa (Family: Scrophulariaceae) is a small perennial herb that grows in northwest India on the slopes of the Himalayas between 3,000 and 5,000 meters. It is an important herb in the traditional Ayurvedic system of medicine, and has been used to treat liver and bronchial problems. Other traditional uses include dyspepsia, bilious fever, chronic dysentery, and scorpion sting. *Picrorhiza* has been shown to protect liver cells from a wide variety of toxins including amanita poisoning, carbon tetrachloride (3), galactosamine (4), ethanol (5), aflatoxin-B1 (6), acetaminophen (7), and thioacetamide (8), in both *in vitro* and *in vivo* experiments. *Picrorhiza kurroa* was found to be a potent immunostimulant, stimulating both cell-mediated and humoral immunity (9). *Picrorhiza kurroa* had been shown to possess anti-asthmatic and anti-allergic activity (10,11). *Picrorhiza* treatment reduced the cellular damage caused by hypoxia, indicating *Picrorhiza* constituents may protect against hypoxia/reoxygenation-induced injuries (12). Other reported activities of *Picrorhiza* include nitric oxide scavenging activity, cardioprotective effect, anti-cancer effect, and anti-viral effect (13). Recently, *Picrorhiza* extract has shown antidiabetic activity through alloxan-induced diabetic rat model (14), found effective in diabetic nephropathy (15) and possess hypolipidemic

*Address correspondence to:

Dr. Vikas Kumar, Department of Pharmaceutics, Institute of Technology, Banaras Hindu University, Varanasi-221 005, India.
e-mail: vikas.phe@itbhu.ac.in

activity (16). In view of these findings and fact that dyslipidemia is the hallmark of type-2 DM, we have evaluated standardized extract of *Picrorhiza* in streptozotocin-nicotinamide induced type-2 diabetes and associated dyslipidemia.

2. Materials and Methods

2.1. Animals

Adult Charles foster rats (180 ± 10 g) were obtained from Central Animal House of Institute of Medical Sciences, Banaras Hindu University, Varanasi, India. The animals were housed in groups of six in polypropylene cages at an ambient temperature of $25 \pm 1^\circ\text{C}$ and 45-55% relative humidity, with a 12:12 h light/dark cycle. Unless stated otherwise, they were provided with commercial food pellets and water *ad libitum*. Animals were acclimatized to laboratory conditions for at least one week before using them for experiments and were subjected only once to the experimental conditions. Principles of laboratory animal care (NIH publication number 85-23, revised 1985) guidelines were followed.

2.2. Plant extract

The standardized aqueous extract of *Picrorhiza kurroa* (standardized to contain 5.00% kutkin, HPTLC) was obtained from Promed Research Centre, Gurgaon, Haryana, India.

2.3. Drug administration

Standardized extract of *Picrorhiza kurroa* was suspended in 0.3% carboxy methyl cellulose (CMC) and administered orally through oral gavage at the doses of 100 and 200 mg/kg of body weight per day. Doses are selected on the basis of available literature on the aqueous extract of *Picrorhiza kurroa* (3,16).

2.4. Oral glucose tolerance test

Oral glucose tolerance test (OGTT) was performed to evaluate the peripheral glucose utilization. Albino rats of either sex were divided into four groups ($n = 6$), fasted overnight and administered as 0.3% CMC suspension, PkE (100 and 200 mg/kg) and glibenclamide (10 mg/kg), respectively. Glucose (2 g/kg) was orally administered 30 min after the drug treatments. Blood glucose levels were determined in blood samples collected at 0 min (prior to glucose administration), 30, 60, and 120 min after glucose administration.

2.5. Induction of type-2 diabetes mellitus

Type-2 DM was induced in overnight fasted male

rats by a single *i.p.* injection of 65 mg/kg dose of streptozotocin (Merck, Germany), 15 min after *i.p.* administration of 120 mg/kg nicotinamide (SD fine Chem, Mumbai, India) (17). Current pharmacology protocols (18) were followed for preparation and administration of streptozotocin solution. Hyperglycemia was confirmed by the elevated glucose level in the blood, determined at 72 h and then on 7th day after injection. The rats found with permanent diabetes were used for antidiabetic study.

2.6. Experimental design

Animals were divided into five groups of six rats each *viz.* Group I: Normal control rats, administered 0.3% CMC for 14 days; Group II: Diabetic control rats, administered 0.3% CMC for 14 days; Group III: Diabetic rats administered PkE 100 mg/kg/day, *p.o.* for 14 days; Group IV: Diabetic rats administered PkE 200 mg/kg/day, *p.o.* for 14 days; Group V: Diabetic rats administered glibenclamide, 10 mg/kg/day, *p.o.* for 14 days. Blood samples were collected by retro-orbital puncture and fasting blood glucose levels were estimated on days 0, 7, and 14 with commercially available biochemical kit (Span Diagnostics Ltd., Surat, India) as in our previous study (19). On 14th day, plasma lipid profiles were estimated using biochemical kits (Span Diagnostics Ltd.) and liver glycogen levels were estimated using anthrone reagent (20). Body weight of rats was also measured periodically.

2.7. Statistical analysis

All the values of the experimental results were expressed as mean \pm standard error of mean (SEM). Statistical analyses were performed by one way analysis of variance (ANOVA) followed by Tukey-Kramer multiple comparisons test. GraphPad InStat (version 3.06) software was used for all statistical analyses.

3. Results

3.1. Effect on OGTT

Figure 1 shows blood glucose levels of normal control, PkE, and glibenclamide treated animals after oral administration of glucose (2 g/kg). Animals treated with PkE and glibenclamide showed a significant decrease in blood glucose levels at 30 and 60 min compared to vehicle control animals. The administration of PkE significantly prevented the increase in blood glucose levels without causing a hypoglycemic state. Maximum effect of PkE was observed 30 min after the oral glucose administration ($p < 0.05$ and 0.001 for PkE 100 and 200 mg/kg, respectively). Effect of higher dose of PkE (200 mg/kg) was found comparable to glibenclamide (10 mg/kg).

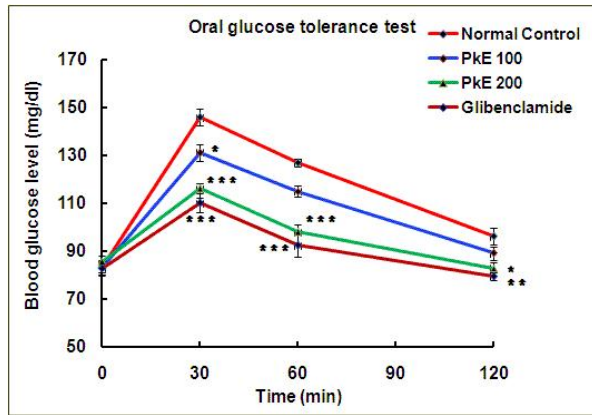


Figure 1. Effect of PkE on oral glucose tolerance test in normal rats. Values are mean ± SEM of 6 animals in each group. **p* < 0.05, ***p* < 0.01, ****p* < 0.001 compared to normal control.

3.2. Effect on fasting blood glucose level and lipid profile

Table 1 illustrates the levels of blood glucose in the control and experimental groups of rats. Diabetic rats showed a significant increase in blood glucose compared with corresponding control rats (*p* < 0.001). Oral administration of PkE (100 and 200 mg/kg) dose dependently and significantly reduced the fasting blood glucose levels on 7th (*p* < 0.05) and 14th day (*p* < 0.001) compared to diabetic control animals. Glibenclamide treatment also significantly reduced the increased blood glucose level of diabetic rats.

Table 2 shows the levels of plasma total cholesterol, triglycerides, and lipoproteins in the control and experimental groups of rats. The levels of plasma total cholesterol (TC), triglycerides (TG), and LDL-cholesterol (LDL-C) were significantly increased, whereas levels of HDL-cholesterol (HDL-C) were significantly

decreased, in diabetic rats as compared to control rats. Oral administration of PkE and glibenclamide to diabetic rats significantly reversed all these changes to near normal level. The effect of PkE (200 mg/kg) was more significant than that of 100 mg/kg and was comparable with that of glibenclamide (10 mg/kg).

3.3. Effect on liver glycogen content

A significant decrease (*p* < 0.001) in liver glycogen content was observed in diabetic rats compared to normal control group. PkE (100 and 200 mg/kg) showed a significant increase (*p* < 0.001) in liver glycogen levels compared to the diabetic control rats. However, results of higher dose of PkE (200 mg/kg) were more significant than lower dose of PkE (100 mg/kg). Glibenclamide treatment also significantly increased (*p* < 0.001) liver glycogen levels compared to diabetic control rats (Table 3).

3.4. Effect on body weight changes

The body weight changes in control, diabetic control and diabetic rats treated with PkE and glibenclamide are shown in Table 4. A significant decrease in body weight was observed in the diabetic rats (*p* < 0.001) compared with the control group. Both doses of PkE as well as glibenclamide resulted in a significant increase in body weight gain (*p* < 0.001) compared with diabetic control animals.

4. Discussion

Streptozotocin and appropriate protective dose of nicotinamide induce a diabetic syndrome with reduced pancreatic insulin stores that mimics some features of

Table 1. Effect of PkE on the blood glucose level of streptozotocin-nicotinamide induced diabetic rats

Group (n = 6) (dose in mg/kg)	Fasting plasma glucose concentration (mg/dL)		
	0 day	7th day	14th day
Normal control	83.03 ± 3.33	80.23 ± 2.99	79.77 ± 3.63
Diabetic control	289.78 ± 21.28 ^a	313.79 ± 15.58 ^a	349.17 ± 11.29 ^a
Diabetic + PkE (100)	325.40 ± 31.06 ^a	176.5 ± 11.30 ^{ab}	133.64 ± 3.40 ^{***}
Diabetic + PkE (200)	345.83 ± 25.97 ^a	137.24 ± 3.55 ^{b††}	94.01 ± 4.98 ^{***††}
Diabetic + Glibenclamide (10)	300.84 ± 21.99 ^a	120.00 ± 3.19 ^{c*}	88.71 ± 2.53 ^{**}

Values are mean ± SEM; n, number of animals in each group. ^a*p* < 0.001, ^b*p* < 0.01, ^c*p* < 0.05 compared to normal control. **p* < 0.05, ***p* < 0.001 compared to diabetic control. †*p* < 0.05, ††*p* < 0.001 compared to PkE 100 mg/kg.

Table 2. Effect of PkE on lipid profile of streptozotocin-nicotinamide induced diabetic rats

Group (n = 6) (dose in mg/kg)	TC (mg/dL)	TG (mg/dL)	HDL-C (mg/dL)	LDL-C (mg/dL)
Normal control	79.53 ± 2.29	46.85 ± 1.47	38.67 ± 0.77	31.48 ± 2.59
Diabetic control	143.27 ± 6.68 ^a	115.31 ± 6.58 ^a	24.47 ± 1.44 ^a	95.75 ± 7.18 ^a
Diabetic + PkE (100)	86.93 ± 1.90 ^{**}	65.41 ± 4.43 ^{***}	27.39 ± 1.44 ^a	46.46 ± 2.37 ^{**}
Diabetic + PkE (200)	71.42 ± 2.64 ^{***}	56.25 ± 1.62 ^{**}	31.71 ± 1.14 ^{b*}	28.46 ± 2.69 ^{***††}
Diabetic + Glibenclamide (10)	73.1 ± 2.55 ^{**}	69.37 ± 2.40 ^{***}	33.94 ± 0.78 ^{**}	25.29 ± 2.71 ^{**}

Values are mean ± SEM; n, number of animals in each group. ^a*p* < 0.001, ^b*p* < 0.01, ^c*p* < 0.05 compared to normal control. **p* < 0.01, ***p* < 0.001 compared to diabetic control. †*p* < 0.05, ††*p* < 0.001 compared to PkE 100 mg/kg.

Table 3. Effect of PkE on liver glycogen content in streptozotocin-nicotinamide induced diabetic rats

Group (n = 6) (dose in mg/kg)	Liver glycogen (mg/g)
Normal control	29.21 ± 0.80
Diabetic control	12.16 ± 0.73 ^a
Diabetic + PkE (100)	19.49 ± 1.12 ^{a*}
Diabetic + PkE (200)	24.45 ± 0.71 ^{b*†}
Diabetic + Glibenclamide (10)	21.80 ± 1.20 ^{a*}

Values are mean ± SEM; n, number of animals in each group. ^a $p < 0.001$, ^b $p < 0.05$ compared to normal control. * $p < 0.001$ compared to diabetic control. † $p < 0.01$ compared to PkE 100 mg/kg.

Table 4. Effect of PkE on body weight of rats

Group (n = 6) (dose in mg/kg)	Body weight (g)	
	Initial (0 day)	Final (14th day)
Normal control	186 ± 2.19	190.67 ± 0.98
Diabetic control	183 ± 2.37	159 ± 1.44 ^a
Diabetic + PkE (100)	184 ± 3.57	180.17 ± 2.77 ^{b*}
Diabetic + PkE (200)	188.17 ± 3.54	192.00 ± 2.80 ^{†*}
Diabetic + Glibenclamide (10)	185.16 ± 3.8	176.5 ± 1.26 ^{a*}

Values are mean ± SEM; n, number of animals in each group. ^a $p < 0.001$, ^b $p < 0.05$ compared to normal control. * $p < 0.001$ compared to diabetic control. † $p < 0.05$ compared to PkE 100 mg/kg.

NIDDM not shared by other established animal models of diabetes (18,21). Streptozotocin causes diabetes by selective depletion of β -cells, which leads to a reduction of insulin release. Decreased insulin release could result in disordered regulation of glucose by decreasing suppression of hepatic glucose production and reducing the efficiency of glucose uptake in insulin-sensitive tissues. Decreased insulin output could also impair adipocyte metabolism, resulting in increased lipolysis and elevated fatty acid level (22).

It is well established that glibenclamide produces hypoglycemia by increasing the secretion of insulin from the existing pancreatic β -cells (23). The hypoglycemic effect of plant extracts is generally dependent upon the degree of β -cell destruction. Treatment in moderate diabetic rats with some plant extracts resulted in the stimulation of β -cells of islets of Langerhans (24,25). In view of this observation, antihyperglycemic effect of PkE may be due to potentiation of insulin secretion (analogous to glibenclamide) from remnant β cells of islet of Langerhans.

Oral administration of PkE to glucose loaded normal rats was associated with a significant decline in blood glucose level compared to normal control animals indicating better tissue glucose utilizing capacity of PkE treated rats. Further, both PkE and glibenclamide treatment elevated the reduced liver glycogen level in diabetic rats which suggest an improvement in the liver glycogenesis. Glycogen is the primary intracellular storable form of glucose and its levels in various tissues are a direct reflection of insulin activity as insulin promotes intracellular glycogen deposition by stimulating glycogen synthase and inhibiting glycogen phosphorylase (26,27).

Type-2 diabetes is associated with marked imbalance in lipid metabolism (28). Diabetic dyslipidemia is characterized by low level of HDL-C as well as elevated level of TG and LDL-C particles (29,30). A significant increase in plasma cholesterol and triglycerides along with a significant decrease in HDL-C, observed in diabetic rats in the present study, are consonant with the pathogenesis of diabetes.

Observed hypolipidemic activity of PkE in diabetic rats is consonant with the earlier studies conducted with *Picrorhiza* extract on different models of hyperlipidemia (16,31). The increase in alanine transaminase (ALT) activity in diabetes is almost always due to hepatocellular damage and is usually accompanied by an increase in aspartate transaminase (AST) activity (32). Several studies with liver tissues of streptozotocin induced diabetic rats indicate a trend towards increased activity of transaminases (33). The AST and ALT activities have been used as an indicator of liver function (34). *Picrorhiza* extract has been reported to reverse the increased AST and ALT activities towards near normalcy (31), which suggests prevention of cellular and tissue damages under diabetic conditions. Therefore, hepatoprotective activity of *Picrorhiza* extract may be partially responsible for the observed antidiabetic activity.

Diabetes is associated with a characteristic loss of body weight in animals. Several hypothesis have been proposed for the body weight loss in diabetic animals like increased muscle wasting (35,36) or loss of muscle proteins due to hyperglycemia (37). Rats treated with PkE extract or glibenclamide showed an increase in body weight as compared to the diabetic control rats suggesting a protective role of PkE on muscle wasting or due to better glycemic control.

5. Conclusion

Our findings have demonstrated for the first time through streptozotocin-nicotinamide induced type-2 diabetes model that standardized extract of *Picrorhiza kurroa* has an antihyperglycemic effect. Therefore, it may be potentially beneficial in type-2 diabetes and associated dyslipidemia.

Acknowledgements

Authors are thankful to Dr. Sateesh Chauhan, Head, Herbal Formulations, Promed Research Centre, Gurgaon, Haryana, India, for providing standardized extract of *Picrorhiza kurroa*. G M Husain is grateful to the University Grants Commission, New Delhi, for providing the financial assistance.

References

1. Wild S, Roglic G, Green A, Sicree R, King H. Global

- prevalence of diabetes: estimates for the year 2000 and projections for 2030. *Diabetes Care*. 2004; 27:1047-1053.
2. Frode TS, Medeiros YS. Animal models to test drugs with potential antidiabetic activity. *J Ethnopharmacol*. 2008; 115:173-183.
 3. Lee HS, Keum KY, Ku SK. Effects of *Picrorrhiza rhizoma* water extracts on the subacute liver damages induced by carbon tetrachloride. *J Med Food*. 2007; 10:110-117.
 4. Dwivedi Y, Rastogi R, Garg NK, Dhawan BN. Picroliv and its components kutkoside and picroside I protect liver against galactosamine-induced damage in rats. *Pharmacol Toxicol*. 1992; 71:383-387.
 5. Rastogi R, Saksena S, Garg NK, Kapoor NK, Agarwal DP, Dhawan BN. Picroliv protects against alcohol-induced chronic hepatotoxicity in rats. *Planta Med*. 1996; 62:283-285.
 6. Dwivedi Y, Rastogi R, Mehrotra R, Garg NK, Dhawan BN. Picroliv protects against aflatoxin B1 acute hepatotoxicity in rats. *Pharmacol Res*. 1993; 27:189-199.
 7. Singh V, Visen PK, Patnaik GK, Kapoor NK, Dhawan BN. Effect of picroliv on low density lipoprotein receptor binding of rat hepatocytes in hepatic damage induced by paracetamol. *Indian J Biochem Biophys*. 1992; 29:428-432.
 8. Dwivedi Y, Rastogi R, Sharma SK, Garg NK, Dhawan BN. Picroliv affords protection against thioacetamide-induced hepatic damage in rats. *Planta Med*. 1991; 57:25-28.
 9. Atal CK, Sharma ML, Kaul A, Khajuria A. Immunomodulating agents of plant origin. I: Preliminary screening. *J Ethnopharmacol*. 1986; 18:133-141.
 10. Dorsch W, Stuppner H, Wagner H, Gropp M, Demoulin S, Ring J. Antiasthmatic effects of *Picrorrhiza kurroa*: androsin prevents allergen- and PAF-induced bronchial obstruction in guinea pigs. *Int Arch Allergy Appl Immunol*. 1991; 95:128-133.
 11. Baruah CC, Gupta PP, Nath A, Patnaik LG, Dhawan BN. Anti-allergic and anti-anaphylactic activity of picroliv-a standardised iridoid glycoside fraction of *Picrorrhiza kurroa*. *Pharmacol Res*. 1998; 38:487-492.
 12. Gaddipati JP, Madhavan S, Sidhu GS, Singh AK, Seth P, Maheshwari RK. Picroliv – a natural product protects cells and regulates the gene expression during hypoxia/reoxygenation. *Mol Cell Biochem*. 1999; 194:271-281.
 13. Luper S. A Review of plants used in the treatment of liver disease: Part I. *Altern Med Rev*. 1998; 3:410-421.
 14. Joy KL, Kuttan R. Anti-diabetic activity of *Picrorrhiza kurroa* extract. *J Ethnopharmacol*. 1999; 167:143-148.
 15. Lee HS, Ku SK. Effect of *Picrorrhiza rhizoma* extracts on early diabetic nephropathy in streptozotocin-induced diabetic rats. *J Med Food*. 2008; 11:294-301.
 16. Lee HS, Yoo CB, Ku SK. Hypolipemic effect of water extracts of *Picrorrhiza kurroa* in high fat diet treated mouse. *Fitoterapia*. 2006; 77:579-584.
 17. Masiello P, Broca C, Gross R, Roye M, Manteghetti M, Hillaire-Buys D, Novelli M, Ribes G. Experimental NIDDM: development of a new model in adult rats administered streptozotocin and nicotinamide. *Diabetes*. 1998; 47:224-229.
 18. Wu KK, Huan Y. Streptozotocin-induced diabetic models in mice and rats. *Curr Protoc Pharmacol*. 2008; 40:1-14.
 19. Husain GM, Singh PN, Kumar V. Anti-diabetic activity of Indian *Hypericum perforatum* L. on alloxan-induced diabetic rats. *Pharmacologyonline*. 2008; 3:889-894.
 20. Van der vies J. Two methods for the determination of glycogen in liver. *J Biol Chem*. 1953; 57:410-416.
 21. Tahara A, Matsuyama-Yokono A, Nakano R, Someya Y, Shibasaki M. Effects of antidiabetic drugs on glucose tolerance in streptozotocin-nicotinamide-induced mildly diabetic and streptozotocin-induced severely diabetic mice. *Horm Metab Res*. 2008; 40:880-886.
 22. Kahn SE, Hull RL, Utzschneider KM. Mechanisms linking obesity to insulin resistance and type 2 diabetes. *Nature*. 2006; 444:840-846.
 23. Proks P, Reimann F, Green N, Gribble F, Ashcroft F. Sulfonylurea stimulation of insulin secretion. *Diabetes*. 2002; 51:368-376.
 24. Atta-ur-Rahman, Zaman K. Medicinal plants with hypoglycemic activity. *J Ethnopharmacol*. 1989; 26:1-55.
 25. Grover JK, Vats V, Rathi SS. Anti-hyperglycemic effect of *Eugenia jambolana* and *Tinospora cordifolia* in experimental diabetes and their effects on key metabolic enzymes involved in carbohydrate metabolism. *J Ethnopharmacol*. 2000; 73:461-470.
 26. Yki-Jarvinen H, Mott D, Young AA, Stone K, Bogardus C. Regulation of glycogen synthase and phosphorylase activities by glucose and insulin in human skeletal muscle. *J Clin Invest*. 1987; 80:95-100.
 27. Groop L, Orho-Melander M. New insights into impaired muscle glycogen synthesis. *PLoS Med*. 2008; 5:e27.
 28. Gadi R, Samaha FF. Dyslipidemia in type 2 diabetes mellitus. *Curr Diab Rep*. 2007; 7:228-234.
 29. Cefalu WT. Diabetic dyslipidemia and the metabolic syndrome. *Diabetes & Metabolic Syndrome: Clinical Research & Reviews*. 2008; 2:208-222.
 30. Mooradian AD. Dyslipidemia in type 2 diabetes mellitus. *Nat Clin Pract Endocrinol Metab*. 2009; 5:150-159.
 31. Lee HS, Ahna HC, Ku SK. Hypolipemic effect of water extracts of *Picrorrhiza rhizoma* in PX-407 induced hyperlipemic ICR mouse model with hepatoprotective effects: a prevention study. *J Ethnopharmacol*. 2006; 105:380-386.
 32. Wolf PL. Biochemical diagnosis of liver disease. *Indian J Clin Biochem*. 1999; 14:59-90.
 33. Rao GM, Morghom LO, Kabur MN, Ben Mohmud BM, Ashibani K. Serum glutamic oxaloacetic transaminase (GOT) and glutamic pyruvic transaminase (GPT) levels in diabetes mellitus. *Indian J Med Sci*. 1989; 43:118-121.
 34. Reichling JJ, Kaplan MM. Clinical use of serum enzymes in liver disease. *Dig Dis Sci*. 1988; 33:1601-1614.
 35. Swanston-Flat SK, Day C, Bailey CJ, Flatt PR. Traditional plant treatment for diabetes: studies in normal and streptozotocin diabetic mice. *Diabetologia*. 1990; 33:462-464.
 36. Mastrocola R, Reffo P, Penna F, Tomasini CE, Boccuzzi G, Baccino FM, Aragno M, Costelli P. Muscle wasting in diabetic and in tumor-bearing rats: role of oxidative stress. *Free Radic Biol Med*. 2008; 44:584-593.
 37. Russell ST, Rajani S, Dhadda RS, Tisdale MJ. Mechanism of induction of muscle protein loss by hyperglycaemia. *Exp Cell Res*. 2009; 315:16-25.

(Received April 30, 2009; Accepted May 26, 2009)

Original Article

Synthesis and reaction mechanism of 3-(4-methoxyphenylazo) acrylic acid

Bing Liu^{1,2}, Runling Wang², Weiren Xu^{1,*}, Guilong Zhao¹, Lida Tang³, Xianchao Cheng², Hui Zhou²¹ Tianjin Key Lab of Molecular Design and Drug Discovery, Tianjin Institute of Pharmaceutical Research, Tianjin, China;² School of Pharmacy, Tianjin Medical University, Tianjin, China;³ Tianjin State Key Lab of Pharmacokinetics and Pharmacodynamics, Tianjin Institute of Pharmaceutical Research, Tianjin, China.

ABSTRACT: Using 4-methoxyphenylhydrazine hydrochloride (**1a**) as starting material, 2-[2-(4-methoxyphenyl) hydrazono] acetic acid (**2a**) was prepared after treatment with 1 equivalent of 2-oxoacetic acid, and 3-(4-methoxyphenyldiazo) acrylic acid (**3a**) was obtained with 2 equivalents of 2-oxoacetic acid through a novel reaction. The mechanism of reaction was analyzed with the help of charge distribution computation. This suggests that the novel reaction depends on the electronegativity of C9, which can be mainly affected by the substituents of the benzene ring.

Keywords: 3-(4-Methoxyphenylazo)acrylic acid, arylhydrazonoacetic acid, reaction mechanism, synthesis

1. Introduction

Arylhydrazines are a class of highly reactive compounds, which are used to synthesize dye and medicine intermediates; such as, indoles, indazoles and pyrazoles (1-5). In our efforts to synthesize 1-aryl-1,2,4-triazolin-5-one derivatives as anticancer agents, a novel reaction was found. Arylhydrazonoacetic acid was prepared from arylhydrazine by treatment with 2-oxoacetic acid as shown in Scheme 1. However, when **1a** was treated with 2 equivalents of 2-oxoacetic acid, product **3a** was isolated. Although the synthesis of **3a** from **1a** through a three step procedure has been published by Cevasco and co-workers (6), our one-pot reaction has not been reported, previously. We report the novel synthesis pathway of **3a** and a possible mechanism.

*Address correspondence to:

Dr. Weiren Xu, Tianjin Key Lab of Molecular Design and Drug Discovery, Tianjin Institute of Pharmaceutical Research, Tianjin 300193, China.
e-mail: xwrtj@yahoo.com.cn

2. Materials and Methods

2.1. Chemical reagents

p-Methoxyphenylhydrazine hydrochloride (**1a**), *p*-tolylhydrazine hydrochloride (**1b**), phenylhydrazine hydrochloride (**1c**) and (4-nitrophenyl)hydrazine hydrochloride (**1d**) were purchased from Linhai Duqiao Fine Chemical Factory, Zhejiang, China. 40% 2-oxoacetic acid was purchased from Shanghai Haiqu Chemical Co. Ltd., Shanghai, China. Acetic acid and sodium acetate were purchased from Tianjin First Chemical Factory, Tianjin, China.

2.2. Chemical experiment

The chemical structures of the compounds were confirmed by ¹H NMR, ¹³C NMR and ESI-MS as described below. **1b**, **1c**, and **1d** were also used to react with two portions of 2-oxoacetic acid under similar reaction conditions for the preparation of **3a**. However, their products were complicated, and no pure corresponding products could be isolated.

2.2.1. [(4-Methoxyphenyl) hydrazono]acetic acid (**2a**)

40% aqueous 2-oxoacetic acid (5.8 g, 31 mmol) was added dropwise to a solution of *p*-methoxyphenylhydrazine hydrochloride (6.0 g, 34 mmol) in water (120 mL) and a yellow precipitate formed. The solution was stirred for 1 h. The precipitate was then collected by filtration and dried *in vacuo* to obtain 2.68 g of 2-[(4-methoxyphenyl)hydrazono]acetic acid (**2a**) in 40% yield. Mp 75°C (dec). ¹H NMR (DMSO-*d*₆, 400 MHz), δ 12.07 (s, 1H), 11.00 (s, 1H), 7.06 (d, 2H, *J* = 7.2 Hz), 7.05 (s, 1H), 6.87 (d, 2H, *J* = 7.2 Hz), 3.69 (s, 3H); ¹³C NMR (DMSO-*d*₆, 400 MHz), δ 165.37, 154.16, 137.23, 124.31, 114.64, 114.29, 55.22. ESI-MS: *m/z* = 195.10 (M+1).

2.2.2. 3-(4-Methoxyphenyldiazo)acrylic acid (**3a**)

40% aqueous 2-oxoacetic acid (6.3 g, 34 mmol) was

added dropwise to a stirred solution of *p*-methoxyphenylhydrazine hydrochloride (**1a**) (3.0 g, 17 mmol), sodium acetate (1.5 g, 17 mmol), acetic acid (100 mL) and water (100 mL) in a three-neck flask at 10°C under a stream of nitrogen. The mixture was stirred for 1.5 h, and the precipitate was collected by filtration. 1.2 g of 3-(4-methoxyphenyldiazo)acrylic acid (**3a**) (in 34% yield) was obtained through recrystallization and dried *in vacuo*. Mp 50°C (dec). ¹H NMR (DMSO-*d*₆, 400 MHz), δ 12.95 (s, 1H), 7.83 (d, 1H, *J* = 14 Hz), 7.81 (d, 2H, *J* = 9 Hz), 7.10 (d, 2H, *J* = 9 Hz), 6.77 (d, 1H, *J* = 14 Hz), 3.86 (s, 3H); ¹³C NMR (DMSO-*d*₆, 400 MHz), δ 166.80, 163.26, 155.96, 146.46, 128.56, 125.33, 114.85, 55.78. ESI-MS: *m/z* = 207.11 (M+1).

2.2.3. (*p*-Tolylhydrazone) acetic acid (**2b**)

Compound **2b** was synthesized from *p*-tolylhydrazine hydrochloride **1b** with a 87% yield under similar reaction conditions for the synthesis of **2a**. Mp 110-111°C. ¹H NMR (DMSO-*d*₆, 400 MHz), δ 12.22 (d, 1H), 1.03 (s, 1H), 7.11 (s, 1H), 7.06 (d, 2H, *J* = 8.4 Hz), 7.02 (d, 2H, *J* = 8.4 Hz), 2.21 (s, 3H); ¹³C NMR (DMSO-*d*₆, 400 MHz), δ 165.31, 141.22, 129.71, 125.08, 119.06, 113.15, 20.23. ESI-MS: *m/z* = 178.10 (M+1).

2.2.4. (Phenylhydrazone)-acetic acid (**2c**)

Compound **2c** was synthesized from phenylhydrazine hydrochloride (**1c**) with a 95% yield under similar reaction conditions for the synthesis of **2a**. Mp

107-108°C. ¹H NMR (DMSO-*d*₆, 400 MHz), δ 12.30 (s, 1H); 11.11 (s, 1H); 7.26 (m, 2H); 7.12 (d, 2H, *J* = 8.8 Hz); 7.10 (s, 1H); 6.88 (t, 1H, *J* = 7.2 Hz); ¹³C NMR (DMSO-*d*₆, 400 MHz), δ 165.26, 143.54, 129.25, 125.94, 121.04, 113.15. ESI-MS: *m/z* = 165.11 (M+1).

2.2.5. [(4-Nitro-phenyl)-hydrazone]-acetic acid (**2d**)

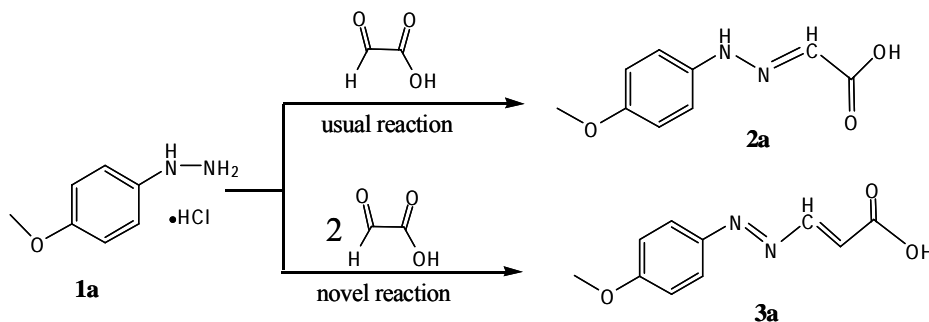
Compound **2d** was synthesized from (4-nitrophenyl) hydrazine hydrochloride (**1d**) with a 77% yield under similar reaction conditions for the synthesis of **2a**. Mp 170-171°C. ¹H NMR (DMSO-*d*₆, 400 MHz), δ 12.70 (s, 1H); 11.73 (s, 1H); 8.16 (d, 2H, *J* = 9.2 Hz); 7.27 (s, 1H); 7.21 (d, 2H, *J* = 9.2 Hz); ¹³C NMR (DMSO-*d*₆, 400 MHz), δ 164.60; 149.29; 140.39; 131.25; 125.68; 112.77. ESI-MS: *m/z* = 210.08 (M+1).

2.3. Computational experiment

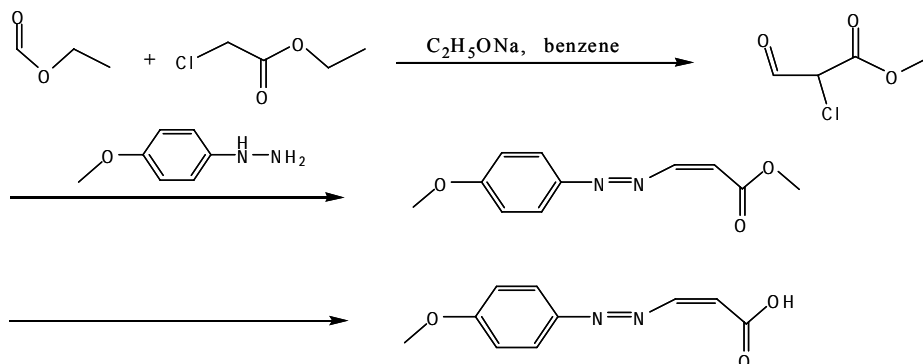
For comparison, the structures of **2a-d** were constructed by ChemOffice software, and then optimized with the density function theory at the B3LPY/6-31G(d) level by the Gaussian 98 software package (7-9). The charge distribution and bond lengths of all structures were calculated using optimized structures by the nature bond orbit method.

3. Results and Discussion

The reaction reported by Cevasco (Scheme 2) (6) used three steps to obtain the final product without any



Scheme 1. The two reactions of *p*-methoxyphenylhydrazine and 2-oxoacetic acid.



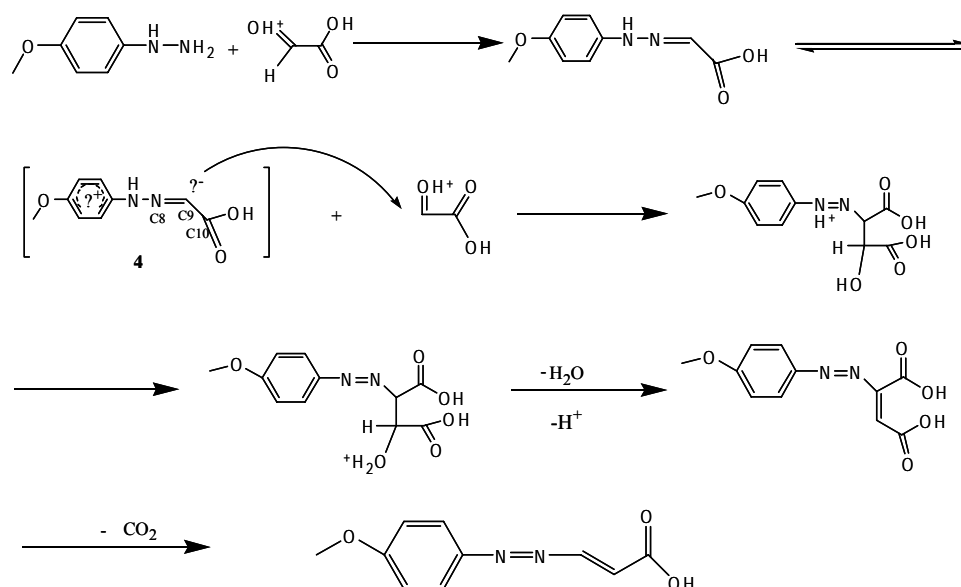
Scheme 2. The reaction reported by Cevasco and his co-workers (6).

disclosed isolated yields. However, some steps required complicated operations and harsh reaction conditions.

As outlined in Scheme 1, 2-[(4-methoxyphenyl)hydrazono]acetic acid (**2a**) was prepared from the usual reaction, while 3-(4-methoxyphenyldiazo)acrylic acid (**3a**) was synthesized through a novel reaction. The different substituents were also screened. The analogues **2b**, **2c**, and **2d** of **2a** can be prepared from *p*-tolylhydrazine hydrochloride (**1b**), phenylhydrazine hydrochloride (**1c**), and (4-nitrophenyl)hydrazine hydrochloride (**1d**) through the usual reaction. Nevertheless, when using **1b**, **1c**, and **1d** as starting materials, the possible analogues **3b**, **3c**, and **3d** were not obtained under similar reaction conditions for the preparation of **3a** from **1a**. The results suggest that the substituents with different electronegativities attached to the benzene ring play a critical role in this pathway.

A possible mechanism was proposed for the novel

reaction, which is shown in Scheme 3. First, 1 equivalent of 2-oxoacetic acid coupled with 1 equivalent of **1a** to form a Schiff's base **2a** through nucleophilic addition and the ensuing dehydration. Second, the electrons were redistributed because of the conjugation within **2a** (**6**), making C9 (following the labeling in Figure 1) and the benzene ring shows electronegativity and electropositivity, respectively. Then the carbonyl group of 2-oxoacetic acid was attacked by C9 through nucleophilic addition, forming a transient state with two carboxyl groups. Finally, **3a** was produced from the transient state through proton translocation, dehydration and decarboxylation in turn. In the whole process, the key point was the conjugated state **4** in which C9 was negative enough. In conjugated state **4**, the electronegativity of atom C9 was strongly enhanced by the substitution of the *p*-methoxy group in **2a**. This explains why the novel reaction could only happen to **2a**.



Scheme 3. The possible mechanism for the novel reaction.

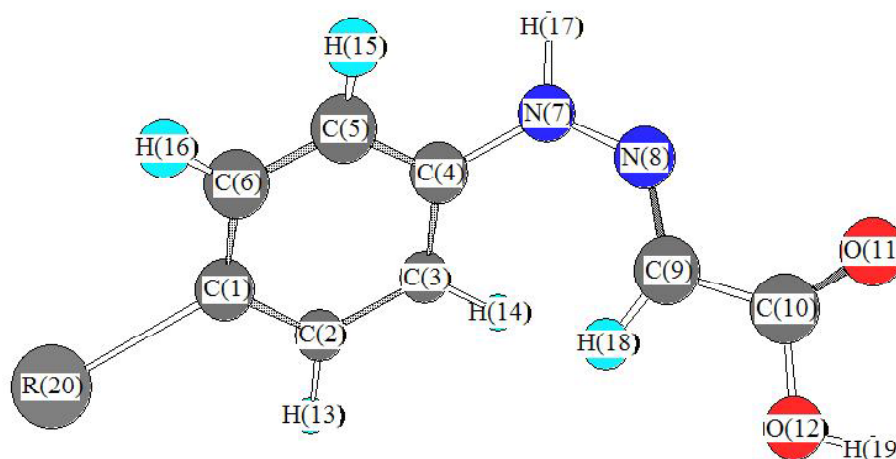


Figure 1. Atom labels of the computational structure.

Table 1. Charge distribution and bond length of compounds 2a-d calculated by B3LYP/6-31G(d) method

Compounds (Substituents)	2a (-OCH ₃)	2b (-CH ₃)	2c (-H)	2d (-NO ₂)
Charge distribution				
R	-0.205	0.034	-----	-0.27
Benzene ring	0.359	0.112	0.139	0.340
N7	-0.358	-0.36	-0.362	-0.365
N8	-0.200	-0.198	-0.198	-0.202
C9	-0.165	-0.159	-0.156	-0.130
C10	0.741	0.742	0.743	0.745
Bond length (pm)				
C4-N7	140.6	140.4	140.4	139.3
N7-N8	131.7	131.8	131.9	132.7
N8-C9	130.2	130.1	130.0	129.6
C9-C10	146.7	146.9	147.0	147.6

In order to support the above hypothesis, the charge distribution of the structures with different substitutions were computed with the DFT method at B3LYP/6-31G(d) level. Atom labels are displayed in Figure 1 for all structures, and the substituents are represented as R(20). As shown in Table 1, the charges of the benzene rings, atoms N7, N8 and C9 were influenced by the different substitutions in the benzenes rings, and it suggests that these fragments are in a large conjugation. The results, in which benzene rings and C9 showed electropositivity and electronegativity respectively, agree with the hypothesis of a conjugated state **4** in Scheme 3.

The postulate that C9 in **2a** had more electronegativity was also supported by the results of calculations. The charge distributions of C9 of **2a**, **2b**, **2c**, and **2d** were -0.165, -0.159, -0.156, and -0.130, respectively. Obviously, the quantity of electric charge of C9 increased with the capability of supplying electrons to substituent groups. The capability to supply electrons from methyl, hydrogen and nitro was weaker than that of methoxy, so the electronegativity of C9 of **2b**, **2c**, and **2d** was weaker than that of **2a**. The weaker electronegativity of C9 led to lower nucleophilicity of C9 of **2b**, **2c**, and **2d**, which could not give dominating products to form a novel reaction under similar conditions.

The strong conjugation in species **4** of Scheme 3 could also be supported by the analysis of bond lengths of structure **2a-2d** from Table 1. It is well known that the length of a standard C-N, C-C, N-N, and C=N are 147.0, 154.0, 140.0, and 128.0 pm, respectively. The bond lengths of C4-N7, N7-N8, and C9-C10 in **2a-2d** were shorter than their standard single bond length, respectively, and that of N8-C9 were longer than a standard double bond. Obviously, these four bonds equilibrated. This phenomenon suggests the fact that there are conjugations in molecule **2a-d**. As the electronegativity of C9 was critical in the reaction, the bond lengths of N8-C9 and C9-C10 were further analyzed for structures **2a-2d**. The structure **4** in Scheme 3 showed that N8-C9 and C9-C10 are double and single bonds. The average degree of these two bonds is related to the conjugation of the molecule. The results in Table 1 show the bond length of N8-C9 of **2a**

was the longest and that of C9-C10 was the shortest in comparison with other compounds. It also suggests that **2a** has more powerful conjugation.

In conclusion, arylhydrazonoacetic acids **2a-d** could be prepared by treatment with one equivalent of 2-oxoacetic acid through the usual pathway, and only 3-(4-methoxyphenyldiazo)acrylic acid **3a** could be synthesized by treatment with 2 equivalents of 2-oxoacetic acid under our reported conditions. We developed a more effective synthetic method for **3a** through this one-pot mild reaction. The mechanism suggests that the novel reaction depends on the degree of electronegativity of C9, which can be largely affected by the substituents of the benzene ring.

Acknowledgements

All authors are grateful to financial support from the Ministry of Science and Technology of the People's Republic of China (No. 2007BA141B01), and Tianjin Municipal Science and Technology Commission (No. 07ZCKFSH00300).

References

- Shandala M, Al-Hajjar F, Al-Jabour N. Reaction of acetylenic β -keto cyanides and β -keto esters with different ammonia derivatives. *J Heterocycl Chem.* 1976; 13:455-459.
- Vicent C, Mazzanti M, Nabferdubu M, Morelli G, Veronese A. Chemosselective synthesis of 3- and 5-pyrazolylacetates. *Heterocycles.* 2000; 53:1285-1292.
- Francesco F, Giovanni G, Francesco R. First synthesis of a bromonitrilimine direct formation of 3-bromopyrazole derivatives. *Tetrahedron Lett.* 1999; 40:2605-2612.
- Kitazaki T, Tamura N, Tasaka A, Matsushita Y, Hayashi R, Okonogi K, Itoh K. Optically active antifungal azoles. VI. Synthesis and antifungal activity of *N*-[(1*R*,2*R*)-2-(2,4-difluorophenyl)-2-hydroxy-1-methyl-3-(1*H*-1,2,4-triazol-1-yl)propyl]-*N'*-(4-substituted phenyl)-3(2*H*,4*H*)-1,2,4-triazolones and 5(1*H*,4*H*)-tetrazolones. *Chem Pharm Bull (Tokyo).* 1996; 44:314-327.
- Parmee ER, Naylor EM, Perkins L, *et al.* Human β_3 -adrenergic receptor agonists containing cyclic ureido benzenesulfonamides. *Bioorg Med Chem Lett.* 1999; 9:749-754.
- Cevasco G, Vigo D, Thea S. The alkaline hydrolysis of aryl (2*E*)-3-(hydroxyphenylazo)propenoates. A kinetic study. *J Org Chem.* 2001; 66:7685-7690.
- Hu CH. Density functional study on the reactivity of carbenes toward 1,2-H shifts. *J Chin Chem Soc-TAIP.* 2001; 48:5-12.
- Lin CL, Chu SY. Comparative study between carbonic and sulfuric acids for dissociation reaction. *J Chin Chem Soc-TAIP.* 2002; 49:777-781.
- Chen PC, Chieh YC. Density functional calculations on the heats of formation of certain aromatic nitro compounds. *J Chin Chem Soc-TAIP.* 2002; 49:791-796.

(Received February 27, 2009; Revised May 20, 2009; Accepted May 26, 2009)

Original Article

A validated stability-indicating HPLC method for analysis of glabridin prodrugs in hydrolysis studies

Warunee Jirawattanapong¹, Ekarin Saifah², Chamnan Patarapanich^{1,*}¹ Department of Pharmaceutical Chemistry, Faculty of Pharmaceutical Sciences, Chulalongkorn University, Bangkok, Thailand;² Department of Pharmaceutical Botany, Faculty of Pharmaceutical Sciences, Chulalongkorn University, Bangkok, Thailand.

ABSTRACT: A simple, selective and precise stability-indicating HPLC method for determination of glabridin diacetate and dihexanoate prodrugs was developed, validated and applied to the enzymatic and chemical hydrolysis studies. The chromatographic separation was achieved on a reverse phase C18 (Thermo Hypersil-Keystone, 250 × 4.6 mm, 5 micron) column using the mixture of acetonitrile and water as mobile phase. Elution of the mobile phase was operated on isocratic (acetonitrile 76%: water 24%) for 9 min, followed by gradient (acetonitrile from 76% to 90%) within 9 min and isocratic (acetonitrile 90%: water 10%) for 12 min at 1 mL/min flow rate, detected at 280 nm. The method was validated for specificity, accuracy, precision, linearity and limit of quantitation following the International Conference on Harmonization (ICH) guidelines. The method is effective for the separation of glabridin diacetate and glabridin dihexanoate from glabridin, its parent drug and successfully used in these prodrugs hydrolysis studies.

Keywords: Glabridin, prodrugs, HPLC, validation, hydrolysis studies

1. Introduction

Glabridin is a major pyranoisoflavan isolated from hydrophobic fraction of European licorice, *Glycyrrhiza glabra* L. var *typica* and var *glandulifera* (1). It has been reported to exhibit a wide range of pharmacological activities such as antimicrobial (2-4), protection of mitochondrial functions against oxidative stress (5), estrogenic and antiproliferative activities in human breast cancer cells (6,7), inhibition of adenosine 3',5'-cyclic monophosphate (cAMP) phosphodiesterase

(8), inhibition of human cytochrome P450s 3A4, 2B6 and 2C9 (9), inhibit melanogenesis and inflammation (10), neuroprotective (11) and prevention of low-density lipoprotein oxidation (12-16).

Even though glabridin (G) is a potent tyrosinase inhibitor and potential for skin whitening preparation, G showed poor skin penetration and instability in formulation (15). One strategy to overcome this problem is the prodrug approach. To improve the stability in formulation, glabridin diacetate (GDA) and glabridin dihexanoate (GDH) esters were synthesized by acylation as prodrug of G (Figure 1). A successful G prodrug must not only undergo enzymatic hydrolysis in physiological condition, but also be chemically stable in formulation. So far, to our present knowledge, most previous analytical methods for determination of G (16-20) have been done in licorice and its extract, but no stability-indicating analytical method for the quantitation of G prodrugs was available in literature. Therefore, it is necessary to develop an analytical method to determine the G, GDA and GDH in hydrolysis studies.

This paper deals with the HPLC assay and method validation for accurate quantitation of G, GDA and GDH. The paper also deals with the application of the method to enzymatic and chemical hydrolysis studies.

2. Materials and Methods

2.1. Chemicals

G was isolated from available licorice extract (PT-40) by conventional column chromatography and obtained

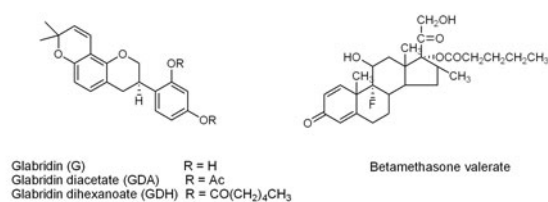


Figure 1. Structure of glabridin (G), its prodrugs and betamethasone valerate (IS).

*Address correspondence to:

Dr. Chamnan Patarapanich, Department of Pharmaceutical Chemistry, Faculty of Pharmaceutical Sciences, Chulalongkorn University, Bangkok 10330, Thailand. e-mail: pchamnan@chula.ac.th

G was finally purified by crystallization from hexane. GDA and GDH were synthesized by acylation with corresponding acid anhydrides. The GDA was purified by column chromatography and recrystallized from methanol, while GDH was purified by column chromatography. The structures of products were elucidated by spectroscopic techniques, mainly NMR, MS, IR spectroscopy and elemental analysis as well as comparison with those of earlier reported ^1H and ^{13}C NMR data of G (21). G, GDA and GDH purity were determined based on HPLC peak purity analysis.

HPLC grade acetonitrile was purchased from Lab-Scan Analytical Sciences (Bangkok, Thailand). Water was purified using a ELGA water purifier (ELGA Ltd., Bucks, England). All other chemicals and solvents were analytical grade.

2.2. Equipment

The quantitation of G, GDA, and GDH was performed on a Shimadzu HPLC system (Kyoto, Japan) consisting of SCL-10ADvp system controller, two LC-10ADvp pumps, SIL-10ADvp autosampler, Diode-array detector SPD-M10Avp, and Class VP software. Shaking water-bath (Maxi shake SBD-50 COLD, Allerod, Denmark), Centrifuge (Hettich Zentrifugen EBA-20, Tuttingen, Germany) and Vortex-2 Genie (Scientific industries, Inc., Bohemia, USA) were used for hydrolysis studies.

2.3. Standard solutions preparation

Each stock solution of G (0.15 mg/mL), GDA (0.20 mg/mL), GDH (0.19 mg/mL) and internal standard (IS), betamethasone valerate (0.41 mg/mL) was prepared in acetonitrile. Working standard solutions for calibration curve were prepared by diluted of each stock solution with acetonitrile to give the final concentration range of 0.075-13.5 $\mu\text{g/mL}$ for G, 0.1-20.0 $\mu\text{g/mL}$ for GDA, and 0.95-16.15 $\mu\text{g/mL}$ for GDH, respectively. The IS solution was added to each working standard solution to obtain the final concentration of 82 $\mu\text{g/mL}$.

2.4. Sample preparation

The stock solutions (0.01 M) of each G, GDA, and GDH were prepared in dimethylsulfoxide and IS solution (82 $\mu\text{g/mL}$) was prepared in acetonitrile. For determination of extraction recovery and precision, 50 μL of the standard solution was added to 450 μL of phosphate buffer solutions (pH 5.5 and 7.4) in a 10-mL screw-capped test tube. One mL of methanol was added and vortexed for 3 sec. The extract was performed by adding 3 mL of chloroform. After 10 sec vortexing, the mixture was centrifuged at 5,000 rpm for 5 min. The aqueous layer was removed and the organic phase was transferred to a new test tube. Two mL of organic phase was evaporated to dryness and reconstituted in 1 mL of

IS solution, then filtered through 0.45 μm nylon filter to obtain a clear sample solution.

2.5. Chromatographic conditions

A reverse phase C18 (250 \times 4.6 mm, 5 micron; Thermo Hypersil-Keystone, Bellefonte, PA, USA) column connected with a guard column (C18; Alltech Associates, Inc., Deerfield, IL, USA) was used. The mobile phase was a mixture of acetonitrile and water at 1 mL/min of flow rate. To separate the sample, three steps of the elution was operated, isocratic elution with the mixture of acetonitrile and water (76:24, v/v) for 9 min followed by linear gradient elution of 76% to 90% acetonitrile for 9 min and finally isocratic elution with the mixture of acetonitrile and water (90:10, v/v) for 12 min. The eluent was monitored at 280 nm. The injection volume was 20 μL of sample solutions.

2.6. Method validation

The validation was performed by spiked placebo technique. The method was validated for specificity, accuracy, precision, linearity and limit of quantitation was determined in accordance with ICH guidelines on analytical validation Q2 (R1) (22).

2.6.1. Specificity

Specificity is the ability of the method to measure the analyte in the presence of impurities and degradation products (22). The specificity of the developed HPLC method for the prodrugs, GDA and GDH were determined by the retention time of GDA, GDH and G in the HPLC system. In addition, the peak purity tests of each standard were performed by the photodiode array detection.

2.6.2. Linearity and range

The linearity of the method was conducted by preparing standard solutions at five different concentrations of analytes within range 0.75-13.5, 0.1-20.0 and 0.95-16.15 $\mu\text{g/mL}$ for G, GDA, and GDH, respectively. Each solution was analyzed in triplicate. Peak area ratio values (ratio AUC/IS) were plotted against the corresponding concentrations of analytes. The linearity of the plot was evaluated by linear regression analysis.

2.6.3. Accuracy

The accuracy of the calibration standards was evaluated in triplicate at three concentrations (4.50, 7.50, and 10.50 $\mu\text{g/mL}$ for G, 6.00, 10.00, and 14.00 $\mu\text{g/mL}$ for GDA and 1.90, 7.60, and 11.40 $\mu\text{g/mL}$ for GDH). To access the accuracy of the samples in spiked phosphate buffer systems, three different concentration levels

(6.49, 8.65, and 10.81 $\mu\text{g/mL}$ for G, 9.73, 12.97, and 16.22 $\mu\text{g/mL}$ for GDA and 9.41, 12.54, and 15.68 $\mu\text{g/mL}$ for GDH) were prepared as described above and injected to HPLC. The percentage of recoveries was calculated from slope and y-intercept of the calibration curve. The criteria for acceptability of accuracy or recovery were the average value within 95-105%.

2.6.4. Precision

The intra-day and inter-day precision of both calibration standards and samples were evaluated at the same concentration levels as those performing for the accuracy. The intra-day precision was performed on the same day and expressed as percentages of relative standard deviations (%RSD) calculated from the analytes of three replicates samples. The inter-day precision was performed on three separate days. The criteria for acceptability of precision was the %RSD for each concentration level not exceed 3%.

2.6.5. Limit of quantitation

The limit of quantitation (LOQ) of the analytes was determined during the evaluation of the linear range of the method. The LOQ was defined as the lowest concentrations yielding a precision with RSD $\leq 10\%$ and acceptable accuracy within 10% of the theoretical value.

2.7. Enzymatic and chemical stabilities

For the enzymatic hydrolysis studies, a purified porcine liver esterase (PLE, carboxylic-ester hydrolase, EC 3.1.1.1; Sigma-Aldrich, St Louis, MO, USA) was dissolved in 0.05 M phosphate buffer solution (pH 7.4, ionic strength = 0.15) to a concentration of 1.01 unit/mL (23,24). Eighty microliters of the 0.01 M stock solution of the prodrug solution in dimethylsulfoxide was added to the enzyme-buffer mixture, mixed well and then kept in a water-bath at $37 \pm 0.1^\circ\text{C}$. At appropriate time intervals (0, 2, 4, 6, 8, 10, 15, 30, 45, 60, 90, and 120 min for GDA and 0, 4, 6, 8, 10, 12, 14, 16, 18, 20, 22, 24, and 31 h for GDH), 500 μL aliquots were withdrawn and 1 mL of methanol was added to quench the reaction. The extract was performed as described in sample preparation. Pseudo-first-order rate constants (k) for the hydrolysis were determined from the slopes of linear plots of the logarithm of residual model prodrugs against time. The half-life of each prodrug was calculated from the equation: $t_{1/2} = 0.693/k$. The experiments were performed in triplicate.

The chemical stability of the prodrug was investigated in aqueous phosphate buffer solutions (pH 7.4 and 5.5, ionic strength = 0.15) at $37 \pm 0.5^\circ\text{C}$, in triplicate experiments. At 24-hour intervals, sample was taken, extracted as the method described above and analyzed by HPLC.

3. Results

3.1. Separation and specification

The developed method showed well chromatographic separation with no interference at the elution time of analytes. Chromatograms of G and its prodrugs sample spiked with IS were recorded at 280 nm according to their absorption maxima as shown in Figure 2. The retention time in HPLC condition were 4.70, 5.27, 7.76, and 25.04 min for G, IS, GDA, and GDH, respectively.

3.2. Linearity and range

Linear calibration plot was obtained from the theoretical concentration versus peak area response within the range of 0.075-13.50, 0.10-20.0, and 0.95-16.15 $\mu\text{g/mL}$ for G, GDA, and GDH, respectively. Response linearity was determined by least squares regression analyses of the calibration plot. The linear regression (r^2) of calibration plots of G, GDA, and GDH showed good linear relationship with $r^2 = 0.9998$, 0.9999, and 0.9999 with respect to peak area (Table 1).

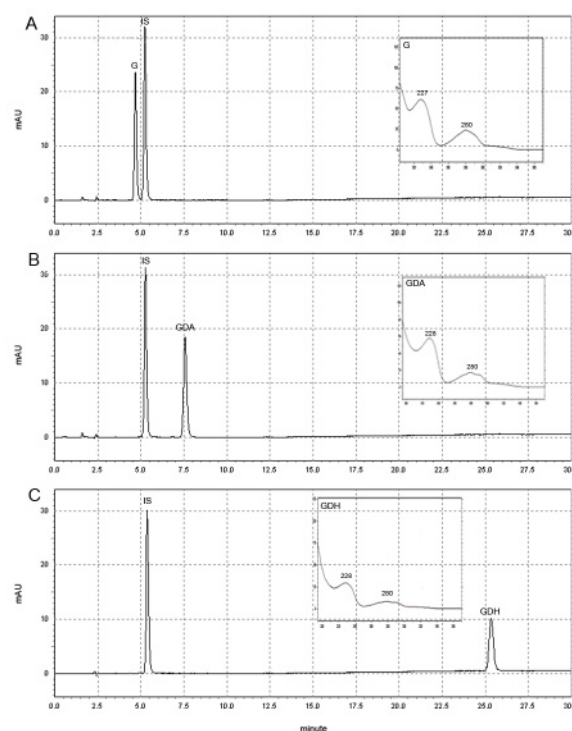


Figure 2. HPLC chromatograms and photodiode array UV absorption spectra of (A) G 4.5 $\mu\text{g/mL}$, (B) GDA 10 $\mu\text{g/mL}$ and (C) GDH 7.6 $\mu\text{g/mL}$, spiked with IS 82 $\mu\text{g/mL}$.

Table 1. Regression data of calibration curves of each reference standard

Analyte	Linear regression	Correlation coefficient (r^2)	n
G	$y = 0.1535x - 0.0023$	0.9998	3
GDA	$y = 0.0818x + 0.0004$	0.9999	3
GDH	$y = 0.0652x + 0.0226$	0.9999	3

3.3. Accuracy and precision

The accuracy and repeatability of samples at three concentration levels were expressed in terms of % recovery and %RSD. The accuracy and precision of the quantitation of calibration standard were shown in Table 2. The assay exhibits acceptable level of accuracy for estimating analyte concentration (95-105%) within percent relative standard deviations (%RSD) < 3%. The percent recovery of the standards ranged from 98.86-101.1%, 98.44-99.74%, and 100.1-102.8% for G, GDA, and GDH, respectively, with precision < 3%. Similar level of accuracy and precision were obtained

from the analysis of the samples in both buffer systems (Tables 3 and 4).

3.4. Limit of quantitation

Limit of quantitation (LOQ) is generally determined by the analysis of samples with known concentrations of analyte and by establishing the minimum level at which the analyte can be quantified with acceptable accuracy and precision. LOQ was determined during the evaluation of the linear range of calibration curve and defined as the lowest concentration yielding a precision with %RSD less than 10, accuracy within 10% of the

Table 2. Accuracy and precision of the quantitation of calibration standard (n = 3)

Analyte	Added ($\mu\text{g/mL}$)	Intra-day			Inter-day		
		Found ($\mu\text{g/mL}$)	Recovery (%)	RSD (%)	Found ($\mu\text{g/mL}$)	Recovery (%)	RSD (%)
G	4.50	4.45	98.86	1.20	4.45	98.84	0.16
	7.50	7.50	100.0	1.05	7.43	99.04	0.90
	10.50	10.61	101.1	0.07	10.38	98.87	1.93
GDA	6.00	5.91	98.44	0.38	5.99	98.87	1.48
	10.00	9.91	99.08	0.93	9.84	98.42	0.65
	14.00	13.96	99.74	1.09	13.95	99.65	0.46
GDH	1.90	1.95	102.8	1.85	1.94	102.0	1.07
	7.60	7.65	100.7	0.51	7.79	102.6	1.60
	11.40	11.41	100.1	1.82	11.56	101.4	2.27

Table 3. Intra-day precision of the quantitation of sample in spiked phosphate buffer systems (n = 3)

Analyte	Added ($\mu\text{g/mL}$)	pH 5.5			pH 7.4		
		Found ($\mu\text{g/mL}$)	Recovery (%)	RSD (%)	Found ($\mu\text{g/mL}$)	Recovery (%)	RSD (%)
G	6.49	6.41	98.75	2.43	6.55	101.0	1.89
	8.65	8.39	97.06	1.17	8.55	98.81	1.49
	10.81	10.88	100.6	1.60	11.03	102.1	2.10
GDA	9.73	9.68	99.50	1.33	9.43	96.90	0.56
	12.97	12.73	98.10	0.67	13.10	101.0	2.26
	16.22	16.43	101.3	1.35	16.04	98.94	0.25
GDH	9.41	9.45	100.5	1.52	9.55	101.6	2.75
	12.54	12.70	101.3	2.53	12.57	100.2	1.24
	15.68	15.55	99.17	1.01	15.53	99.06	1.83

Table 4. Inter-day precision of the quantitation of sample in spiked phosphate buffer systems (n = 3)

Analyte	Added ($\mu\text{g/mL}$)	pH 5.5			pH 7.4		
		Found ($\mu\text{g/mL}$)	Recovery (%)	RSD (%)	Found ($\mu\text{g/mL}$)	Recovery (%)	RSD (%)
G	6.49	6.40	98.61	0.49	6.57	101.4	0.54
	8.65	8.49	98.19	1.05	8.63	99.76	1.60
	10.81	11.06	102.3	1.54	10.83	100.2	1.59
GDA	9.73	9.83	101.0	1.79	9.40	96.90	0.52
	12.97	12.66	97.62	1.78	12.86	99.14	2.15
	16.22	16.38	101.0	0.75	16.21	99.94	1.13
GDH	9.41	9.53	101.3	2.05	9.56	101.7	2.23
	12.54	12.68	101.2	0.29	12.55	100.1	1.18
	15.68	15.58	99.37	0.49	15.63	99.73	1.16

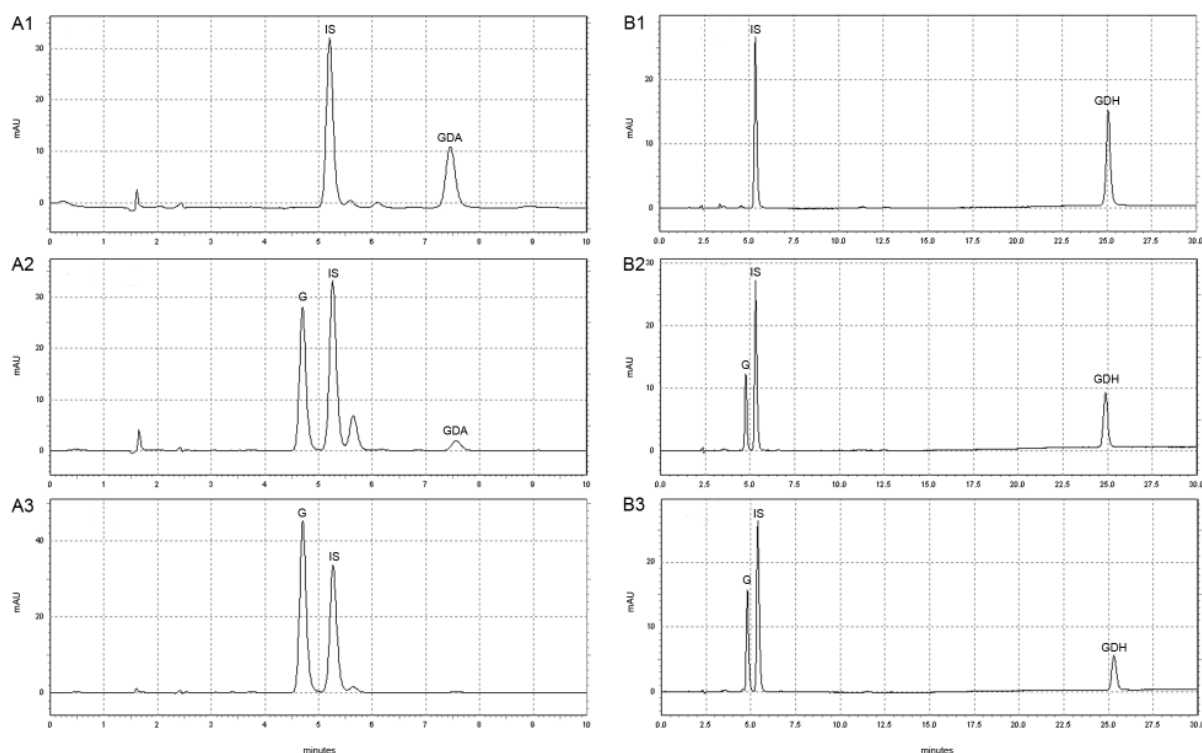


Figure 3. HPLC chromatograms of samples from enzymatic hydrolysis studies of GDA (A) at 0 min (A1), 6 min (A2), and 120 min (A3) as well as GDH (B) at 0 h (B1), 10 h (B2) and 24 h (B3).

theoretical value (90-110%R). The established LOQ were 0.075, 0.1, and 0.95 $\mu\text{g/mL}$ for G, GDA, and GDH, respectively.

3.5. Application to enzymatic and chemical stability studies

The validated method was further evaluated for its applicability in analyzing G, GDA, and GDH in stability studies. In this study, the porcine esterase was used as a tool for enzymatic hydrolysis study of G prodrugs and the chemical hydrolysis was determined in phosphate buffer (pH 5.5 and 7.4). The chromatograms of analytes from enzymatic hydrolysis of GDA and GDH were shown in Figure 3 and chemical hydrolysis time course profiles of GDA and GDH were demonstrated in Figure 4. The enzymatic half-life of GDA was 2.36 min and that of GDH was 14.8 h, while chemical hydrolysis half-lives of both prodrugs were more than 15 days.

4. Discussion

The main target of this chromatographic method is to develop a single HPLC system for the simultaneous separation of both GDA and GDH prodrugs from its parent drug. The developed method was based on different polarity, amenable to reverse-phase HPLC and UV detectable at 280 nm of each analyte. In addition, the liquid-liquid extraction was employed as sample

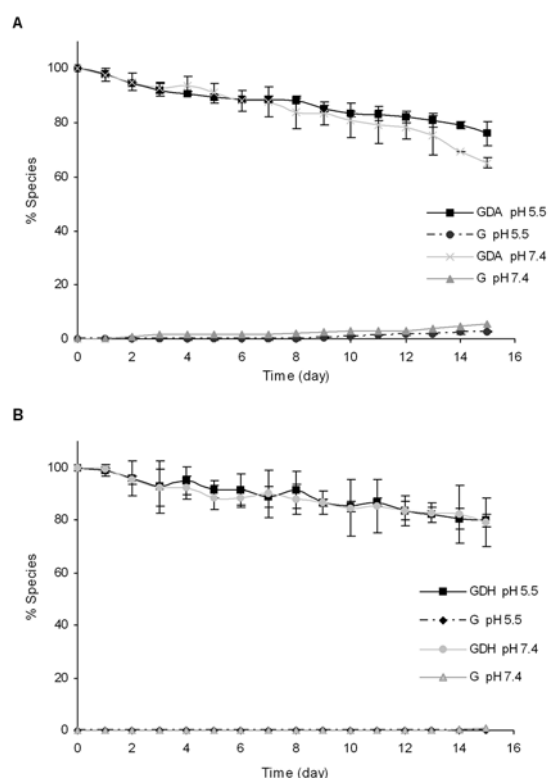


Figure 4. Chemical hydrolysis time course for GDA (A) and GDH (B) including its parent drug, G, in phosphate buffer systems.

preparation method.

Several compounds, quercetin, plumbagin, berberine, diclofenac, fluroseamide, chloramphenicol,

propyl-paraben, prednisolone, and betamethasone valerate were tested as internal standard. The peaks of all selected compounds except betamethasone valerate were not completely separated from the peak of either G or its prodrugs. Only betamethasone valerate was well separated from G, GDA, and GDH, and thus it is used as internal standard.

Various combinations of organic modifiers such as acetonitrile, tetrahydrofuran as well as methanol and water were investigated. Besides, both isocratic and gradient HPLC elutions were also examined. Finally, the optimal condition was achieved using the mixture of acetonitrile and water as mobile phase, which operated on isocratic (acetonitrile 76%: water 24%) for 9 min, followed by gradient (acetonitrile from 76% to 90%) within 9 min and finally, isocratic (acetonitrile 90%: water 10%) for 12 min at 1 mL/min of flow rate. The linear regression analysis data for the calibration plots of G, GDA, and GDH showed good linear relationship with $r^2 = 0.9998$, 0.9999 , and 0.9999 with respect to peak area, for the concentration range 0.075-13.50, 0.10-20, and 0.95-16.15 $\mu\text{g/mL}$, respectively. The accuracy of each analyte was determined to be within 5% (95-105%) with a relative standard deviation $< 3\%$. Thus the developed sample preparation and liquid chromatographic condition were found to be specific for GDA and GDH prodrugs including their parent drug, G.

The validated method was also tested for its ability to support the quantitative analysis of GDA and GDH prodrugs in stability studies. Since the precondition of prodrug approach is that the prodrug can be converted to the parent drug in order to exert biological effects. The evaluation of enzymatic and chemical hydrolysis of these prodrugs was studied. As porcine liver esterase is a good model of the esterase found in the skin and, as such, is important in predicting the use of certain prodrugs as topical treatment. Chromatograms shown in Figure 3 indicated that the porcine liver esterase can easily catalyze hydrolysis of phenol ester of GDA prodrug, lead to the release of its parent drug, G. The hydrolysis of GDA was found to proceed in two steps reaction. Firstly, one of the ester moiety was hydrolyzed to yield the intermediate, G acetate which underwent spontaneous hydrolysis to G. While GDH was hydrolyzed with more slower rate. Therefore, the varying size of the acyl group from acetate (C2) group of GDA to hexanoate (C6) group of GDH may cause steric hindrance to the esterase. Moreover, the stability of prodrug against the spontaneous chemical hydrolysis is of importance, especially for the cosmetic products and topical formulation. The chemical hydrolysis in this study was performed to evaluate the effect of pH on degradation of G prodrugs. The result indicated that the chemical stabilities of both prodrugs at both pH were quite similar. However, the degradation rate was very slow as comparison with enzymatic hydrolysis. The

half-lives of hydrolysis in both pH buffer solution were more than 15 days, suggesting the sufficient chemical stability.

5. Conclusion

A simple, sensitive, accurate and precise HPLC method was developed, validated and subsequently successfully applied to stability studies of glabridin prodrugs. The stabilities of these prodrugs in enzyme solution and phosphate buffer systems (pH 5.5 and 7.4) were examined by monitoring the remained level of prodrugs as well as the appearance of their degradation product, glabridin, under the experimental conditions. Therefore, the chromatographic condition and sample preparation method of this present study is suitable to conduct stability studies for glabridin prodrugs.

References

1. Fukai T, Satoh K, Nomura T, Sakagami H. Preliminary evaluation of antinephritis and radical scavenging activities of glabridin from *Glycyrrhiza glabra*. *Fitoterapia*. 2003; 74:624-629.
2. Fukai T, Marumo A, Kaitou K, Kanda T, Terada S, Nomura T. Antimicrobial activity of licorice flavonoids against methicillin-resistant *Staphylococcus aureus*. *Fitoterapia*. 2002; 73:536-539.
3. Fukai T, Marumo A, Kaitou K, Kanda T, Terada S, Nomura T. Anti-*Helicobacter pylori* flavonoids from licorice extract. *Life Sci*. 2002; 71:1449-1463.
4. Mitscher LA, Park YH, Clark D. Antimicrobial agents from higher plants: antimicrobial isoflavanoids and related substances from *Glycyrrhiza glabra* L. var. *typical*. *J Nat Prod*. 1980; 43:259-269.
5. Haraguchi H, Yoshida N, Ishikawa H, Tamura Y, Mizutani K, Kinoshita T. Protection of mitochondrial functions against oxidative stresses by isoflavans from *Glycyrrhiza glabra*. *J Pharm Pharmacol*. 2000; 52:219-223.
6. Somjen D, Knoll E, Vaya J, Stern N, Tamir S. Estrogen-like activity of licorice root constituents: glabridin and glabrene, in vascular tissues *in vitro* and *in vivo*. *J Steroid Biochem Mol Biol*. 2004; 91:147-155.
7. Tamir S, Eizenberg M, Somjen D, Stern N, Shelach R, Kaye A, Vaya J. Estrogenic and antiproliferative properties of glabridin from licorice in human breast cancer cells. *Cancer Res*. 2000; 60:5704-5709.
8. Kusano A, Nikaïdo T, Kuge T, Ohmoto T, Monache GD, Botta B, Botta M, Saitoh T. Inhibition of adenosine 3',5'-cyclic monophosphate phosphodiesterase by flavonoids from licorice roots and 4-arylcoumarins. *Chem Pharm Bull*. 1991; 39:930-933.
9. Kent UM, Aviram M, Rosenblat M, Hollenberg PF. The licorice root derived isoflavan glabridin inhibits the activities of human cytochrome P450s 3A4, 2B6, and 2C9. *Drug Metab Dispos*. 2002; 30:709-715.
10. Yokota T, Nishio H, Kubota Y, Mizoguchi M. The inhibitory effect of glabridin from licorice extracts on melanogenesis and inflammation. *Pigment Cell Res*. 1998; 11:355-361.
11. Yu XQ, Xue CC, Zhou ZW, Li CG, Du YM, Liang J,

- Zhou SF. *In vitro* and *in vivo* neuroprotective effect and mechanisms of glabridin, a major active isoflavan from *Glycyrrhiza glabra* (licorice). *Life Sci*. 2008; 82:68-78.
12. Aviram M. Flavonoids-rich nutrients with potent antioxidant activity prevent atherosclerosis development: the licorice example. *Int Congr Ser*. 2004; 1262:320-327.
 13. Belinky PA, Aviram M, Fuhrman B, Rosenblat M, Vaya J. The antioxidative effects of the isoflavan glabridin on endogenous constituents of LDL during its oxidation. *Atherosclerosis*. 1998; 137:49-61.
 14. Belinky PA, Aviram M, Mahmood S, Vaya J. Structural aspects of the inhibitory effect of glabridin on LDL oxidation. *Free Radic Biol Med*. 1998; 24:1419-1429.
 15. Rosenblat M, Belinky P, Vaya J, Levy R, Hayek T, Coleman R, Merchav S, Aviram M. Macrophage enrichment with the isoflavan glabridin inhibits NADPH oxidase-induced cell-mediated oxidation of low density lipoprotein: a possible for protein kinase C. *J Biol Chem*. 1999; 274:13790-13799.
 16. Vaya J, Belinky PA, Aviram M. Antioxidant constituents from licorice roots: isolation, structure elucidation and antioxidative capacity toward LDL oxidation. *Free Radic Biol Med*. 1997; 23:302-313.
 17. Rauchensteiner F, Matsumura Y, Yamamoto Y, Yamaji S, Tani T. Analysis and comparison of *radix Glycyrrhizae* (licorice) from Europe and China by capillary-zone electrophoresis (CZE). *J Pharm Biomed Anal*. 2005; 38:594-600.
 18. Yan H, Tian M, Row KH. Selective solid-phase extraction of glabridin from licorice root using molecularly imprinted polymer. *Separ Sci Technol*. 2009; 44:359-369.
 19. Aoki F, Nakagawa K, Tanaka A, Matsuzaki K, Arai N, Mae T. Determination of glabridin in human plasma by solid-phase extraction and LC-MS/MS. *J Chromatogr B*. 2005; 828:70-74.
 20. Shanker K, Fatima A, Negi AS, Gupta VK, Darokar MP, Gupta MM, Khanuja SPS. RP-HPLC method for the quantitation of glabridin in Yashti-madhu (*Glycyrrhiza glabra*). *Chromatographia*. 2007; 65:771-774.
 21. Kinoshita T, Kajiyama K, Hiraga Y, Takahashi K, Tamura Y, Mizutani K. Isoflavan derivatives from *Glycyrrhiza glabra* (licorice). *Heterocycles*. 1996; 43:581-588.
 22. International Conference on Harmonization (ICH). Validation of analytical procedures text and methodology, Q2 (R1). 2005. <http://www.ich.org/LOB/media/MEDIA417.pdf> (accessed March 20, 2008).
 23. Wang B, Zhang H, Zheng A, Wang W. Coumarin-based prodrugs. Part 3: Structure effects on the release kinetics of esterase-sensitive prodrugs of amines. *Bioorg Med Chem*. 1998; 6:417-426.
 24. Xu CR, He HT, Song X, Siahaan TJ. Synthesis and comparison of physicochemical, transport, and antithrombic properties of a cyclic prodrug and the parent RGD peptidomimetic. *Tetrahedron*. 2003; 59:2861-2869.

(Received April 10, 2009; Accepted May 2, 2009)

Original Article**Correlation of *in vitro* dissolution rate and apparent solubility in buffered media using a miniaturized rotating disk equipment: Part I. Comparison with a traditional USP rotating disk apparatus**Anita M. Persson^{1,*}, Anders Sokolowski², Curt Pettersson¹¹ Division of Analytical Pharmaceutical Chemistry, Uppsala University, BMC, SE-751 23 Uppsala, Sweden;² AS Consulting, Hugo Alfvéns väg 26, SE-756 49 Uppsala, Sweden.

ABSTRACT: A correlation of the logarithmic values of the *in vitro* dissolution rate, *G*, and the apparent solubility, *S*, was evaluated in phosphate and ammonium acetate buffer at an initial pH of 7. The dissolution rates were determined with a newly designed and build miniaturized rotating disk equipment, as well as with a traditional rotating disk apparatus. The two apparatuses gave the same correlation pattern of log*G* and log*S*. Thirteen diverse drug substances from all of the classes in the Biopharmaceutics Classification System (BCS) were used for the correlation in the phosphate buffer system, with the results from the miniaturized apparatus only. A coefficient of determination, *R*², of 0.982 was found if bases formulated as hydrochloride salts were excluded in the correlation.

The miniaturized equipment is used for rapid screening of the dissolution rate, approximately 10 min for one run, and consumes small amounts of substance (about 5 mg) and dissolution media. All quantifications were performed by using reversed phase high-performance liquid chromatography (RP-HPLC) with a diode array detector (DAD), integrated with the miniaturized rotating disk equipment.

Keywords: Dissolution rate, solubility, *in vitro* models, correlation, HPLC (high-performance liquid chromatography)

1. Introduction

Solubility and dissolution rate are two important physicochemical properties during the lead selection and optimization process in drug discovery (1,2).

*Address correspondence to:

M.Sc. Anita M. Persson, Division of Analytical Pharmaceutical Chemistry, Uppsala University, BMC, SE-751 23 Uppsala, Sweden.
e-mail: anita.persson@farmkemi.uu.se

Great effort in preformulation studies can sometimes circumvent insufficient solubility of a drug substance, but more cost- and time-effective strategies are preferred. Due to the large number of lead candidates in early development of drugs it would be desirable to develop a fast and adequate accurate method to measure the solubility, while consuming only minute amount of substances and media. Furthermore it should be advantageous to predict the solubility directly by simply studying the dissolution rate of a drug substance.

Good correlation between the solubility and the *in vitro* dissolution rate has previously been found for a number of compounds (3-6). However, it should always be stressed that this correlation will be dependent on the instrumental setup and the media used. The chemical properties of the dissolution medium (pH, buffer and additional components, *etc.*) play a decisive role for the dissolution rate studies (7-10). Furthermore the correlation can differ between free bases or acids and their respective salt forms (11,12). Additional studies of the correlation between solubility and dissolution rate are necessary in order to validate a predictive value of solubility from dissolution rate data due to the differences stated above.

Several different methods are used to determine the solubility of new substances (13,14), with the traditional shake-flask method as the most frequently used technique. Unfortunately, not all of the methods are adapted to the high throughput needs in modern drug discovery. Some methods that minimize the amount of substances while determining the solubility are *e.g.* the miniaturized shake-flask (15), pSol method (16), GLpKa/CheqSol method (17,18) and a multichanneled miniaturized device (19). The shake-flask method most often determines the solubility at a specific pH and buffer capacity (β) at a defined shake-time, which gives the apparent solubility. A problem during this solubility determination is the possibility of a degradation of the drug substance. The experimental determination of solubility can also be affected by buffer or additional components in the solution, *e.g.* due to the common ion effect, as well as the ionic strength (20-22).

Many rotating disk theories of the dissolution rate are based on the diffusion layer model (23), where the dissolution rate is assumed to be controlled by the diffusion of the investigated drug substance through a stagnant layer near the drug surface. The hydrodynamics is thus a combination of laminar and convective fluids (23,24) and the disturbance of the diffusion layer will probably increase the dissolution rate. Even if media mimicking gastric and small intestinal environments are used, the simulation of the *in vivo* hydrodynamics is still difficult to achieve. Different techniques have been used in dissolution rate studies, *e.g.* USP rotating disk method (25), flow-through cell or channel flow methods (5,26,27), microcalorimetry (28) and a newly designed miniaturized equipment (29) as well as a miniaturized intrinsic dissolution rate apparatus (30,31).

In this study a comparison of the correlation between the logarithmic values of the *in vitro* dissolution rates (G) obtained with a newly designed miniaturized equipment and a traditional rotating disk apparatus, and the logarithmic values of the apparent solubilities (S) determined by a conventional shake-flask method at a volume of 1.5 mL was made. The evaluations were done with six different drug substances in an ammonium acetate and a phosphate buffer. In an extended study, thirteen substances in the correlation between the dissolution rate and the solubility was performed, using only the phosphate buffer and the miniaturized equipment. The initial pH was chosen to be biorelevant (32,33) and applied to the guidelines from the Federation International Pharmaceutic (FIP). FIP recommend USP buffer solutions in the pH range of 4.5 to 8.0 in dissolution testing (34,35).

The aim of the present study was to compare the possibility to predict the solubility based on the dissolution rate determined by a traditional rotating disk apparatus and a newly established miniaturized rotating disk equipment (29). The miniaturized system has the advantage of only consuming minute amount of substance, as well as dissolution medium. Furthermore, it also provides a value of the dissolution rate simply by one measurement. The comparison between the two dissolution systems is vital. If they give equal results, the newly developed instrument can be used in further studies of the correlation of $\log G$ and $\log S$.

2. Theoretical

The stoichiometric apparent solubility (S) can theoretically be calculated by using the stoichiometric intrinsic solubility of a solute (S_0), pH of the solution and the stoichiometric pK_a -value of the solute at the actual ionic strength for both monoacidic (Eq. 1) and monobasic (Eq. 2) drugs. The stoichiometric pK_a -value is dependent on the ionic strength, which consequently will affect the apparent solubility (36,37). The intrinsic solubility relates to the solubility of the completely

unionized substance. These equations of ionizable substances are based on the Henderson-Hasselbalch relationship, cf. (38-40).

$$S = S_0 [1 + 10^{(pH - pK_a)}] \quad \text{Eq. 1}$$

$$S = S_0 [1 + 10^{(pK_a - pH)}] \quad \text{Eq. 2}$$

During solubility studies with shake-flask methodology the pH can differ from the start to the end of the experiments if protolytic drug substances are examined, as often is the case. It is therefore necessary to measure the pH in the medium before drug substance is added and particularly after the defined shake time.

At constant flow rate and rotation speed in the rotating disk experiments, the thickness of the diffusion layer above the rotating disk of drug substance will be constant. Assuming that no other side reactions, beside protolysis, exist in the experiments and that sink conditions is prevailed the modified Noyes-Whitney equation can be expressed as Eq. 3 (41):

$$G = \frac{D}{h} \cdot S = k \cdot S \quad \text{Eq. 3}$$

where G is the *in vitro* dissolution rate, k is a constant based on the thickness of the diffusion layer adjacent the disk surface, h , and the diffusion coefficient, D , of the substance in the dissolution medium at a certain temperature. S is the apparent solubility (as defined above) of the drug substance in the dissolution medium at a certain temperature. The logarithmated form of the equation will give a straight line when plotting $\log G$ versus $\log S$, Eq. 4, cf. (3).

$$\log G = \log S + \log k \quad \text{Eq. 4}$$

3. Materials and Methods

3.1. Chemicals

Naproxen, ketoprofen and griseofulvin met USP specifications, enalapril maleate, nortriptyline hydrochloride, chlorpromazine hydrochloride, clomipramine hydrochloride, prednisone, bendroflumethiazide, furosemide and terfenadine were minimum 98% and carbamazepine 99%, were all purchased from Sigma-Aldrich (Chemie GmbH, Steinheim, Germany). Ciprofloxacin $\geq 98.0\%$ was obtained from Fluka BioChemika, (Chemie GmbH, Buchs, Switzerland). Sodium di-hydrogen phosphate monohydrate ($\text{NaH}_2\text{PO}_4 \cdot \text{H}_2\text{O}$) *p.a.*, Acros Organics (Springfield, NJ, USA), di-sodium hydrogen phosphate dihydrate ($\text{Na}_2\text{HPO}_4 \cdot 2\text{H}_2\text{O}$) *p.a.* and trifluoroacetic acid $\geq 99.0\%$, were both from Fluka Chemika (Chemie GmbH, Buchs, Switzerland). Ammonium acetate (NH_4Ac) *p.a.*, was bought from Riedel-de Haën, Sigma-Aldrich (Laborchemikalien GmbH, Seelze, Germany). Acetonitrile, HPLC grade was bought from Fisher

Scientific (UK Limited, Leicestershire, UK). The water used in this study was purified in a Milli-Q[®] Academic system (18.2 MΩ-cm/0.22 μm), Millipore, (Burlington, MA, USA).

3.2. Experimental

3.2.1. Dissolution media and drug substances

Sodium phosphate buffer pH 7.0 ± 0.1 (65.5 mM) and ammonium acetate buffer pH 6.8 ± 0.3 (10 mM) had the ionic strengths of 150 mM and 10 mM respectively. These buffers were prepared by dissolving 3.21 g NaH₂PO₄·H₂O and 7.52 g Na₂HPO₄·2H₂O in 1000 mL Milli-Q[®] water and 0.757 g NH₄Ac in 1000 mL Milli-Q[®] water. The pK_a-values used for phosphoric acid are 1.89, 6.67, and 11.68 (I = 0.165 M, 25.0°C) (42), for ammonium 9.20 and for acetic acid 4.53 (both at I = 0.15 M) (43). The drug substances used in this study were from all of the classes in the BCS, and is an assortment of bases, acids, ampholytes and aprotic compounds. The structures of the substances and their pK_a-values are shown in Table 1. The pK_a-value from reference (44) was determined by using the Sirius PCA100 instrument, while the pK_a-

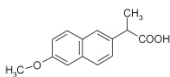
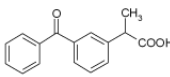
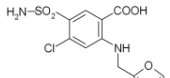
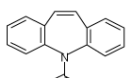
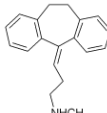
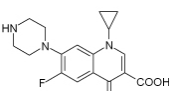
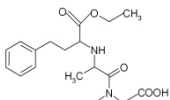
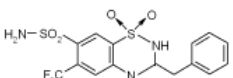
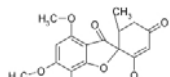
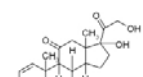
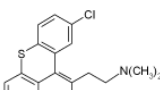
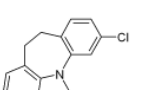
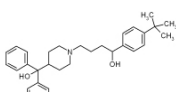
values from reference (45) were determined by using the Sirius GLpKa instrument.

3.2.2. Stability study of the drug solutions

For the stability and solubility (section 1.2.3) determinations microtubes MCT-200-C homo-polymer (2.0 mL) from Axygen scientific (Union City, CA, USA), a horizontal shaker from KABI AB (Stockholm, Sweden) and Spectrafuge 16M microcentrifuge from Labnet International Inc. (Woodbridge, NJ, USA) were used. The pH monitoring was carried out using a pH Meter 744, Metrohm (Herisau, Switzerland) with electrode CMAW711 (Ø 4.5 mm) from Thermo Russell (Auchtermuchty Fife, Scotland).

Two different concentrations of the substances in phosphate buffer were used in the stability study. One was made by using saturated solutions of the drug substances in room temperature with the shake-flask methodology. The other concentration was approximately 15 μM, stored at different temperatures. In the saturated solutions each drug substance was added in excess (2-50 mg) to 1.5 mL of the phosphate buffer. The drug-buffer suspensions were shaken

Table 1. Structures and pK_a-values of the drug substances (N/A = not applicable)

Substance name [salt form] pK _a	Structure (not salt)	Substance name [salt form] pK _a	Structure (not salt)
Naproxen 4.18 (16)		Ketoprofen 3.95 (45)	
Furosemide 3.52 (16)		Carbamazepine N/A (46)	
Nortriptyline [HCl] 10.21 (18)		Ciprofloxacin 6.20 8.59 (47)	
Enalapril [maleate] 2.99 5.39 (45)		Bendroflumethiazide 8.77 (48)	
Griseofulvin N/A (49)		Prednisone N/A (50)	
Chlorprotixene [HCl] 8.80 (51)		Clomipramine [HCl] 8.83 (44)	
Terfenadine 9.25 (50)			

at room temperature ($21.0 \pm 1.5^\circ\text{C}$) for up to seven days, including the centrifugation at 14000 rpm for 10 min to find an optimal shake-time. The end of the experiments was chosen so that two following analyses of the supernatant gave the response (chromatographic peak area), $\pm 15\%$, and pH value, ± 0.15 . Four samples of each drug substance were analyzed in duplicate at each time-point. Each drug substance of $15 \mu\text{M}$ were measured for eventual concentration changes at different time intervals at room temperature ($21.0 \pm 1.5^\circ\text{C}$), in refrigerator ($+4^\circ\text{C}$) and in freezer (-20°C). The acceptance criterion was set to $\geq 85\%$ of the initial drug substance concentration (at μM range) in room temperature.

3.2.3. Apparent solubility determination by shake-flask methodology

Each drug was added in excess (2-50 mg) to 1.5 mL of dissolution media, phosphate or ammonium acetate buffer, and was shaken at room temperature ($21.0 \pm 1.5^\circ\text{C}$) for 24 h. Centrifugation was used in separating the excess of substance from the dissolution medium after the defined shake-time. This was made instead of filtration to avoid problems with adsorption to filters, which had been noticed during initial dissolution studies of some of the substances. The pH was always measured before a substance was added into the buffer and after reaching the end of the study, but pH was not adjusted afterwards. The supernatant was diluted 600 times in mobile phase before HPLC analysis due to high absorbance and to avoid precipitation. Three samples of each drug substance were made for the shake-flask study. Double injections of each analyte were used for the apparent solubility determination and the average values with the relative standard deviations (RSD) were calculated.

3.2.4. In vitro dissolution rate studies

The conventional dissolution bath was a Dissolutest, Prolabo (Paris, France) and the thermometer a Testo 110 from Testo Inc. (Lenzkirch, Germany). The newly designed miniaturized equipment has been described previously (29). The disk in the miniaturized apparatus had a diameter of 1.5 mm. A magnetic stirrer with graded rotating speeds was obtained from Heidolph MR 3001K (Steinheim, Germany). The cell of Plexiglas was integrated with a HPLC (high-performance liquid chromatography) system using DAD (diode array detector) for analysis, see Figure 1. An external HPLC pump was connected to the cell for the distribution of dissolution medium, which was deairedated. The flow into the chamber of Plexiglas was always 1.0 mL/min (29). For the traditional rotating disk experiments a manual laboratory press from Perkin-Elmer (Waltham, MA, USA) with a stainless steel rotating disk die

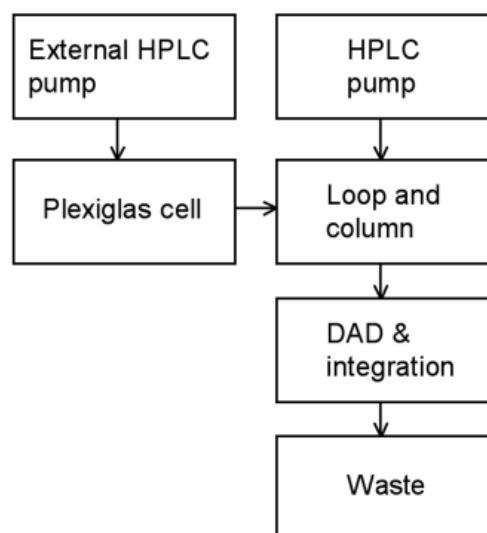


Figure 1. The setup for the miniaturized apparatus when measuring the *in vitro* dissolution rate, G. The sampling loop was positioned in the switching valve.

($\varnothing 8$ mm disk) similar to that proposed by Wood (52) was used. The making of the traditional, 195 MPa, and miniaturized, 182 MPa, disks were according to the previously described method in (29). Three disks in total of each drug substance were used in all experiments. The miniaturized disks of ciprofloxacin were always pre-wetted in the dissolution medium to remove any crust of substance above the disk surface that occurred by swelling. This was done to diminish the risk of breaking the Plexiglas cell due to obstruction of the peek tubing cf. (29). The effect on the dissolution rate value due to this pre-wetting of the ciprofloxacin disk was found to be negligible since the first run always was discarded during analysis to eliminate substance debris not firmly attached to the magnetic bar after compression. The magnetic bar with the attached ciprofloxacin disk was immediately placed in the cell after pre-wetting and the dissolution rate study was started.

For the traditional rotating disk equipment rotation speeds of 25 rpm, 50 rpm, 100 rpm and 150 rpm were used, whereas 100 rpm, 300 rpm, 500 rpm and 1000 rpm were applied for the miniaturized apparatus. When studying the correlation of $\log G$, and $\log S$, for all thirteen drug substances in the phosphate buffer, 300 rpm were used in the miniaturized apparatus. In order to improve the rotation robustness of the magnetic bar in the dissolution cell (with the flow of medium over the disk), 300 rpm was found to give more repeatable dissolution rate values compared to 100 rpm. The Plexiglas cell in this work was a newly constructed one and not the same as used in the previously study by (29), but with identical design and dimensions.

The chromatography was performed on an Agilent 1100 Series HPLC system with a binary pump, degasser, autosampler and DAD, Agilent Technologies Inc. (Palo Alto, CA, USA). A six-position switching valve with

a 20 μL stainless steel loop attached to it was also purchased from Agilent Technologies Inc. The analysis by HPLC was described earlier in (29). The mobile phases were prepared so that the retention factor, k , was between 2.5 and 6.5. No analysis was longer than two min, which gives a total run time of less than three min. The analytical column was a Zorbax SB-C8 (2.1×50 mm, $5 \mu\text{m}$) from Agilent Technologies Inc. The temperature of the column compartment was measured to $25\text{-}28^\circ\text{C}$ and was constant within approximately 2°C in one experiment. The dissolution media were used at room temperature ($21.0 \pm 1.5^\circ\text{C}$). The external HPLC-pump was a Jasco PU-1585, Jasco Inc. (Tokyo, Japan). The data were collected by ChemStation Rev.A.10.02 from Hewlett Packard, Agilent Technologies Inc. A schematic view of the experimental setup can be found in Figure 1.

The system suitability criterion for the chromatographic system was set to a precision within 1% in retention time and area of the main peak. This was tested by injecting a standard solution ($n = 6$) with a concentration equivalent to the middle concentration in the standard curve.

4. Results and Discussion

4.1. Stability of drug substances and shake-time determination

The stability of the drug substances ($15 \mu\text{M}$) was studied in different temperatures to optimize the shake-time and to confirm the repeatability of the solubility values, according to Figure 2. Shake-flask samples were also analyzed, but only in room temperature (see section 2.2 below).

As observed, 24 h can be used as shake-time in the phosphate buffer without noteworthy degradation of the drug substances at room temperature (ciprofloxacin at micro molar level is shown as an example in Figure 2). The percent remaining of the initial concentration was between 87% and 101% for all of the substances at room temperature at a maximum of 24 h, fulfilling the criterion set for stability.

The spectra in the diode array chromatograms during the stability study were investigated for extra

peaks eluting prior to the main peak that could be related to degradation products. The spectrum of the main substance peak from an injected sample was also compared to the spectrum of the main peak from an injection of a newly prepared solution to confirm that no noteworthy chemical alterations had occurred. No changes of the main peak spectrum could be seen, thus it was assumed that the drug substance was stable during the study according to the set criterion, *i.e.* $\pm 15\%$ in response area. Only a few small extra peaks could be detected in the chromatograms for some of the substances.

4.2. Determination of apparent solubility using the shake-flask methodology

The shake-flask studies were ended after 24 h, determined by the criterion set for degradation as discussed in section 2.1. The response peak areas were compared at each time-point to compare the percent remaining of the initial substance amount. The solubility of ciprofloxacin in the phosphate buffer at different shake times is presented in Figure 3. No difference in solubility was observed from 5 h to 2 days, whereas the degradation study showed a decreased stability beyond 24 h (Figure 2). Thus, 24 h was set as the shake-flask time in the determinations of the solubility.

The solubility results from the shake-flask experiments are summarized in Table 2. Six drug substances were tested in both ammonium acetate and phosphate buffer and further seven substances were tested in the phosphate buffer. The phosphate buffer had the best buffer capacity (β) (53), see Table 2, and it is also the buffer recommended as USP buffer by FIP. Acetate has been used to simulate fed state intestinal fluid (FeSSIF), while phosphate has been used in the fasted state simulated intestinal fluid (FaSSIF) (54) and acetate may have different impact on solubility of certain substances (55). ΔpH is the change in pH before addition of drug substance in the medium to the stop at 24 h in the shake-flask study.

As expected, the phosphate buffer showed the best buffer capacity at the chosen pH of approximately 7 since ΔpH in this study is consistently lower compared to in

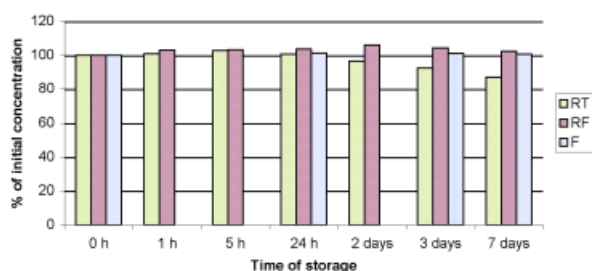


Figure 2. The stability study of ciprofloxacin (μM) in phosphate buffer. Stored at room temperature, RT, ($21.0 \pm 1.5^\circ\text{C}$), refrigerator, RF, ($+4^\circ\text{C}$) and freezer, F, (-20°C).

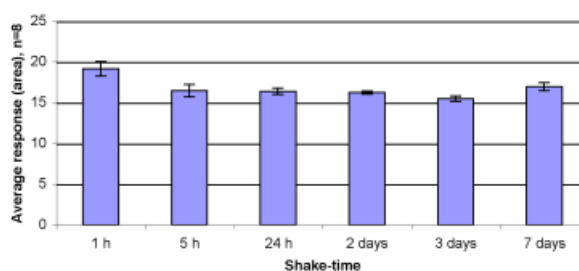


Figure 3. Determination of the shake-time of ciprofloxacin. The dissolution medium was phosphate buffer pH 7.0 at room temperature ($21.0 \pm 1.5^\circ\text{C}$). The main bars are the average area responses of four different samples using double injections ($n = 8$) at each time-point. The error bars show the standard deviation.

Table 2. The apparent solubility, S , measured after 24 h at room temperature ($21.0 \pm 1.5^\circ\text{C}$). S , is the average of eight values (four samples with double injections). RSD = relative standard deviation ($n = 8$). pH is the value after defined shake-time, 24 h, and ΔpH is the change in pH before addition of drug substance in the medium to the stop at 24 h. N/A = not applicable

Substance	Phosphate buffer pH 7.0 ± 0.1 ($\beta = 0.0328$ M)				Ammonium acetate buffer pH 6.8 ± 0.3 ($\beta = 0.00021$ M)			
	S (mM)	RSD (%)	pH 24 h	ΔpH	S (mM)	RSD (%)	pH 24 h	ΔpH
Naproxen	17	0.30	6.73	-0.41	1.6	7.5	5.30	-1.16
Ketoprofen	35	1.8	6.08	-1.02	4.5	3.9	4.80	-1.72
Furosemide	21	5.4	6.61	-0.53	1.6	1.8	5.24	-1.28
Carbamazepine	0.74	3.6	7.14	± 0.00	0.79	3.2	6.40	-0.12
Nortriptyline HCl	2.8	11	7.10	-0.04	54	7.5	6.13	-0.42
Ciprofloxacin	0.22	9.2	7.16	+0.02	0.23	6.7	6.60	-0.13
Enalapril maleate	74	1.5	3.35	-3.75				
Bendroflumethiazide	0.34	5.2	7.15	+0.01				
Griseofulvin	0.13	4.5	7.14	+0.02				
Prednisone	0.76	16	7.10	+0.02				
Chlorprotixene HCl	0.92	32	6.80	-0.32			N/A	
Clomipramine HCl	2.4	2.2	7.10	-0.02				
Terfenadine	0.019	16	7.13	+0.05				

the ammonium acetate buffer. A significant difference in pH is achieved for enalapril maleate, which had a high solubility in the phosphate buffer. This high solubility significantly decreases the pH of the medium. A large excess was needed to reach equilibrium solubility, *i.e.* to maintain the excess of the drug substance throughout the experiment (24 h and beyond). The concentration of enalapril and maleate after 24 h is higher than the buffer capacity of the phosphate buffer. Since the lower acidic pK_a -value of enalapril is 2.99 and the pK_a -value of the protonated carboxylic group of maleate is 5.72 (45), this will generate the drastic decrease in pH as can be seen in Table 2. A noticeable decrease in pH is also observed for ketoprofen. The solubility of ketoprofen is 34.8 mM in the phosphate buffer, which is somewhat higher than the buffer capacity of the buffer. The acidic pK_a -value of 3.95 combined with the high concentration of ketoprofen will decrease the pH in the medium.

The apparent solubility, S , of the three monoprotic acids, *i.e.* naproxen, ketoprofen and furosemide, is approximately ten times lower in the ammonium acetate buffer compared to S in the phosphate buffer. From Table 2 it can be concluded that the ammonium acetate buffer has a much lower buffer capacity at a pH around 7. Thus a much larger decrease in pH after 24 h was found in the ammonium acetate buffer compared to in the phosphate buffer. By using Eq. 1 the solubility, S , can be calculated to be ten times lower when pH is decreased one unit provided that the ionic strength is constant.

4.3. Dissolution rate determination with two types of rotating disk apparatuses

Previous publications correlated the pH when determining the apparent solubility to the pH in the diffusion layer of a substance that dissolves in a dissolution medium (30,56-59). It can be assumed that pH of the medium in equilibrium with a solid drug, *i.e.*

pH of a saturated solution, is an approximation of pH in the diffusion layer. This assumption was also used in this study, and no adjustment of pH was therefore made after the final shake-time of 24 h.

The average *in vitro* dissolution rates, G , for the six substances in the two buffers are presented in Table 3. for the traditional rotating disk studies and in Table 4 for the miniaturized rotating disk experiments. Four different rotation speeds were used for both apparatuses, 25-150 rpm for the traditional setup and 100-1000 rpm for the miniaturized setup. The RSD for the dissolution rate values in the studies were lower than 20% for all of the drug substances.

As has been found previously (29) a relative consistent ratio is found when dividing the dissolution rate values for the phosphate buffer with the values for the ammonium acetate buffer at the respective rotation speeds. The consistency of these ratios indicates that similar results of the two in-house constructed Plexiglas cells were achieved.

The high dissolution rate of nortriptyline HCl in both buffers is assumed to be a result of that the base is formulated as a salt. A difference between free bases or acids and their respective salt forms has been discussed by *e.g.* (11,12). The functional groups of drug substances might have different interactions with different buffer species (9,60,61). This may be seen for *e.g.* the drug substances containing weak carboxylic acids in Table 3 and 4. Problems associated with swelling of the disks of ciprofloxacin, *cf.* (29), were minimized by pre-wetting prior the miniaturized rotating disk study but this substance was still difficult to handle. In the traditional rotating disk equipment no extra preparation of the ciprofloxacin disk was performed preceding the dissolution rate study. The dissolution rate in the ammonium acetate buffer showed no clear trend at higher rotation speeds. The disks swelled in this apparatus as well and maybe this may explain the deviating trend of the influence of a change in flow pattern nearby the disk surface and the adjacent diffusion layer.

Table 3. Average *in vitro* dissolution rates, *G*, (*n* = 3). Six drug substances dissolved in two different buffer media using a traditional rotating disk apparatus

		Naproxen	Ketoprofen	Furosemide	Carbamazepine	Nortriptyline HCl	Ciprofloxacin
Phosphate buffer pH 7.0	G ₂₅ (μg/s/cm ²)	2.7	6.7	4.5	0.26	24	0.042
	G ₅₀ (μg/s/cm ²)	3.6	9.0	5.4	0.29	26	0.053
	G ₁₀₀ (μg/s/cm ²)	5.4	12	8.4	0.35	31	0.081
	G ₁₅₀ (μg/s/cm ²)	6.1	15	9.1	0.44	40	0.15
Ammonium acetate buffer pH 6.8	G ₂₅ (μg/s/cm ²)	0.27	0.76	0.39	0.27	17	0.038
	G ₅₀ (μg/s/cm ²)	0.35	1.1	0.62	0.35	22	0.039
	G ₁₀₀ (μg/s/cm ²)	0.48	1.4	0.83	0.48	30	0.080
	G ₁₅₀ (μg/s/cm ²)	0.59	1.7	0.86	0.49	35	0.080

Table 4. Average *in vitro* dissolution rates, *G*, (*n* = 3). Six drug substances dissolved in two different buffer media using the miniaturized rotating disk apparatus

		Naproxen	Ketoprofen	Furosemide	Carbamazepine	Nortriptyline HCl	Ciprofloxacin
Phosphate buffer pH 7.0	G ₁₀₀ (μg/s/cm ²)	16	34	22	1.3	81	0.49
	G ₃₀₀ (μg/s/cm ²)	21	40	26	1.8	106	0.63
	G ₅₀₀ (μg/s/cm ²)	22	51	40	2.6	140	0.92
	G ₁₀₀₀ (μg/s/cm ²)	29	71	50	4.6	218	1.8
Ammonium acetate buffer pH 6.8	G ₁₀₀ (μg/s/cm ²)	1.9	4.8	2.3	1.4	72	1.2
	G ₃₀₀ (μg/s/cm ²)	2.5	6.0	3.2	1.8	95	1.7
	G ₅₀₀ (μg/s/cm ²)	2.9	7.6	4.1	2.6	139	4.8
	G ₁₀₀₀ (μg/s/cm ²)	3.7	11	5.4	4.9	211	11

4.4. Correlation of *in vitro* dissolution rate and apparent solubility

To compare the new miniaturized rotating disk apparatus with traditional rotating disk equipment, six drug substances were tested in ammonium acetate and a phosphate buffer at four different rotation speeds, see Tables 3 and 4. The correlation of the logarithmic values of the *in vitro* dissolution rate, *G*, and the apparent solubility, *S*, (from Table 2) for both buffer media are presented in Figures 4 A-B and 5 A-B respectively. Triplicates of log*G* are shown in the figures, while average values are used for log*S*. The correlation of dissolution rate and solubility will for most substances be done in a pH interval of roughly 6.1 to 7.1 in the phosphate buffer and in the region of 4.8 to 6.8 in the ammonium acetate buffer, cf. Table 2.

The hydrochloride salt of nortriptyline is deviating from the more linear correlation pattern in the phosphate buffer for both rotating disk systems used. This can possibly be related to the fact that this is the only drug substance formulated as a salt during this study. The dissolution rates are found to be similar in the buffers, while the solubility is about twenty times higher in the ammonium acetate buffer compared to the phosphate buffer. This difference can partly be explained by the pH difference in the two buffers, which should result in a ten times higher solubility (cf. Eq. 2). Since the visual pattern of the correlations presented in Figures 4 and 5 are similar comparing the traditional and newly designed rotating disk equipments, only the miniaturized apparatus was used for further correlation studies in the phosphate buffer.

The correlation for all thirteen drug substances in the

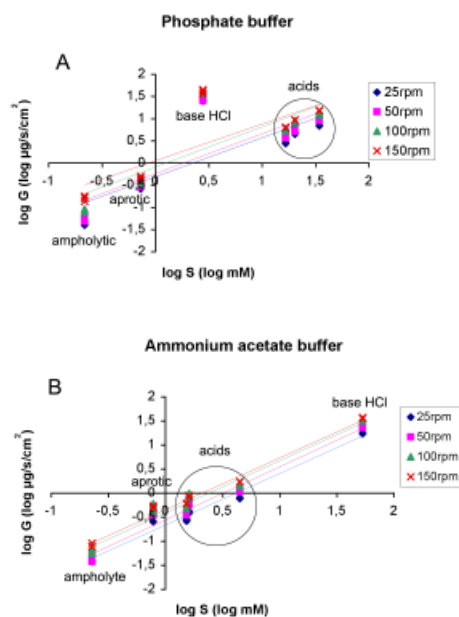


Figure 4. The correlation of the logarithmic average values of dissolution rate, *G*, and solubility, *S*, using the miniaturized rotating disk apparatus. The study was performed at 300 rpm (flow 1.0 mL/min) in phosphate buffer at the initial pH of 7.0 ± 0.1 at room temperature (21.0 ± 1.5°C) for thirteen different drug substances.

phosphate buffer (pH 7.0) at 300 rpm is shown in Figure 4. A good correlation (R^2 of 0.982, dashed line with the equation written in italic) was observed, provided that the substances formulated as hydrochloride salts were excluded from the series. All basic substances formulated as salts were found to depart from the more linear regression of the other substances tested. However, the free base terfenadine with a pK_a -value similar to chlomipramine is not deviating from the linear trend in Figure 6. Interestingly it seems that a linear correlation

is possible to achieve even though an assortment of different BCS substances are used in the correlation of *in vitro* dissolution rates and apparent solubility in aqueous buffer media. The ammonium acetate buffer gave a better correlation of the logarithmic dissolution rate and solubility values for the hydrochloride salt

of nortriptyline, compared to the correlation found in the phosphate buffer. An optimization of the buffer composition might improve the possibility to obtaining a good correlation of dissolution rate and solubility for more substances, *e.g.* in early screening of solubility of drug candidates.

5. Comparison of the throughput for the two apparatuses

The applicability of the new miniaturized equipment is focused on low consumption of substance and dissolution media, while giving sufficient accurate values for screening studies of solubility in early drug development. The miniaturized equipment is also easy to use and it is straightforward to shift media during the experiments. The throughput of analyses for the two rotating disk apparatuses was compared during the dissolution rate studies, Table 5. Manual sampling was used in the traditional rotating disk determinations according to the previously described method (29).

By using the miniaturized equipment savings can be done in analysis time, amount of drug substances as well as dissolution media. If only one disk should be screened in one buffer using the miniaturized methodology, approximately 10 min is needed from making of the disk to finishing the chromatographic analysis. To speed up the screening further, more development work must be performed concerning the disk making. The reduction in volume of the dissolution medium can further be optimized by decreasing the void volume of the chromatographic system and by decreasing the total chromatographic analysis time (retention volume). This can *e.g.* be achieved by using ultra performance liquid chromatography (UPLC) or further miniaturization of the cell of Plexiglas.

6. Conclusions

The miniaturized apparatus for the *in vitro* dissolution rate is rapid compared to the traditional rotating disk method. Smaller amounts of samples and dissolution media are consumed by using the miniaturized system. The two rotating disk instruments were found to give similar logarithmic correlations of the *in vitro* dissolution rate versus the apparent solubility, as well as precision in the determinations. Consequently, the extended study of the correlation was only performed using the miniaturized apparatus. The logarithmic correlation of the

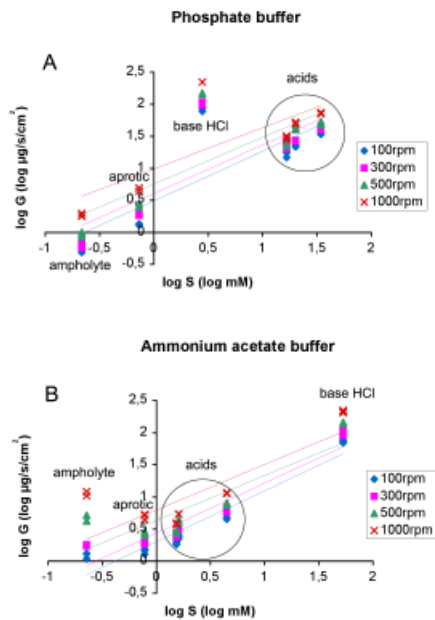


Figure 5. The correlation of the logarithmic values of the *in vitro* dissolution rate, *G*, and the solubility, *S*, using the miniaturized rotating disk apparatus. Four different rotation speeds and two dissolution media A. phosphate buffer pH 7.0 ± 0.1 and B. ammonium acetate buffer pH 6.8 ± 0.3 both at room temperature (21.0 ± 1.5°C).

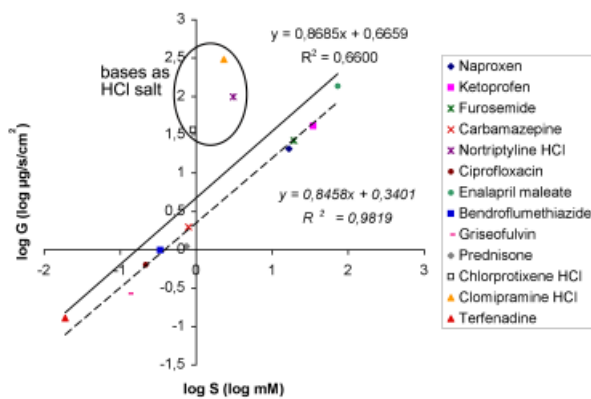


Figure 6. The correlation of the logarithmic average values of dissolution rate, *G*, and solubility, *S*, using the miniaturized rotating disk apparatus. The study was performed at 300 rpm (flow 1.0 mL/min) in phosphate buffer at the initial pH of 7.0 ± 0.1 at room temperature (21.0 ± 1.5°C) for thirteen different drug substances.

Table 5. Performance of the new miniaturized rotating disk equipment and the traditional rotating disk apparatus (using manual sampling)

Rotating disk apparatus	Total time for three disks at four different rotation speeds in both buffer systems per drug substance	Approximately amount of drug substance per disk	Approximately volume of dissolution medium per disk
Miniaturized	2 days	5 mg	35 mL
Traditional	8 days	100 mg	500 mL

dissolution rate and the solubility for ten drug substances in the phosphate buffer became as good as $R^2 = 0.982$, if the three substances formulated as hydrochloride salts were excluded. Interestingly, it seems that the correlation of dissolution rate and solubility for the hydrochloride salt of nortriptyline is not deviating from other drug substances in the ammonium acetate buffer. This correlation might be of interest to investigate, especially if the discrepancy is valid for other media and other salts formulations than hydrochlorides. A linear correlation by the use of an optimized medium for all types of substances might accordingly be used to estimate the apparent solubility from the *in vitro* dissolution rate in early screening.

Acknowledgements

We would like to thank Walter Lindberg, AstraZeneca Mölndal, Sweden, for lending us the miniaturized equipment for the dissolution rate studies as well as Anders AS. Karlsson and Anders S. Carlsson at AstraZeneca Mölndal, Sweden for providing some of the drug substances used in this study. Elisabeth Gäfvert, Biovitrum Stockholm, Sweden is also thanked for performing the GLpKa-measurements of the pK_a -values for ketoprofen and enalapril maleate. Special thanks to the Swedish Academy of Pharmaceutical Sciences which financed participation at the 2nd BBBB conference on Pharmaceutical Sciences in Tallinn/Tartu, Estonia, 2007, with a grant from "APS resestipendie".

References

- Panchagnula R, Thomas NS. Biopharmaceutics and pharmacokinetics in drug research. *Int J Pharm.* 2000; 201:131-150.
- Bolger MB, Fraczekiewicz R, Entzeroth M, Steere B. Exploiting Chemical Diversity for Drug Discovery. *Exploiting Chemical Diversity for Drug Discovery*, Royal Society of Chemistry, Cambridge, UK, 2006; pp. 343-348.
- Nicklasson M, Brodin A, Nyqvist H. Studies on the relationship between solubility and intrinsic rate of dissolution as a function of pH. *Acta Pharm Suec.* 1981; 18:119-128.
- Hamlin WE, Northam JI, Wagner JG. Relationship between *in vitro* dissolution rates and solubilities of numerous compounds representative of various chemical species. *J Pharm Sci.* 1965; 54:1651-1653.
- Shah AC, Nelson KG. Evaluation of a convective diffusion drug dissolution rate model. *J Pharm Sci.* 1975; 64:1518-1520.
- Nelson KG, Shah AC. Convective diffusion model for a transport-controlled dissolution rate process. *J Pharm Sci.* 1975; 64:610-614.
- McNamara DP, Amidon GL. Reaction plane approach for estimating the effects of buffers on the dissolution rate of acidic drugs. *J Pharm Sci.* 1988; 77:511-517.
- Ramtoola Z, Corrigan OI. Influence of the buffering capacity of the medium on the dissolution of drug-excipient mixtures. *Drug Dev Ind Pharm.* 1989; 15:2359-2374.
- Aunins JG, Southard MZ, Myers RA, Himmelstein KJ, Stella VJ. Dissolution of carboxylic acids. III: The effect of polyionizable buffers. *J Pharm Sci.* 1985; 74:1305-1316.
- Mooney KG, Mintun MA, Himmelstein KJ, Stella VJ. Dissolution kinetics of carboxylic acids II: effect of buffers. *J Pharm Sci.* 1981; 70:22-32.
- Berge SM, Bighley LD, Monkhouse DC. Pharmaceutical salts. *J Pharm Sci.* 1977; 66:1-19.
- Anderson BD, Conradi RA. Predictive relationships in the water solubility of salts of a nonsteroidal anti-inflammatory drug. *J Pharm Sci.* 1985; 74:815-820.
- Avdeef A. Physicochemical profiling (solubility, permeability and charge state). *Curr Top Med Chem.* 2001; 1:277-351.
- Yalkowsky SH, Banerjee S. *Aqueous Solubility (Methods of estimation for organic compounds)*. MARCEL DEKKER, INC. New York, USA 1992.
- Glomme A, Marz J, Dressman JB. Comparison of a miniaturized shake-flask solubility method with automated potentiometric acid/base titrations and calculated solubilities. *J Pharm Sci.* 2005; 94:1-16.
- Avdeef A, Berger CM, Brownell C. pH-metric solubility. 2: correlation between the acid-base titration and the saturation shake-flask solubility-pH methods. *Pharm Res.* 2000; 17:85-89.
- Stuart M, Box K. Chasing equilibrium: measuring the intrinsic solubility of weak acids and bases. *Anal Chem.* 2005; 77:983-890.
- Box KJ, Volgyi G, Baka E, Stuart M, Takacs-Novak K, Comer JE. Equilibrium versus kinetic measurements of aqueous solubility, and the ability of compounds to supersaturate in solution-a validation study. *J Pharm Sci.* 2006; 95:1298-1307.
- Chen XQ, Venkatesh S. Miniature device for aqueous and non-aqueous solubility measurements during drug discovery. *Pharm Res.* 2004; 21:1758-1761.
- Serajuddin ATM, Mufson D. pH-solubility profiles of organic bases and their hydrochloride salts. *Pharm Res.* 1985; 2:65-68.
- Fini A, Fazio G, Feroci G. Solubility and solubilization properties of non-steroidal anti-inflammatory drugs. *Int J Pharm.* 1995; 126:95-102.
- Serajuddin AT, Sheen PC, Augustine MA. Common ion effect on solubility and dissolution rate of the sodium salt of an organic acid. *J Pharm Pharmacol.* 1987; 39:587-591.
- Grijseels H, Crommelin DJA, De Blaeij CJ. Hydrodynamic approach to dissolution rate. *Pharm Weekbl Sci Ed.* 1981; 3.
- Southard MZ, Green DW, Stella VJ, Himmelstein KJ. Dissolution of ionizable drugs into unbuffered solution: a comprehensive model for mass transport and reaction in the rotating disk geometry. *Pharm Res.* 1992; 9:58-69.
- USP. *Intrinsic dissolution*. U.S. Pharmacopeia National Formulary. 2006; 29(chapter 1087):2923-2924.
- Sun W, Larive CK, Southard MZ. A mechanistic study of danazol dissolution in ionic surfactant solutions. *J Pharm Sci.* 2003; 92:424-435.
- Peltonen L, Liljeroth P, Heikkilä T, Kontturi K, Hirvonen J. Dissolution testing of acetylsalicylic acid by a channel flow method-correlation to USP basket and intrinsic dissolution methods. *Eur J Pharm Sci.* 2003; 19:395-401.

28. Terada K, Kitano H, Yoshihashi Y, Yonemochi E. Quantitative correlation between initial dissolution rate and heat of solution of drug. *Pharm Res.* 2000; 17:920-924.
29. Persson AM, Baumann K, Sundelof LO, Lindberg W, Sokolowski A, Pettersson C. Design and characterization of a new miniaturized rotating disk equipment for *in vitro* dissolution rate studies. *J Pharm Sci.* 2008; 97:3344-3355.
30. Avdeef A, Tsinman O. Miniaturized rotating disk intrinsic dissolution rate measurement: effects of buffer capacity in comparisons to traditional wood's apparatus. *Pharm Res.* 2008; 25:2613-2627.
31. Berger CM, Tsinman O, Voloboy D, Lipp D, Stones S, Avdeef A. Technical note: miniaturized intrinsic dissolution rate (Mini-IDR™) measurement of griseofulvin and carbamazepine. *Dissolut Technol.* 2007; 14:39-41.
32. Dressman JB, Amidon GL, Reppas C, Shah VP. Dissolution testing as a prognostic tool for oral drug absorption: immediate release dosage forms. *Pharm Res.* 1998; 15:11-22.
33. Zhao YH, Abraham MH, Le J, Hersey A, Luscombe CN, Beck G, Sherborne B, Cooper I. Rate-limited steps of human oral absorption and QSAR studies. *Pharm Res.* 2002; 19:1446-1457.
34. Aiache JM, Aoyagi N, Blume H, Dressman JB, Friedel HD, Grady LT. FIP Guidelines for dissolution testing of solid oral products. *Dissolut Technol.* 1997; 4:5-14.
35. Corrigan OI, Devlin Y, Butler J. Influence of dissolution medium buffer composition on ketoprofen release from ER products and *in vitro-in vivo* correlation. *Int J Pharm.* 2003; 254:147-154.
36. Sirius. Applications and Theory Guide to pH-metric pK_a and logP Determination. Sirius Analytical Instruments Ltd. UK 1993.
37. Butler JN. Ionic Equilibrium (Solubility and pH Calculations). John Wiley & Sons, Inc. New York, USA 1998; pp. 202-237.
38. Avdeef A. High-throughput measurements of solubility profiles. *Pharmacokinetic optimization in drug research*, Verlag Helvetica Chimica Acta and WileyVCH, Zürich and Weinheim, 2001; pp. 305-325.
39. Schill G. Photometric determination of amines and quaternary ammonium compounds with bromthymol blue, Part 5. Determination of dissociation constants of amines. *Acta Pharm Suec.* 1965; 2:99-108.
40. Krebs HA, Speakman JC. Dissociation constant, solubility, and the pH value of the solvent. *J Chem Soc.* 1945; 593-595.
41. Wagner JG. *Biopharmaceutics* 18. Rate of dissolution part III. Methods of measuring and interpreting *in vitro* rates. *Drug Intell and Clin Pharm.* 1970; 4:77-82.
42. Sirius. Sirius Technical Applications Notes (STAN). Sirius Analytical Instruments Ltd., (UK) 1994; pp. 1.
43. Sirius. RefinementPro2 Sirius Analytical Instruments Ltd., (UK).
44. Sokolowski A. AS Consulting, Uppsala, Sweden. 2007.
45. Gäfvert E. Biovitrum, Stockholm, Sweden. Personal communication 2007.
46. Yu LX, Carlin AS, Amidon GL, Hussain AS. Feasibility studies of utilizing disk intrinsic dissolution rate to classify drugs. *Int J Pharm.* 2004; 270:221-227.
47. Escribano E, Calpena AC, Garrigues TM, Freixas J, Domenech J, Moreno J. Structure-absorption relationships of a series of 6-fluoroquinolones. *Antimicrob Agents Chemother.* 1997; 41:1996-2000.
48. Zhou C, Jin Y, Kenseth JR, Stella M, Wehmeyer KR, Heineman WR. Rapid pK_a estimation using vacuum-assisted multiplexed capillary electrophoresis (VAMCE) with ultraviolet detection. *J Pharm Sci.* 2005; 94:576-589.
49. Bergstrom CA, Norinder U, Luthman K, Artursson P. Experimental and computational screening models for prediction of aqueous drug solubility. *Pharm Res.* 2002; 19:182-188.
50. Sköld C, Winiwarter S, Wernevik J, Bergström F, Engström L, Allen R, Box K, Comer J, Mole J, Hallberg A, Lennernäs H, Lundstedt T, Ungell AL, Karlén A. Presentation of a structurally diverse and commercially available drug data set for correlation and benchmarking studies. *J Med Chem.* 2006; 49:6660-6671.
51. Wiczling P, Kawczak P, Nasal A, Kaliszczan R. Simultaneous determination of pK_a and lipophilicity by gradient RP HPLC. *Anal Chem.* 2006; 78:239-249.
52. Wood J, Syarto J, Letterman H. Improved holder for intrinsic dissolution rate studies. *J Pharm Sci.* 1965; 54:1068.
53. Van Slyke DD. On the measurement of buffer values and on the relationship of buffer value to the dissociation constant of the buffer and the concentration and reaction of the buffer solution. *J Biol Chem.* 1922; 52:525-570.
54. Galia E, Nicolaides E, Horter D, Lobenberg R, Reppas C, Dressman JB. Evaluation of various dissolution media for predicting *in vivo* performance of class I and II drugs. *Pharm Res.* 1998; 15:698-705.
55. Wagner D, Glube N, Berntsen N, Tremel W, Langguth P. Different dissolution media lead to different crystal structures of talinolol with impact on its dissolution and solubility. *Drug Dev Ind Pharm.* 2003; 29:891-902.
56. Serajuddin AT, Jarowski CI. Effect of diffusion layer pH and solubility on the dissolution rate of pharmaceutical acids and their sodium salts. II: Salicylic acid, theophylline, and benzoic acid. *J Pharm Sci.* 1985; 74:148-154.
57. Serajuddin AT, Jarowski CI. Effect of diffusion layer pH and solubility on the dissolution rate of pharmaceutical bases and their hydrochloride salts. I: Phenazopyridine. *J Pharm Sci.* 1985; 74:142-147.
58. Li S, Wong S, Sethia S, Almoazen H, Joshi YM, Serajuddin AT. Investigation of solubility and dissolution of a free base and two different salt forms as a function of pH. *Pharm Res.* 2005; 22:628-635.
59. Pudipeddi M, Zannou EA, Vasanthavada M, Dontabhaktuni A, Royce AE, Joshi YM, Serajuddin AT. Measurement of surface pH of pharmaceutical solids: a critical evaluation of indicator dye-sorption method and its comparison with slurry pH method. *J Pharm Sci.* 2008; 97:1831-1842.
60. Vertzoni M, Fotaki N, Kostewicz E, Stippler E, Leuner C, Nicolaides E, Dressman J, Reppas C. Dissolution media simulating the intraluminal composition of the small intestine: physiological issues and practical aspects. *J Pharm Pharmacol.* 2004; 56:453-462.
61. Levis KA, Lane ME, Corrigan OI. Effect of buffer media composition on the solubility and effective permeability coefficient of ibuprofen. *Int J Pharm.* 2003; 253:49-59.

(Received April 2, 2009; Accepted April 23, 2009)

Original Article**Correlation of *in vitro* dissolution rate and apparent solubility in buffered media using a miniaturized rotating disk equipment: Part II. Comparing different buffer media**Anita M. Persson^{1,*}, Curt Pettersson¹, Anders Sokolowski²¹ Division of Analytical Pharmaceutical Chemistry, Uppsala University, BMC, SE-751 23 Uppsala, Sweden;² AS Consulting, Hugo Alfvéns väg 26, SE-756 49 Uppsala, Sweden.

ABSTRACT: A correlation of the logarithmic values of the *in vitro* dissolution rate, *G*, and apparent solubility, *S*, was made for seven different drug substances from all of the classes in the Biopharmaceutics Classification System (BCS), in four different phosphate buffers. The effect of inorganic salts added as sodium chloride, sodium nitrate, sodium phosphate and sodium sulfate in the buffer media was investigated for the correlation. Triethanolammonium acetate buffer was also included in the study of the correlation of log*G* vs. log*S*. The pH was 7.0 ± 0.1 in all of the buffers to mimic a pH condition in intestinal fluids.

The dissolution rate was determined with a newly constructed miniaturized rotating disk equipment, which enables fast determinations and consumes only minute quantities of substance (about 5 mg). The solubility was determined by conventional shake-flask methodology, using 1.5 mL solution volumes. All quantifications were performed with reversed phase high-performance liquid chromatography (RP-HPLC) and diode array detection (DAD).

The different inorganic anions seemed to affect the solubility more than the dissolution rate. The phosphate and nitrate ions decreased the solubility for amines compared to the chloride ion. The best correlations of log*G* and log*S* were however obtained with a triethanolammonium acetate buffer. The good correlation ($R^2 = 0.991$) may be sufficient in initial screening of drug solubility, based on dissolution rates in aqueous buffer media.

Keywords: Dissolution rate, solubility, *in vitro* models, correlation, HPLC (high-performance liquid chromatography)

*Address correspondence to:

M.Sc. Anita M. Persson, Division of Analytical Pharmaceutical Chemistry, Uppsala University, BMC, SE-751 23 Uppsala, Sweden.

e-mail: anita.persson@farmkemi.uu.se

1. Introduction

The dissolution rate for a drug substance that goes into solution in the gastrointestinal (GI) tract is one of the important factors for systemic absorption of the drug using oral administration (1). This dissolution is a complex process and the factors affecting it can generally be divided into three sections (2,3). Physicochemical properties of the drug represent the first part *i.e.* p*K*_a, solubility, stability, diffusivity and lipophilicity. Physiological factors characterize the second part and include GI pH, gastric emptying, intestinal transit, GI blood flow, gut wall metabolism, active transport including drug efflux and other absorption mechanisms. Moreover surface tension, solubilisation, osmolality, viscosity, buffer capacity and the volume of the luminal content play a vital role for the dissolution (4,5). The third part comprises the formulation factors *e.g.* surface area and drug particle size, crystal form, salt formulation and type of dosage form. Kinetic factors concerning the drug dissolution as described by the Noyes-Whitney model (6-10) are dependent on the three parts stated above. The physiological factors will in addition vary with the position in the gastrointestinal tract, as well as by the ingestion of food (11).

It has been found that the ionic strength can affect drug solubility and dissolution (12-14). The so called common ion effect can also have an impact on dissolution and solubility for *e.g.* hydrochloride formulated weak bases in chloride containing solutions (15-17). The effect on solubility and dissolution rate of different added ions in the media have been investigated (16-19), however only few studies (13,20-22) were found to use anions as additives to a buffer as in this study.

The experimental medium composition is a key for obtaining a good *in vitro-in vivo* correlation (IVIVC), where drug solubility and permeability are principal parameters according to the Biopharmaceutics Classification System (BCS) (23). *In vitro* dissolution testing is used at several stages during the drug

development. Valuable information can thereby be achieved for the drug substance itself (by the rotating disk method) or for a certain formulation (by USP apparatuses), and for the selection of appropriate excipients in a formulation (24). The effect of buffer media composition on the *in vitro* solubility and dissolution have been studied extensively (25-28) and the type of buffer can have a pronounced effect on dissolution and solubility of a substance (13,29). The composition of biorelevant media are now based on maleate buffers (30), but phosphate buffer has traditionally been used in the fasted state simulated intestinal fluid (FaSSIF) and acetate buffer in the simulated fed state intestinal fluid (FeSSIF) (27).

In this study, based on the Noyes-Whitney equation, the correlation of the logarithmic values of the *in vitro* dissolution rate, G , and the apparent solubility, S , was evaluated. Seven different test substances and six different buffer media were used in the correlation studies. To be physiological relevant, a pH of 7 was chosen since this mimics a pH in intestinal fluids as well as gastric pH under some conditions (11). The triethanolammonium acetate buffer was chosen to obtain a high buffer capacity at pH 7.0 compared to ammonium acetate buffer, which has a very low buffer capacity at this pH (31). Different anions were added to a phosphate buffer in this study to investigate if this generates an effect on dissolution rate and/or solubility, at a constant ionic strength. The aim of the study was to evaluate the possibility to predict the solubility in different aqueous buffer media from the dissolution rate, determined by a miniaturized rotating disk equipment.

2. Materials and Methods

2.1. Chemicals

Naproxen met USP specifications, enalapril maleate, nortriptyline hydrochloride, chlorprotixene hydrochloride, clomipramine hydrochloride, prednisone, bendroflumethiazide and terfenadine were minimum 98%, carbamazepine 99%, sodium chloride (NaCl) minimum 99.5%, sodium nitrate (NaNO₃) minimum 99.0% di-sodium sulfate (Na₂SO₄) ACS Reagent Grade, all from Sigma-Aldrich (Chemie GmbH, Steinheim, Germany). Sodium dihydrogen phosphate monohydrate (NaH₂PO₄·H₂O) *p.a.*, Acros Organics (Springfield, NJ, USA), di-sodium hydrogen phosphate dihydrate (Na₂HPO₄·2H₂O) *p.a.* and trifluoroacetic acid $\geq 99.0\%$, both from Fluka Chemika (Chemie GmbH, Buchs, Switzerland). Ammonium acetate (NH₄Ac) *p.a.*, Riedel-de Haën, Sigma-Aldrich (Laborchemikalien GmbH, Seelze, Germany). Triethanolamine ((CH₂CH₂OH)₃N) *p.a.* and acetic acid (CH₃COOH) 99.8%, Riedel-de Haën, RdH Laborchemikalien GmbH & Co., Seelze, Germany.

Acetonitrile, HPLC grade, was bought from Fisher Scientific (UK Limited, Leicestershire, UK). The water in this study was purified in a Milli-Q® Academic system (18.2 MΩ·cm/0.22 μm), Millipore, (Burlington, MA, USA).

2.2. Experimental

2.2.1. Dissolution media and drug substances

Sodium phosphate buffer pH 7.0 ± 0.1 (65.5 mM), PB, and ammonium acetate buffer pH 6.8 ± 0.3 (10 mM), AmAc, were prepared as described previously (32). The buffer capacity, β , (33) in PB was 32.8 mM (32). Triethanolammonium acetate buffer 7.0 ± 0.1, TeAmAc, was prepared by mixing 173.8 mM triethanolamine and 150.5 mM acetic acid in Milli-Q® water as diluent. TeAmAc had an ionic strength of 150 mM while AmAc had an ionic strength of 10 mM. In TeAmAc, β was 50.8 mM compared to 0.21 mM in AmAc. The phosphate buffer, PB, was diluted ten times, Dil_PB, (6.55 mM) and the ionic strength was calculated to 13 mM. The ionic strength will not be one tenth of the ionic strength in the PB due to changes in the stoichiometric acidity constants of phosphate buffer system (34,35). The pH remained constant during dilution. In Table 1, Dil_PB buffer was considered to be an initial buffer, and to this buffer different anions were added to investigate the eventual effect of different ions in the phosphate buffer system. The addition were NaNO₃ (Dil_PB+NO₃), NaCl (Dil_PB+Cl) or Na₂SO₄ (Dil_PB+SO₄) to obtain an ionic strength of 150 mM, See Table 1. The pH was still constant at 7.0 ± 0.1. In Dil_PB the buffer capacity was calculated to 3.8 mM. This is also valid for the phosphate buffers with the presence of chloride, nitrate or sulfate. In Dil_PB the concentration of sodium ions is 11 mM and with addition of sodium chloride or nitrate the concentration is raised to 147 mM.

The stoichiometric pK_a-values used for the phosphate buffer preparation for I = 0.15 M were 1.89, 6.67 and 11.68 and for I = 0.013 M 2.19, 6.99 and 12.10 (36). For the preparation of the triethanolammonium acetate buffer the pK_a-value for acetic acid was 4.53 (I = 0.15 M) (37) and 7.77 for triethanolamine (38). The pK_a-value

Table 1. The phosphate media compositions and ionic strengths. The pH was 7.0 ± 0.1. For clarification of the abbreviations, see the text section above the table.

Medium	Additive (anionic)	Concentration of additive (mM)	Ionic strength (mM)
Dil_PB	-	-	13
PB	H ₂ PO ₄ ⁻	18.8	150
	HPO ₄ ²⁻	40.2	
Dil_PB+Cl	Cl ⁻	136	150
Dil_PB+NO ₃	NO ₃ ⁻	136	150
Dil_PB+SO ₄	SO ₄ ²⁻	45.6	150

of ammonium used in the ammonium acetate buffer preparation was 9.20 ($I = 0.15 \text{ M}$) (37). The structures of the drug substances used in this study was given in (31) and pK_a -values were as followed; naproxen (4.18), carbamazepine (N/A), nortriptyline HCl (10.21), bendroflumethiazide (8.77), prednisone (N/A), terfenadine (9.25), enalapril maleate (2.99 and 5.39), clomipramine HCl (8.83) and chlorprotixene HCl (8.80). N/A = not applicable, aprotic.

2.2.2. Apparent solubility determination by shake-flask methodology

For the apparent solubility determinations microtubes MCT-200-C homo-polymer (2.0 mL) from Axygen scientific (Union City, CA, USA), a horizontal shaker from KABI AB (Stockholm, Sweden) and Spectrafuge 16 M microcentrifuge from Labnet International Inc. (Woodbridge, NJ, USA) were used. The pH monitoring was carried out using a pH Meter 744, Metrohm (Herisau, Switzerland) with electrode CMAW711 ($\varnothing 4.5 \text{ mm}$) from Thermo Russell (Auchtermuchty Fife, Scotland).

Each drug substance was added in an excess to 1.5 mL of dissolution media. The amount added to achieve this excess was between 2 mg and 50 mg in the phosphate systems. In the triethanolammonium acetate buffer 100 mg of nortriptyline HCl was required. Enalapril maleate was too soluble in the triethanolammonium acetate buffer to be studied, more than 200 mg per 1.5 mL of medium was necessary. Noticeable was that nortriptyline HCl in $\text{DiI}_{\text{PB}}+\text{NO}_3$ seemed to re-crystallize and was found attached along the walls of the microtubes.

The drug-buffer suspensions were shaken at room temperature ($21.0 \pm 1.5^\circ\text{C}$) for 24 h. Centrifugation was used in separating the excess of substance from the dissolution medium. The pH was always measured in the buffers before addition of drug substance and after the centrifugation, but was not adjusted after the completed experiments. Solid phase of terfenadine and bendroflumethiazide were partly located at the medium surface (supernatant) after centrifugation, which generated experimental difficulties when diluting aliquots in mobile phase. In order to avoid precipitation and due to high absorbance, the supernatant was diluted 600 times in mobile phase before HPLC analysis. Four samples were analyzed in duplicates for each substance and buffer. The solubility, S , was reported as the average value together with the relative standard deviation (RSD), $n = 8$.

2.2.3. In vitro dissolution rate studies

The miniaturized equipment has been described previously (31,32). A magnetic stirrer with graded rotating speeds was obtained from Heidolph MR

3001K (Lenzkirch, Germany). The external HPLC-pump was a Jasco PU-1585, Jasco Inc. (Tokyo, Japan). For the dissolution rate studies the chromatography was performed on an Agilent 1100 Series HPLC system with a binary pump, degasser, autosampler and diode-array detector (DAD), Agilent Technologies Inc. (Palo Alto, CA, USA). A six-position switching valve with a 20 μL stainless steel loop attached to it. The analytical column, Zorbax SB-C8 ($2.1 \times 50\text{mm}$, 5 μM), was also purchased from Agilent Technologies Inc. The temperature of the column compartment was ambient ($25\text{-}28^\circ\text{C}$) and constant within approximately 2°C in one experiment. Data were collected by ChemStation Rev.A.10.02 from Hewlett Packard, Agilent Technologies Inc.

The dissolution media were used at room temperature ($21.0 \pm 1.5^\circ\text{C}$) and were deaerated. The making of the miniaturized disks were according to the method in (31,32). The Plexiglas cell was the same as used in the previously study (31). The flow into the chamber of Plexiglas was always 1.0 mL/min and the rotation speed was 300 rpm (32). Triplicates of the disks were analyzed for all substances in the different media. The average values were calculated together with the relative standard deviations (RSD), $n = 3$. The analysis by HPLC has been described earlier in the references by Persson *et al.* (31,32).

3. Results and discussion

The newly constructed miniaturized equipment for dissolution rate determinations is suited for screening studies. The dissolution rates are to be used for prediction of apparent solubilities in drug development. In order to evaluate the usefulness of this approach, some general factors (*e.g.* common ion effect, type of counter ions and buffer capacity) affecting the solubility and/or the determination of dissolution rate were investigated.

3.1. Apparent solubility (S) determination

The results from the solubility study are shown in Figure 1 and 2. Figure 1 shows the logarithmic apparent solubility values and Figure 2 the ΔpH , which is the change in pH before addition of drug substance in the medium to the stop at 24 h in the shake-flask study. The data from PB and AmAc originates from reference (31). The triethanolammonium acetate buffer was used for comparison to AmAc since the latter, despite the low buffer capacity, was found to give a good correlation when plotting $\log G$ versus $\log S$ cf. (31). Good precision was obtained in general, $\text{RSD} \leq 10\%$, in the solubility determinations. Highest RSD-values were obtained for drug substances which were partially located at the medium surface after centrifugation (see Experimental).

The two acids, naproxen and bendroflumethiazide,

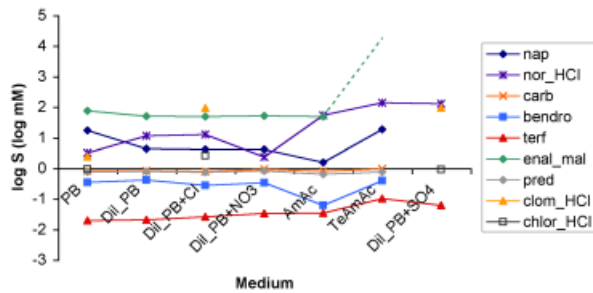


Figure 1. The average logarithmic apparent solubilities, logS, in aqueous dissolution media (24 h in room temperature). See Experimental for the media abbreviations. nap = naproxen, nor_HCl = nortriptyline hydrochloride, carb = carbamazepine, bendro = bendroflumethiazide, terf = terfenadine, enal_mal = enalapril maleate, pred = prednisone, clom_HCl = clomipramine hydrochloride and chlor_HCl = chlorprotixene hydrochloride. The raw data can be found in the Supplementary data section.

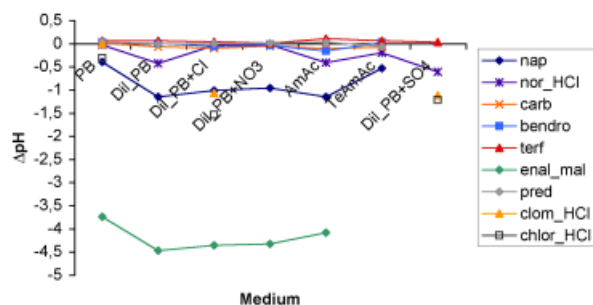


Figure 2. ΔpH, which is the change in pH before addition of drug substance in the medium to the stop at 24 h in the shake-flask study in aqueous dissolution media (24 h in room temperature). See Experimental for the media abbreviations and Figure 1 for the substance abbreviations. The raw data can be found in the Supplementary data section.

shows similar solubility properties in all media as can be seen in Figure 1. The decreased solubility of bendroflumethiazide in AmAc can partly be explained by the decrease in pH (Figure 2), compared to the other buffer media. The solubility of naproxen is higher in PB compared to the Dil_PB media. As expected, the better buffer capacity in the buffer media, the higher solubility of acidic drug compounds. The concentration of sodium ion in the different buffers had no effect on the solubility of the acids in this study, which is in agreement with reference (25). However, the finding contradicts some previously published results cf. (39,40).

There are small differences in the solubility of the aprotic substances (carbamazepin and prednisone) in the different buffers, Figure 1. Apparently, the ionic composition in the media is of less importance for their solubility in these buffer systems.

A significant decrease in pH was found in all media when dissolving enalapril added as the salt maleate, Figure 2. Enalapril maleate was too soluble in TeAmAc to be studied practically (indicated as a dotted line in Figure 1). At a concentration of 271 mM the solution was still not saturated. As was observed for the acids the solubility of enalapril was dependent on the buffer capacity, cf. PB and Dil_PB in Figure 2. When changing

anions in the diluted phosphate buffers, no effect on the solubility of the ampholytic enalapril was obtained as observed for another ampholytic drug substance (doxycycline) in water with added anions, cf. (41). This divergence might be due to the very high solubility of enalapril maleate in this study.

The solubility of nortriptyline seems to be dependent on the type of anion added to the diluted phosphate buffer, see Figure 1. Phosphate and nitrate ions in the media decreased the solubility of nortriptyline, whereas additional chloride ions in the buffer gave the same solubility as observed in Dil_PB (despite the change in ionic strength). This indicates that it is not mainly the common ion effect that decreases the solubility of nortriptyline hydrochloride in this study. However, it has been established that the common ion effect at low pH-values do effect the solubility of an amine salt (16,19,42,43). Furthermore, the effect on solubility by different counter ions, as observed in this study and by previously published results (e.g. (16,17,19)) will depend on the physico-chemical properties of the drug substance. These properties are often described by the solubility product, K_{sp} , and this value for a given protolyte is dependent on the counter ion used. This complicates the choice of a general dissolution medium in the screening of solubility for a drug candidate.

In order to further investigate the effect of the common ion and/or counter ion on the solubility, three different amines formulated as hydrochloride salts and one free base were studied. The selected screening media for this purpose were phosphate buffers with chloride and sulfate additives respectively, Figure 1 and 2. It can be seen that all hydrochloride salts have higher solubilities in Dil_PB+Cl compared to PB. This verifies that the phosphate ion ($H_2PO_4^-$ and/or HPO_4^{2-}) decreases the solubility more than the chloride ion for the hydrochloride bases, at an initial pH of 7 in the media. The results indicate that the K_{sp} for the phosphate ion is lower than for the chloride ion. This was also seen for haloperidol in reference (44). In Dil_PB+SO₄ the solubility is equal for clomipramine HCl compared to in Dil_PB+Cl, while nortriptyline HCl and terfenadine shows increased solubility. However, the solubility of chlorprotixene HCl is decreased in Dil_PB+SO₄ compared to in the chloride containing media. The conclusion was drawn that the types of counter ions added in the medium have different impact on the solubilities of the amines at a certain pH in the media.

A complementary investigation (Experimental not shown) of the solubility for nortriptyline, formulated as the hydrochloride salt, was also made. The media was based on Milli-Q® water of different pH containing dissolved salt of chloride, nitrate or sulfate to an ionic strength of 0.15 M. Regulation of pH was made by adding hydrochloric or nitric acid to the water medium. As reference, a solution of pure Milli-Q® water was used. The concentration of nortriptyline was determined

after 24 h and two weeks respectively. The chloride ion concentration was also determined after two weeks by use of a chloride selective electrode. In the reference solution, the nortriptyline concentration was 12 mM and the chloride concentration was 13 mM. In the pH region (2.4-6.5) where the positively charged form of nortriptyline dominates, the concentration was 31 mM while the chloride concentration was 26 mM. The solubility of the amine in the 0.15 M chloride containing medium was lower (8.9 mM), which is in agreement with the theory based on the common ion effect. In the 0.15 M nitrate medium however, the concentration of nortriptyline was even lower (1.7 mM). The chloride ion concentration was here found to be 22 mM, even though the chloride only originates from the nortriptyline hydrochloride itself. The K_{sp} for the nitrate salt is obviously lower than for the chloride salt. In the reference solution and the two media mentioned above, the nortriptyline concentration was found to be constant after 24 h and two weeks. In the sulfate containing medium on the contrary the nortriptyline concentration was very high after 24 h, 100 mM, but after two weeks it had decreased to 21 mM. The chloride concentration after two weeks in this medium was 110 mM, which approximately corresponds to the nortriptyline concentration determined after 24 h. The results in the sulfate medium indicate that the solubility equilibrium is slow, and also that nortriptyline might form a sulfate salt. This is important to account for when comparing the solubility results of the four amines in Dil_PB+SO₄ with the results in the other the media stated above.

The solubility in the different buffer systems (phosphate and acetate) was mainly dependent on the protolytic properties of the drug compound, Figure 1 and 2. In TeAmAc, the solubilities of nortriptyline HCl and terfenadine are higher than in PB, whereas acids have about the same solubility in these media. All of the drug substances, but the aprotic ones, seems to have increased solubility in TeAmAc compared to in AmAc. The triethanolammonium ion itself might generate an amplified effect of the solubility due to its organic character. This divergence might indicate that there are differences in the solubility product of the phosphate and acetate salts for the amines. The K_{sp} for the acetate salt may have a higher value compared to the phosphate salts. The buffer capacity of the medium is of course important for the solubility determinations of the protolytic drug substances.

3.2. *In vitro* dissolution rate (*G*) determination using the miniaturized apparatus

The logarithmic *in vitro* dissolution rates in the different media at 300 rpm for the drug substances are shown in Figure 3. RSD was at maximum 16% during the dissolution rate studies.

As also observed in the solubility study (Figure

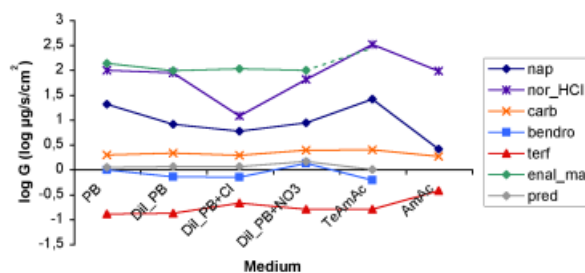


Figure 3. The logarithmic *in vitro* dissolution rate, log*G*, in aqueous dissolution media (300 rpm with 1.0 mL/min in room temperature). See Experimental for the media abbreviations and Figure 1 for the substance abbreviations. The raw data can be found in the Supplementary data section.

1), there is no significant difference in the dissolution rates of the aprotic substances in the different buffers. Furthermore, the effect of the altered media on the dissolution rate of acids was similar as to the solubility results, see Figure 1. This may indicate that the pH in the saturated medium of a drug substance is approximately the pH in the diffusion layer for that substance, cf. (42,44-47). As stated before, a better buffer capacity in the diffusion layer will generate a more stable pH-value and as a consequence higher dissolution rates and solubilities will be achieved for the acids. No major influence on the dissolution rate by an increased sodium ion concentration was observed.

The two drug substances formulated as salts, nortriptyline HCl and enalapril maleate, have the highest dissolution rates of all compounds in all of the buffer media. The dissolution rate of enalapril maleate was very high in TeAmAc, why it was difficult to experimentally measure an accurate value (shown as a dotted line in Figure 3). This difficulty has previously been observed using the miniaturized rotating disk apparatus with the small substance disk in combination with high dissolution rate of a drug substance, cf. (32). In contrary to the observations of the solubility of nortriptyline HCl in Dil_PB+Cl, the dissolution rate is significant lower than for the rates in the other buffer media possibly due to the common ion effect cf. (48-50). The nature of buffer media was of less importance for the dissolution rate of terfenadine, see Figure 3.

3.3. Correlation of dissolution rate and apparent solubility

The modified Noyes-Whitney equation has previously been used to correlate solubility and dissolution rate (31, 51-54). In this study, the applicability of the equation to correlate apparent solubility and *in vitro* dissolution rate using a miniaturized rotating disk apparatus was tested. The usefulness of the equation would be to predict solubility from dissolution rate data. The logarithmic form of the modified Noyes-Whitney equation will give a straight line when plotting log*G* versus log*S* according to Eq. 1 (cf. (31)).

$$\log G = \log S + \log k \quad \text{Eq. 1}$$

The logarithmic values of G and S were correlated in Figure 4 A-E for the different buffer media and substances. Triplicates of $\log G$ are shown in the figures, while average values are used for $\log S$. The correlation was made at the pH in the solubility solutions after 24 h. This will according to references (42,44-47) be the pH of the diffusion layer, rather than to the pH of the bulk solution in the rotating disk experiments.

Since the dissolution rate of the substances in the different media do not always follow the same pattern as the solubility, the different media will obviously give different correlations of dissolution rate versus solubility. Previously it was seen that nortriptyline HCl was deviating from the more linear correlation pattern in PB (31), which also was found in this study (Figure 4A). A deviation in the correlation of dissolution rate

and solubility was also observed for nortriptyline HCl in other buffer media. Interestingly the best correlation, as described by the coefficient of determination (R^2) was however found in TeAmAc ($R^2 = 0,991$, $n = 6$). In TeAmAc only six substances were used for correlation since enalapril maleate was excluded due to the high solubility. Dil_PB+Cl, which might be comparable to the buffers used in biorelevant media, gave a good correlation as well including nortriptyline HCl ($R^2 = 0.952$, $n = 7$). So far, TeAmAc and Dil_PB+Cl seem to be best suitable for predicting the solubility from the experimental *in vitro* dissolution rate at pH 7.

Presented in Figure 5 is the correlation of the dissolution rate and the solubility for all drug compounds and buffer media tested thus far. It is seen that nortriptyline HCl, nor_HCl, deviates from the correlation line in three of the buffers as discussed above. If these three values of nortriptyline HCl are discarded the R^2 value will be 0.967 (shown as dashed line and italic equation). This correlation

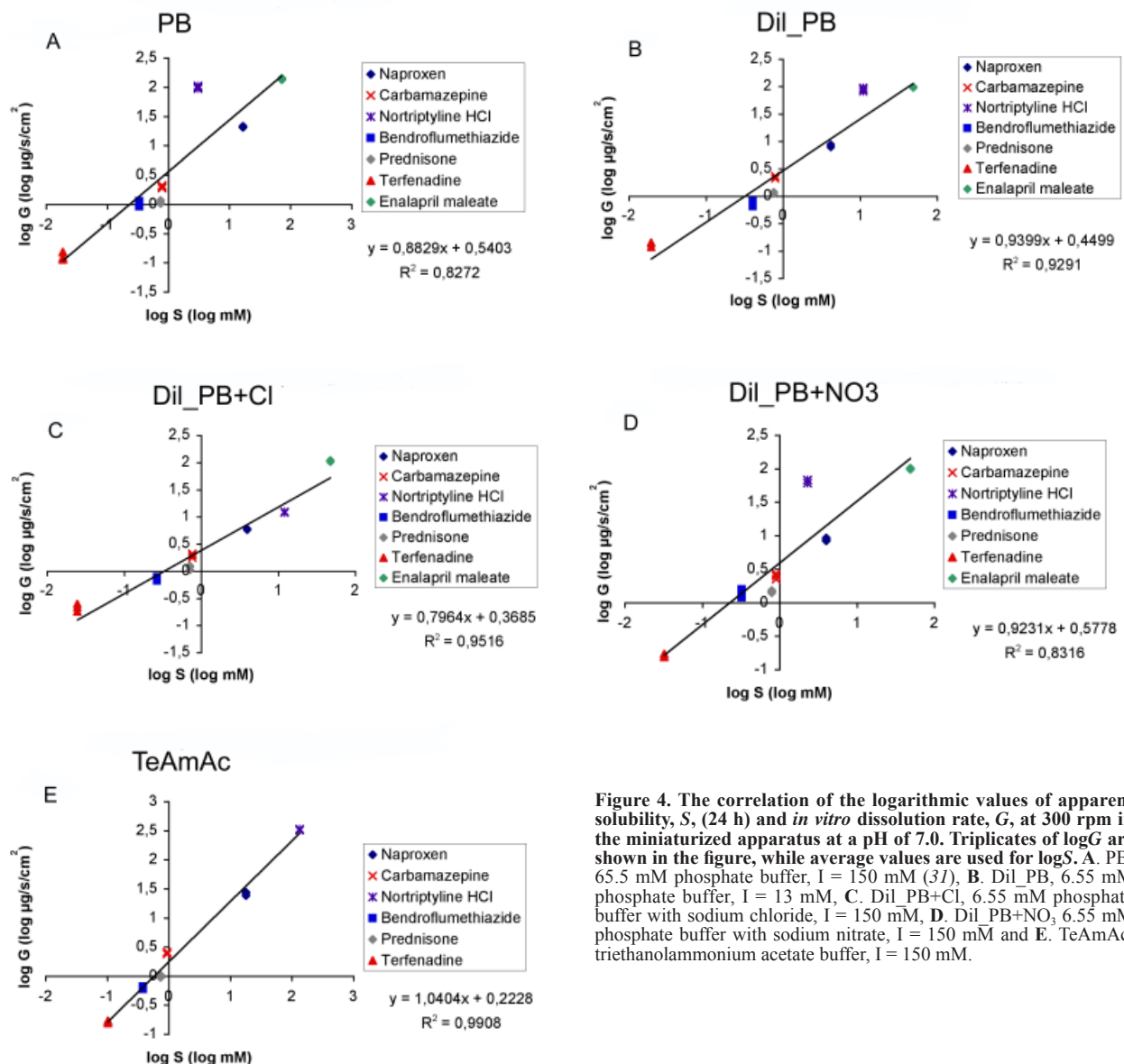


Figure 4. The correlation of the logarithmic values of apparent solubility, S , (24 h) and *in vitro* dissolution rate, G , at 300 rpm in the miniaturized apparatus at a pH of 7.0. Triplicates of $\log S$ are shown in the figure, while average values are used for $\log S$. A. PB, 65.5 mM phosphate buffer, $I = 150$ mM (31), B. Dil_PB, 6.55 mM phosphate buffer, $I = 13$ mM, C. Dil_PB+Cl, 6.55 mM phosphate buffer with sodium chloride, $I = 150$ mM, D. Dil_PB+NO₃, 6.55 mM phosphate buffer with sodium nitrate, $I = 150$ mM and E. TeAmAc, triethanolammonium acetate buffer, $I = 150$ mM.

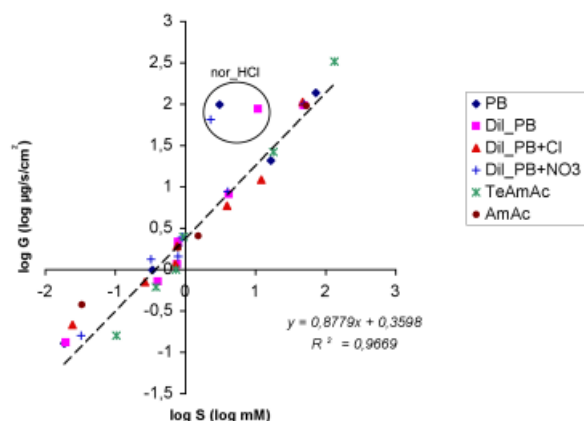


Figure 5. The correlation of the logarithmic values of apparent solubility, S , (24 h) and *in vitro* dissolution rate, G , at 300 rpm in the miniaturized apparatus at a pH of 7.0. The six different media were; PB, $I = 150$ mM (31), Dil_PB, $I = 13$ mM, Dil_PB+Cl, $I = 150$ mM, Dil_PB+NO₃, $I = 150$ mM, TeAmAc, $I = 150$ mM and AmAc = ammonium acetate buffer pH 6.8, $I = 10$ mM (31,32).

would probably be acceptable in a screening study of solubility from dissolution rate data during early phases in drug discovery. However, to obtain a general buffer where $\log G$ versus $\log S$ shows a good correlation for all types of drug substances, more types of buffers and drug substances both in free form and as salts have to be investigated.

4. Conclusions

A correlation study, based on the modified Noyes-Whitney equation, of solubility and dissolution rate was made. The apparent solubilities of seven different compounds were measured by a conventional shake-flask methodology. The dissolution rates were determined using a newly introduced miniaturized rotating disk apparatus. The rotating disk equipment decreased the time for determining the *in vitro* dissolution rate, whilst only consuming minute quantities of substance amount in the disks.

The influence of buffer system and buffer capacity as well as the common ion effect on the correlation was investigated using six different buffer media. The best correlations of $\log G$ versus $\log S$ were obtained with a triethanolammonium acetate buffer ($R^2 = 0.991$, $n = 6$). However, to compare the correlation with buffer used in biorelevant media, a phosphate buffer with the addition of chloride gave a good correlation for the drug substances in this study ($R^2 = 0.952$, $n = 7$). These results are encouraging, but more studies are needed in order to be able to select an optimal buffer for predicting the solubility based on dissolution rate data. Future studies, preferably by including multivariate data analysis, should include more buffer types and diverse substances. It should also be of interest to investigate the correlation of $\log G$ and $\log S$ in simulated intestinal fluids, *i.e.* FeSSIF and FaSSIF.

Acknowledgements

We would like to thank Walter Lindberg, AstraZeneca Mölndal, Sweden, for lending us the miniaturized equipment for the dissolution rate studies as well as Anders AS. Karlsson and Anders S. Carlsson at AstraZeneca Mölndal, Sweden for providing some of the drug substances used in this study.

Reference

- Zhao YH, Abraham MH, Le J, Hersey A, Luscombe CN, Beck G, Sherborne B, Cooper I. Rate-limited steps of human oral absorption and QSAR studies. *Pharm Res.* 2002; 19:1446-1457.
- Varma MV, Sateesh K, Panchagnula R. Functional role of P-glycoprotein in limiting intestinal absorption of drugs: contribution of passive permeability to P-glycoprotein mediated efflux transport. *Mol Pharm.* 2005; 2:12-21.
- Yu LX, Lipka E, Crison JR, Amidon GL. Transport approaches to the biopharmaceutical design of oral drug delivery systems: prediction of intestinal absorption. *Adv Drug Deliv Rev.* 1996; 19:359-376.
- Kostewicz ES, Wunderlich M, Brauns U, Becker R, Bock T, Dressman JB. Predicting the precipitation of poorly soluble weak bases upon entry in the small intestine. *J Pharm Pharmacol.* 2004; 56:43-51.
- Klein S, Butler J, Hempenstall JM, Reppas C, Dressman JB. Media to simulate the postprandial stomach I. Matching the physicochemical characteristics of standard breakfasts. *J Pharm Pharmacol.* 2004; 56:605-610.
- Noyes AA, Whitney WR. The rate of solution of solid substances in their own solutions. *J Am Chem Soc.* 1897; 19:930-934.
- Nernst W. Theory of reaction velocity in heterogenous systems. *Zeitschrift für Physikalische Chemie.* 1904; 47:52-55.
- Levich VG. *Physicochemical Hydrodynamics.* Prentice-Hall, NJ, USA, 1962; pp. 162-171.
- Bruner L, Tolloczko S. On the velocity of solution of solid bodies. *Zeitschrift für Physikalische Chemie.* 1900; 35:283-290.
- Brunner E. Reaction velocity in heterogenous systems. *Zeitschrift für Physikalische Chemie.* 1904; 47:56-102.
- Dressman JB, Amidon GL, Reppas C, Shah VP. Dissolution testing as a prognostic tool for oral drug absorption: immediate release dosage forms. *Pharm Res.* 1998; 15:11-22.
- Kararli TT, Kirchoff CF, Truelove JE. Ionic strength dependence of dissolution for Eudragit S-100 coated pellets. *Pharm Res.* 1995; 12:1813-1816.
- Wagner D, Glube N, Berntsen N, Tremel W, Langguth P. Different dissolution media lead to different crystal structures of talinolol with impact on its dissolution and solubility. *Drug Dev Ind Pharm.* 2003; 29:891-902.
- Fini A, Fazio G, Feroci G. Solubility and solubilization properties of non-steroidal anti-inflammatory drugs. *Int J Pharm.* 1995; 126:95-102.
- Serajuddin AT, Sheen PC, Augustine MA. Common ion effect on solubility and dissolution rate of the sodium salt of an organic acid. *J Pharm Pharmacol.* 1987; 39:587-591.
- Streng WH, Hsi SK, Helms PE, Tan HG. General treatment of pH-solubility profiles of weak acids and bases and the effects of different acids on the solubility of a weak base. *J Pharm Sci.* 1984; 73:1679-1684.

17. Li S, Doyle P, Metz S, Royce AE, Serajuddin AT. Effect of chloride ion on dissolution of different salt forms of haloperidol, a model basic drug. *J Pharm Sci.* 2005; 94:2224-2231.
18. Agharkar S, Lindenbaum S, Higuchi T. Enhancement of solubility of drug salts by hydrophilic counterions: properties of organic salts of an antimalarial drug. *J Pharm Sci.* 1976; 65:747-749.
19. Dittert LW, Higuchi T, Reese DR. Phase solubility technique in studying the formation of complex salts of triamterene. *J Pharm Sci.* 1964; 53:1325-1328.
20. Miyazaki S, Inoue H, Nadai T, Arita T, Nakano M. Solubility characteristics of weak bases and their hydrochloride salts in hydrochloric acid solutions. *Chem Pharm Bull.* 1979; 27:1441-1447.
21. Miyazaki S, Nakano M, Arita T. A comparison of solubility characteristics of free bases and hydrochloride salts of tetracycline antibiotics in hydrochloric acid solutions. *Chem Pharm Bull.* 1975; 23:1197-1204.
22. Miyazaki S, Oshiba M, Nadai T. Unusual solubility and dissolution behavior of pharmaceutical hydrochloride salts in chloride-containing media. *Int J Pharm.* 1980; 6:77-85.
23. Amidon GL, Lennernas H, Shah VP, Crison JR. A theoretical basis for a biopharmaceutical drug classification: The correlation of *in vitro* drug product dissolution and *in vivo* bioavailability. *Pharm Res.* 1995; 12:413-420.
24. Sugano K, Okazaki A, Sugimoto S, Tavnornvipas S, Omura A, Mano T. Solubility and dissolution profile assessment in drug discovery. *Drug Metab Pharmacokinet.* 2007; 22:225-254.
25. Levis KA, Lane ME, Corrigan OI. Effect of buffer media composition on the solubility and effective permeability coefficient of ibuprofen. *Int J Pharm.* 2003; 253:49-59.
26. Ozturk SS, Palsson BO, Dressman JB. Dissolution of ionizable drugs in buffered and unbuffered solutions. *Pharm Res.* 1988; 5:272-282.
27. Galia E, Nicolaides E, Horter D, Lobenberg R, Reppas C, Dressman JB. Evaluation of various dissolution media for predicting *in vivo* performance of class I and II drugs. *Pharm Res.* 1998; 15:698-705.
28. Iga K, Ogawa Y. Effect of buffer species, pH and buffer strength on drug dissolution rate and solubility of poorly-soluble acidic drugs: experimental and theoretical analysis. *Takeda Kenkyusho Hô.* 1996; 55:173-187.
29. Vertzoni M, Fotaki N, Kostewicz E, Stippler E, Leuner C, Nicolaides E, Dressman J, Reppas C. Dissolution media simulating the intraluminal composition of the small intestine: physiological issues and practical aspects. *J Pharm Pharmacol.* 2004; 56:453-462.
30. Jantratid E, Janssen N, Reppas C, Dressman JB. Dissolution media simulating conditions in the proximal human gastrointestinal tract: An update. *Pharm Res.* 2008; 25:1663-1676.
31. Persson AM, Sokolowski A, Pettersson C. Part I: Correlation of *in vitro* dissolution rate and apparent solubility in buffered media using a new miniaturized rotating disk equipment. *Drug Discov Ther.* 2009; 3:104-113.
32. Persson AM, Baumann K, Sundelof LO, Lindberg W, Sokolowski A, Pettersson C. Design and characterization of a new miniaturized rotating disk equipment for *in vitro* dissolution rate studies. *J Pharm Sci.* 2008; 97:3344-3355.
33. Van Slyke DD. On the measurement of buffer values and on the relationship of buffer value to the dissociation constant of the buffer and the concentration and reaction of the buffer solution. *J Biol Chem.* 1922; 52:525-570.
34. Sirius. Applications and Theory Guide to pH-metric pK_a and logP Determination. Sirius Analytical Instruments Ltd., UK, 1993.
35. Butler JN. Ionic Equilibrium (Solubility and pH Calculations). John Wiley & Sons, Inc. New York, USA 1998:202-237.
36. Sirius. Sirius Technical Applications Notes (STAN). Sirius Analytical Instruments Ltd., UK, 1994;1.
37. Sirius. RefinementPro2 Sirius Analytical Instruments Ltd.,UK.
38. Hall HK, Jr. Correlation of the base strengths of amines. *J Am Chem Soc.* 1957; 79:5441-5444.
39. Chowhan ZT. pH-solubility profiles of organic carboxylic acids and their salts. *J Pharm Sci.* 1978; 67:1257-1260.
40. Anderson BD, Conradi RA. Predictive relationships in the water solubility of salts of a nonsteroidal anti-inflammatory drug. *J Pharm Sci.* 1985; 74:815-820.
41. Bogardus JB, Blackwood RK, Jr. Solubility of doxycycline in aqueous solution. *J Pharm Sci.* 1979; 68:188-194.
42. Li S, Wong S, Sethia S, Almoazen H, Joshi YM, Serajuddin AT. Investigation of solubility and dissolution of a free base and two different salt forms as a function of pH. *Pharm Res.* 2005; 22:628-635.
43. Serajuddin ATM, Mufson D. pH-solubility profiles of organic bases and their hydrochloride salts. *Pharm Res.* 1985; 2:65-68.
44. Serajuddin ATM, Jarowski CI. Effect of diffusion layer pH and solubility on the dissolution rate of pharmaceutical bases and their hydrochloride salts I: Phenazopyridine. *J Pharm Sci.* 1985; 74:142-147.
45. Serajuddin ATM, Jarowski CI. Effect of diffusion layer pH and solubility on the dissolution rate of pharmaceutical acids and their sodium salts II: Salicylic acid, theophylline, and benzoic acid. *J Pharm Sci.* 1985; 74:148-154.
46. Avdeef A, Tsinman O. Miniaturized rotating disk intrinsic dissolution rate measurement: effects of buffer capacity in comparisons to traditional wood's apparatus. *Pharm Res.* 2008; 25:2613-2627.
47. Pudipeddi M, Zannou EA, Vasanthavada M, Dontabhaktuni A, Royce AE, Joshi YM, Serajuddin AT. Measurement of surface pH of pharmaceutical solids: a critical evaluation of indicator dye-sorption method and its comparison with slurry pH method. *J Pharm Sci.* 2008; 97:1831-1842.
48. Bogardus JB, Blackwood RK, Jr. Dissolution rates of doxycycline free base and hydrochloride salts. *J Pharm Sci.* 1979; 68:1183-1184.
49. Miyazaki S, Oshiba M, Nadai T. Dissolution properties of salt forms of berberine. *Chem Pharm Bull.* 1981; 29:883-886.
50. Lin SL, Lachman L, Swartz CJ, Huebner CF. Preformulation investigation I: Relation of salt forms and biological activity of an experimental antihypertensive. *J Pharm Sci.* 1972; 61:1418-1422.
51. Nelson KG, Shah AC. Convective diffusion model for a transport-controlled dissolution rate process. *J Pharm Sci.* 1975; 64:610-614.
52. Nicklasson M, Brodin A, Nyqvist H. Studies on the relationship between solubility and intrinsic rate of dissolution as a function of pH. *Acta Pharm Suec.* 1981; 18:119-128.
53. Shah AC, Nelson KG. Evaluation of a convective diffusion drug dissolution rate model. *J Pharm Sci.* 1975; 64:1518-1520.
54. Hamlin WE, Northam JI, Wagner JG. Relationship between *in vitro* dissolution rates and solubilities of numerous compounds representative of various chemical species. *J Pharm Sci.* 1965; 54:1651-1653.

(Received April 2, 2009; Accepted April 23, 2009)

Supplementary data 1

Raw data for the solubility study in six dissolution media, 24 h in room temperature. The apparent solubility, S , is the average of eight values (four samples with double injections). RSD = relative standard deviation ($n = 8$). pH is the value after the defined shake-time, 24 h, and Δ pH is the change in pH before addition of drug substance in the medium to the stop at 24 h.

Medium and experimental values		Naproxen	Carbamazepine	Nortriptyline HCl	Bendroflu -methiazide	Prednisone	Terfenadine	Enalapril maleate
PB	S (mM)	17	0.74	2.8	0.34	0.76	0.019	74
	RSD (%)	0.30	3.6	11	5.2	16	16	1.5
	pH (24 h)	6.73	7.14	7.10	7.15	7.10	7.13	3.35
	Δ pH	-0.41	± 0.00	-0.04	+0.01	+0.02	+0.05	-3.75
Dil_PB	S (mM)	4.2	0.80	11	0.41	0.77	0.020	50
	RSD (%)	2.1	2.9	3.8	13	8.7	5.8	2.2
	pH (24 h)	5.96	7.06	6.70	7.09	7.00	7.13	2.66
	Δ pH	-1.16	-0.08	-0.44	-0.01	-0.02	+0.05	-4.48
Dil_PB+Cl	S (mM)	4.0	0.78	12	0.27	0.73	0.025	48
	RSD (%)	4.5	5.7	0.85	16	7.9	11	2.2
	pH (24 h)	6.00	6.98	7.06	6.99	6.95	7.02	2.59
	Δ pH	-1.02	-0.11	-0.05	-0.07	-0.01	+0.03	-4.37
Dil_PB+NO ₃	S (mM)	4.1	0.92	2.3	0.33	0.81	0.033	50
	RSD (%)	2.6	6.1	1.6	21	3.8	19	1.7
	pH (24 h)	6.01	6.97	6.99	6.94	6.93	6.98	2.62
	Δ pH	-0.97	-0.06	-0.03	-0.05	± 0.00	± 0.00	-4.34
AmAc	S (mM)	1.6	0.79	54	0.057	0.63	0.034	48
	RSD (%)	7.5	3.2	7.5	20	0.60	18	1.0
	pH (24 h)	5.30	6.40	6.13	6.57	6.85	6.56	2.78
	Δ pH	-1.16	-0.12	-0.42	-0.17	+0.02	+0.10	-4.09
TeAmAc	S (mM)	18	0.95	137	0.39	0.74	0.10	>271
	RSD (%)	1.7	3.4	0.89	20	4.1	30	
	pH (24 h)	6.58	7.06	6.77	7.10	7.08	7.08	
	Δ pH	-0.54	-0.09	-0.21	+0.01	-0.07	+0.05	

Supplementary data 2

Solubility raw data for the basic drug substances in three different phosphate buffer media ($n = 8$). clom HCl = clomipramine HCl, chlor HCl = chlorproprizine HCl, nor HCl = nortriptyline HCl and terf = terfenadine.

Drug Substance	PB				Dil_PB+Cl				Dil_PB+SO ₄			
	S (mM)	RSD (%)	pH (24 h)	Δ pH	S (mM)	RSD (%)	pH (24 h)	Δ pH	S (mM)	RSD (%)	pH (24 h)	Δ pH
clom HCl	2.4	2.2	7.10	-0.02	93	1.9	5.99	-1.08	92	0.60	5.95	-1.13
chlor HCl	0.92	32	6.80	-0.32	2.6	1.5	5.52	-1.55	0.89	2.9	5.85	-1.23
nor HCl	2.8	11	7.10	-0.04	12	0.85	7.06	-0.05	127	1.1	6.46	-0.62
terf	0.019	16	7.13	+0.05	0.025	11	7.02	+0.03	0.055	14	7.03	+0.02

Supplementary data 3

The raw data for the *in vitro* dissolution rate values, G , in five dissolution media (300 rpm at a flow of medium at 1.0 mL/min). The values are presented as average values of three disks. RSD = relative standard deviation ($n = 3$). N/A = not applicable.

Medium and experimental values		Naproxen	Carbamazepine	Nortriptyline HCl	Bendroflu -methiazide	Prednisone	Terfenadine	Enalapril maleate
PB	G ($\mu\text{g/s/cm}^2$)	20	1.9	97	0.98	1.1	0.13	135
	RSD (%)	2.8	4.9	5.1	11	6.5	16	3.3
Dil_PB	G ($\mu\text{g/s/cm}^2$)	8.0	2.1	86	0.71	1.1	0.13	95
	RSD (%)	6.3	5.9	8.0	13	3.2	9.9	1.5
Dil_PB+Cl	G ($\mu\text{g/s/cm}^2$)	5.8	1.9	12	0.69	1.1	0.21	104
	RSD (%)	2.0	9.1	2.7	8.7	8.6	16	3.4
Dil_PB+NO ₃	G ($\mu\text{g/s/cm}^2$)	8.6	2.4	64	1.3	1.4	0.16	98
	RSD (%)	5.0	9.1	6.2	15	3.7	5.8	1.9
TeAmAc	G ($\mu\text{g/s/cm}^2$)	26	2.4	323	0.60	0.98	0.16	N/A
	RSD (%)	6.8	3.9	2.6	5.3	5.5	5.8	

Original Article**Formulation and optimization of sustained release terbutaline sulfate microspheres using response surface methodology**Ibrahim Khattab^{1,*}, Farzana Bandarkar¹, Ahmed Lila²¹ Department of Pharmaceutics, Faculty of Pharmacy, Kuwait University, Kuwait;² Department of Pharmaceutics, Faculty of Pharmacy, Al-Azhar University, Egypt.

ABSTRACT: The present study reports the optimization of sustained release microspheres of terbutaline sulfate (TS) and Eudragit RSPM using response surface methodology. The microspheres were prepared by the emulsion solvent evaporation process utilizing Eudragit RSPM as release retarding agent. A 3² full factorial design was utilized by taking the drug: Eudragit RSPM ratio (X₁), the percent of Span 80 (X₂) and the speed of rotation (X₃) as the independent variables; particle size (Y₁) and percent drug released (Y₂) were the dependent variables. The resultant microspheres were subjected to various physico-chemical analysis, viz., drug content, micrometrics, photo-microscopy and *in vitro* drug release. The percent of drug release at 8 h of dissolution decreased from 90.7% to 61.3% with increase in polymer concentration from 4 to 8%. It was observed that an increase in surfactant concentration from 1 to 2% and speed of rotation from 500 to 900 rpm decreased the size of microspheres (350-330 μm). The results of the present study indicate that optimized sustained release microspheres of terbutaline sulfate could be successfully prepared by the emulsion solvent evaporation method by emulsifying the drug and polymer in the ratio of 1:8, at a speed of 500 rpm, utilizing 1.5% of span 80 as emulsifying agent.

Keywords: Terbutaline sulfate, Eudragit RSPM, sustained release microspheres, response surface methodology, Box-Behnken design

1. Introduction

Much of the research effort in developing novel drug delivery systems has been focused on oral sustained release dosage forms. Among them, in the last decade,

multiple unit dosage forms, such as micro particles have gained in popularity for different reasons when compared to non-disintegrating single-unit dosage forms (1). They distribute more uniformly in the gastrointestinal tract, resulting in more uniform drug absorption and reduced local irritation, and also avoid the unwanted intestinal retention of the polymeric material. It is also desirable to release drugs at a constant rate, thereby maintaining drug concentration within the therapeutic range and eliminating the need for frequent dosages. The rate of drug release from solid dosage forms may be modified by the technologies which, in general, are based on modifying drug dissolution by controlling access of biologic fluids to the drug through the use of barrier coatings, controlling drug diffusion rates from dosage forms and chemical interactions between the drug substance or its pharmaceutical barrier and site-specific biologic fluids (2).

One of the most effective techniques for preparing sustained release particles is by microencapsulation (3-6). This method has been employed in pharmaceutical practice for a variety of purposes. It is useful for reducing toxicity and adverse effects, separating reactive or incompatible components, controlling the rate and site of release of a drug and providing greater patient convenience and compliance. Microcapsules are small particles that contain an active agent or core material surrounded by a coating or shell. At present, there is no universally accepted size range that particles must have in order to be classified as microcapsules. However, many workers classify capsules smaller than 1 μm as nanocapsules and capsules larger than 1,000 μm as macrocapsules. Commercial microcapsules typically have a diameter between 3 and 800 μm and contain 10-90 weight percent cores. Microcapsules can have a variety of structures. Some have a spherical geometry with a continuous core region surrounded by a continuous shell; others have an irregular geometry and contain a number of small droplets or particles of core material (7). The micro encapsulation process in which the removal of the hydrophobic polymer solvent is achieved by evaporation has been widely reported in recent years for the preparation of microcapsules

*Address correspondence to:

Dr. Ibrahim S. Khattab, Faculty of Pharmacy, Kuwait University, Kuwait.
e-mail: i_khattab@hotmail.com (or Khattab@hsc.edu.kw)

(8-10). This process is known as the emulsion solvent (ESE) technique and has been used successfully in the preparation of drug microspheres or capsules using different biocompatible polymers (11-15). Many formulation factors can influence the preparation of microcapsules by the ESE process (16-20).

In the present study, terbutaline sulfate (TS), a selective beta 2-adrenergic agonist was chosen as the model drug, as it has a short biological half-life (3-4 h). It is widely used as a bronchodilator for the treatment of bronchial asthma, chronic bronchitis and emphysema (21-24). Currently available treatments for asthma and bronchitis, although generally effective, are limited by the necessity for frequent drug administration and/or the possibility of unpleasant or debilitating side effects. Thus, a long acting TS formulation which would maximize the duration of active drug concentration in extra-cellular fluid is desirable to improve patient compliance. There are several studies in the literature regarding prolongation of its release using various polymers. Prolongation of TS release from all these formulations has been demonstrated by means of *in vitro* dissolution studies (25-28).

Modern sustained-release dosage forms require reliable excipients to ensure a release rate of the active drug which is reproducible in a narrow range. Eudragit polymers fulfill this requirements to a very high extent and enable research and development to create tailor-made solutions. In the present study, Eudragit RSPM (hydrophobic polymer) was used as the microcapsule wall-former because of its wide use as a coating material in the pharmaceutical industry. It is a copolymer with a low content of quaternary ammonium groups. Since, Eudragit RSPM film is only slightly permeable, drug release through the film is relatively retarded. Several sustained-release formulations using Eudragit RSPM, such as coated tablets and matrix type tablets, have been reported (29-32).

Response surface methodology, an empirical modeling technique devoted to the evaluation of the relationship of a set of controlled experimental factors and observed results was employed in the present research work (33). It requires prior knowledge of the process to achieve a statistical model. Basically this optimization process involves three major steps, performing the statistically designed experiments, estimating the coefficients in a mathematical model, predicting the response and checking the adequacy of the model. This design is suitable for exploration of a quadratic response surface and constructs a second order polynomial model, thus helping in optimizing a process using a small number of experimental runs. Various formulation studies have been optimized and reported using this design. In all these studies, the observed responses were in close agreement with the predicted values of the optimized formulation (34-38).

There are comparatively few reports on sustained

release TS microcapsules, none of which have been optimized by the factorial design approach (25-28). The present study was thus designed to formulate TS containing microspheres using the ESE technique by applying Box-Behnken design, multiple regression analysis and response surface modeling. The objective was to investigate the influence of independent variables on the particle size distribution and drug release properties of the TS microcapsules.

2. Materials and Methods

2.1. Materials

Terbutaline sulfate (TS) was a generous gift from Chemical Industrial Development Co., CID (Giza, Egypt). Eudragit RSPM was kindly supplied by Rohm Pharma, and GMBH (Weitestadt, Germany) was a gift sample. Aluminum tristearate was received from Morgan Co. (Cairo, Egypt). Methylene chloride, ethanol absolute (99%) and cyclohexane were purchased from Prolabo (Briare, France). *n*-Hexane was purchased from Honil Limited (London, UK). Chloroform was bought from Labscan Ltd. (Dublin, Ireland). Light liquid paraffin was purchased from Chemaject (Egypt). Span 80 was purchased from Sigma Chemical Co. (Steinheim, Germany). Hydrochloric acid was purchased from Carloerba (Milano, Italy). Potassium chloride and monobasic potassium hydrogen phosphate were purchased from Merck (Darmstadt, Germany). All of the above materials were of analytical grade and were used without further purification. De-ionized double distilled water was used throughout the study.

2.2. Preparation of TS microcapsules

Microspheres were prepared by the ESE technique. Polymer solution of Eudragit RSPM was prepared in methylene dichloride. TS was dispersed in this polymeric solution to form the internal phase. Different drug-polymer ratios, *viz.*, 1:4, 1:6, and 1:8 were used to prepare the microcapsules. Known amounts of Aluminum tristearate were dispersed in the different internal phases as smoothing agent. This dispersion was added drop wise to liquid paraffin (external phase) containing several different concentrations of Span 80 as emulsifying agent. Emulsification was achieved by stirring at various rotation speeds. Stirring was continued at room temperature until complete evaporation of the solvent (methylene chloride), for approximately 2 h. Liquid paraffin was decanted and the microspheres produced were collected by filtration through Whatman No.1 filter paper. The filtrate was washed three times with *n*-hexane and three times with cyclohexane to remove the remaining oily phase and then dried overnight at room temperature.

2.3. Optimization of TS microspheres using response surface methodology

In the present study, a three-factors, three levels Box-Behnken design with speed (X_1), drug-polymer ratio (X_2) and concentration of span 80 (X_3) as independent variables were selected for the formulation. Three levels of speed used were 500, 700, and 900 rpm which equals to -1, 0, and +1 values for the above design. Drug-polymer ratios of 1:4, 1:6, and 1:8 reflect the -1, 0, and +1 values. While span 80 concentrations of 1, 1.5, and 2% were equal to the -1, 0, and +1 values. The various levels used are shown in Table 1. This design is suitable for exploration of quadratic response surface and constructs a second order polynomial model, thus helping in optimizing a process using a small number of experimental runs. The model constructed was as follows:

$$Y = a_0 + a_1X_1 + a_2X_2 + a_3X_3 + a_4X_1X_2 + a_5X_2X_3 + a_6X_1X_3 + a_7X_1^2 + a_8X_2^2 + a_9X_3^2 + E$$

Where a_0 to a_9 are the regression coefficient, X_1 , X_2 , and X_3 are the factors studied, Y is the measured response associated with each factor level combination and E is the error term.

2.4. Drug content determination of TS microcapsules

The drug content of TS microspheres was determined by an extraction method reported by Kim *et al.* (25). Microspheres (25 mg) were added to chloroform (20 mL) to dissolve the polymer matrix. Terbutaline sulfate was then extracted with distilled water (100

mL). The amount of terbutaline sulfate in the aqueous phase was analyzed by UV spectrophotometry (Jenway 6305 UV/Vis Spectrophotometer, Essex, UK) at 278 nm after suitable dilution.

2.5. Evaluation of micromeritic characteristics of TS microcapsules

The prepared TS microspheres were evaluated for the following parameters:

2.5.1. Particle size distribution

According to the sieve analysis method stated by U.S.P. XXIV for testing powder fineness, a definite weight of TS microspheres was placed on the mechanical sieve shaker and analyzed for particle size distribution (USP, 2002). The powder was shaken for a defined period of time (15 min) using a range of standard sieves with openings from 100 to 900 μm . The material that passes through one sieve and was retained on the next fine sieve was collected and weighed. The obtained batches were separated into different fractions based on their particle size (900, 715, 565, 407.5, 282.5, 225, and 100 μm). The logarithm of the particle size was plotted against the cumulative percent frequency on a probability scale and a linear relationship was observed. From this linear plot, both the geometric mean diameter (d_g) and geometric standard deviation were measured for the TS microspheres equivalent to 50% on the probability scale. The geometric standard deviation was calculated from the slope of the line and the geometric standard deviation which was the quotient of the ratio of 50% size and 16% undersize.

Table 1. Box-Behnken design

Formula No.	Independent variables*		
	Speed (X_1)	Drug: polymer (X_2)	Span 80 (X_3)
T1	-1	-1	0
T2	0	-1	-1
T3	0	-1	+1
T4	+1	-1	0
T5	-1	0	-1
T6	-1	0	+1
T7	0	0	0
T8	0	0	0
T9	0	0	0
T10	+1	0	-1
T11	+1	0	+1
T12	-1	+1	0
T13	0	+1	-1
T14	0	+1	+1
T15	+1	+1	0

Coded values	Actual values*		
	X_1 (rpm)	X_2 (ratio)	X_3 (%)
-1	500	1:4	1
0	700	1:6	1.5
+1	900	1:8	2

2.5.2. Density

For determination of bulk density of the microcapsules, a sample of 50 g was poured into a 100 mL graduated cylinder (38). The cylinder was then dropped from a height of 1 inch onto a hard surface three times at 2 sec intervals. The volume of the powder was then read and used to calculate the bulk density by dividing the weight in (g) by the volume in (cm³). For determination of tap density of the microcapsules, tapping onto a hard surface was carried out until a constant volume was achieved. This volume was taken and used to calculate the tap density of the microcapsules.

2.5.3. Hausner ratio

Hausner ratio is the ratio between bulk density and tap density. It gives an idea about the flow characteristics of powder particles. The powder has good flow when the ratio is less than 1.2, while if the ratio is more than 1.2 this indicates poor flow.

2.5.4. Compressibility percent

Compressibility is indirectly related to the relative flow rate, cohesiveness, and particle size of a powder. A compressible material has generally less flow, and powders with compressibility values greater than 20-21% have been found to exhibit poor flow properties (39). The compressibility of a material can be estimated as follows:

$$\text{Compressibility \%} = (\rho_{\text{tap}} - \rho_{\text{bulk}} / \rho_{\text{tap}}) \times 100$$

2.5.5. Photomicroscopic observation of TS microspheres

Photomicroscopy has the advantage of providing a direct visual representation of the particles being measured. A photomicroscope can provide details about shape, crystal habit, and homogeneity of the tested sample. In the present study a diluted suspension of TS microspheres in liquid paraffin was mounted on a slide, and then a photograph for each microsphere was taken from the prepared slide.

2.6. Preparation and assay of TS capsules

Capsules were prepared by putting the equivalent of 7.5 mg of TS in the microsphere form into hard gelatin capsule of zero size. The procedure was done for each suggested formula based on their drug content. For assay, each TS capsule was emptied and its microsphere content was dissolved in methylene chloride and the drug was determined spectrophotometrically at 278 nm. The assay was done in triplicate.

2.7. In vitro dissolution and kinetic studies of TS capsules

In vitro drug release was studied according to the USP XXIV basket method using Dissolution Apparatus Type I (Pharma Test PTWII, Hamburg, Germany). The dissolution medium employed was 900 mL of HCl (pH 1.2) for 2 h which was then changed to 900 mL phosphate buffer (pH 6.8) at 37 ± 0.5°C. The basket speed was 50 rpm. At appropriate time intervals, 5 mL of each sample was taken and replaced by fresh dissolution media. The samples were analyzed at 278 nm by UV/VIS spectrophotometry.

3. Results and Discussion

3.1. Optimization results for preparation of microspheres

Box-Behnken design was used for formulating TS microspheres. This design deals with optimization of formulation variables to improve *in-vitro* release of TS capsules. A three-factors, three levels Box-Behnken design with speed (X₁), drug-polymer ratio (X₂) and percent of span 80 (X₃) as independent variables were selected for the formulation.

TS microspheres were prepared by the ESE technique. This method is generally known to be simple, reproducible and economical. Eudragit RSPM was used to control the release of TS from the microcapsules. The drug polymer ratios employed were 1:4, 1:6, and 1:8. Microspheres were formed in the presence of a small amount of aluminum tristearate. Flocculation was clearly recognized when no aluminum tristearate was added to the system. Specifically, with 5% aluminum tristearate, the microspheres were nearly uniform and free flowing with good reproducibility. Aluminum tristearate reduces the interfacial tension and prevents electrification and flocculation during the preparation of microspheres. Addition of excess aluminum tristearate (10-20%) to the system resulted in a large amount of aggregates. The action of aluminum tristearate as smoothing agent and liquid paraffin as external phase were used as part of the ESE technique while the surfactant (Span 80) was used as emulsifying agent.

3.2. Drug content determination

The production yield is a measure of accuracy of the microencapsulation technique, since it measures the actual weight of the prepared microspheres (drug and other excipients). This value was calculated by dividing the actual weight of the prepared TS microspheres by the theoretical weight. While the drug content determination measures the actual weight of TS itself inside the microspheres. The range of the production yield of the prepared microspheres was found to be between 46.7% and 98.7% as shown in Table 2. The greatest yield appeared in formula T₁₄ (98.7%) while

the lowest yield appeared in formula T₂ (46.7%). Formulae T₃, T₄, T₆, T₇, T₈, T₉, T₁₀, T₁₁, and T₁₂ showed a production yield above 85%. Formulae T₁ and T₅ had a production yield of 78.7 and 78.2%, respectively. The rank order of the drug content was measured by the deviation from the theoretical weight. Formula T₁₅ gave the best drug content of the prepared TS microspheres (140.1%), while formula T₂ showed the lowest value (51.8%).

3.3. Micromeritic properties

3.3.1. Particle size distribution

The particle size distribution of different formulae of TS microspheres was determined by the sieve analysis method. Formulae T₃, T₄, T₇, T₈, and T₉ exhibited the best distribution pattern as the largest weight determined lied between 500-315 µm. While, formulae T₇, T₁₀, and T₁₁ gave the second best group distribution as largest weight calculated lied between 800-500 µm. The remaining formulae exhibited either low or high distribution as the largest weight determined lied either below 200 µm or above 800 µm. The sieve analysis data of each formula was used to determine the average arithmetic mean diameter. The results obtained were in agreement with the weight distribution. The arithmetic mean diameters of low distribution gave values between 250-330 µm. while that of high distribution gave values between 500-610 µm. At the same time, the arithmetic mean diameter of the good distribution formulae lied between 330-500 µm. Probability scales were used to calculate the geometric mean diameter and geometric standard deviation. These values were obtained by plotting the particle size in micrometers on the x-axis versus the cumulative percent frequency under size (probability scale) on the y-axis. The geometric mean diameter for each formula was determined at the 50% size while the geometric standard deviation was

calculated by dividing the 50% size / 16% undersize.

3.3.2. Density, Hausner ratio, and compressibility index

The bulk densities of TS microspheres ranged from 0.190 g/cm³ to 0.467 g/cm³. While, the tap densities ranged from 0.333 g/cm³ to 0.666 g/cm³. Formula F₁₅ gave the lowest values for both bulk and tap densities. While, formulae T₅ and T₁₂ gave the highest values. The values of Hausner ratio below 1.2 indicated good flow while the values above 1.2 indicated poor flow properties. Formulae T₁, T₅, T₆, T₉, and T₁₀ showed good flow while the remaining formulae exhibited a values higher than 1.2. The values of percent compressibility below 20-21% exhibit good flow while the values greater than 21% indicate poor flow. Formulae T₁, T₅, T₆, T₉, and T₁₀ showed good flow while the remaining formulae exhibited values higher than 21%. It is obvious from the data in Table 3 that there was an inverse proportionality between the particle size and the particle number for TS microcapsules studied. The best formulae in terms of micromeritic properties were found to be T₂, T₁, T₁₅, T₁₃, and T₁₂.

3.3.3. Photo-microscopic determination of TS microcapsules

Photo-microscopic technique was used to get a clear view of the surface morphology of the prepared TS microspheres. Also, this technique reflects the efficiency of the ESE process. It was found that the majority of TS microcapsules were irregular in shape except formulae T₃ and T₉ in which the shape of the particles were semi-spherical, as observed in Figure 1.

3.4. In vitro release of TS capsules

In vitro release studies of TS capsules containing different drug-polymer ratios were evaluated by

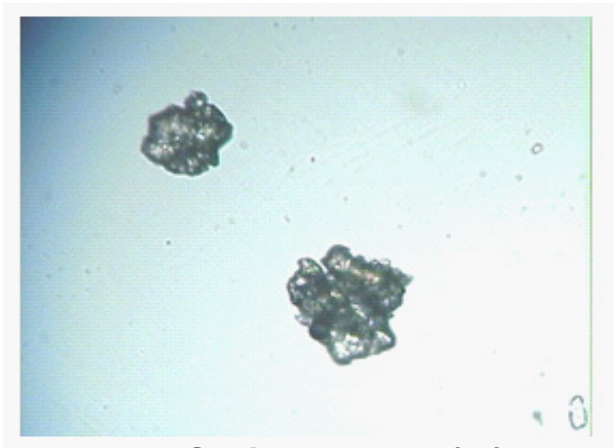
Table 2. Production yield and percentage recovery of TS microcapsules

Formula No.	Core/coat ratio	Production yield (%)	Theoretical drug content (mg)	Actual drug content (mg)	Drug content (%)
T ₁	1:4	78.7	20.00	26.76	133.80
T ₂	1:4	46.7	20.00	10.36	51.80
T ₃	1:4	91.2	20.00	13.76	68.80
T ₄	1:4	87.6	20.00	15.84	79.20
T ₅	1:6	78.2	14.26	9.42	66.05
T ₆	1:6	91.2	14.26	11.41	80.01
T ₇	1:6	92.2	14.26	13.53	94.88
T ₈	1:6	88.2	14.26	8.89	62.34
T ₉	1:6	90.3	14.26	13.44	94.24
T ₁₀	1:6	86.3	14.26	10.25	71.87
T ₁₁	1:6	96.3	14.26	9.36	56.63
T ₁₂	1:8	95.7	11.11	11.33	101.90
T ₁₃	1:8	80.3	11.11	13.07	117.60
T ₁₄	1:8	98.7	11.11	8.83	79.47
T ₁₅	1:8	83.3	11.11	15.56	140.10

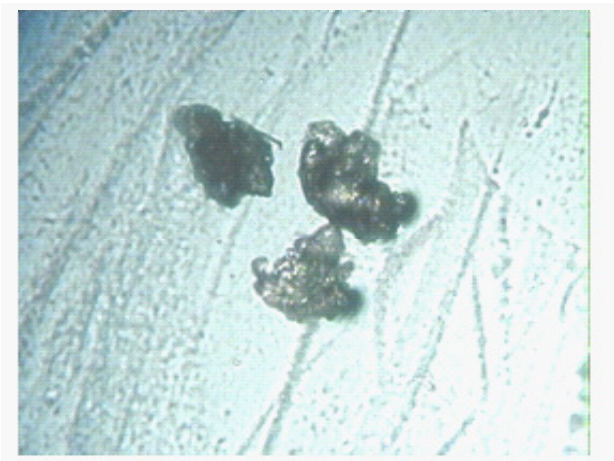
Table 3. Determination of density, Hausner ratio, % compressibility and specific surfaces of TS microcapsules

Formula No.	Density (g/cc)		Hausner ratio	Compressibility %	Specific surfaces	
	Bulk	Tap			S _w [†]	S _v ^{††}
T ₁	0.285	0.333	1.16	14.4	775	221
T ₂	0.400	0.533	1.33	24.9	458	183
T ₃	0.363	0.500	1.37	27.4	343	124
T ₄	0.200	0.307	1.54	34.8	907	181
T ₅	0.467	0.540	1.15	13.5	210	98
T ₆	0.414	0.462	1.11	10.3	218	90
T ₇	0.300	0.480	1.60	37.5	421	126
T ₈	0.375	0.502	1.33	25.2	366	137
T ₉	0.400	0.470	1.12	14.8	369	148
T ₁₀	0.446	0.480	1.07	07.1	244	109
T ₁₁	0.285	0.400	1.40	28.8	510	145
T ₁₂	0.421	0.666	1.58	36.8	339	143
T ₁₃	0.300	0.429	1.43	30.1	666	200
T ₁₄	0.401	0.546	1.36	26.5	288	115
T ₁₅	0.190	0.333	1.75	42.9	1162	221

[†] Surface area per unit weight; ^{††} Surface area per unit volume.



A: TS microcapsule (T₃)



B: TS microcapsule (T₀)

Figure 1. Photomicroscope images of TS microspheres.

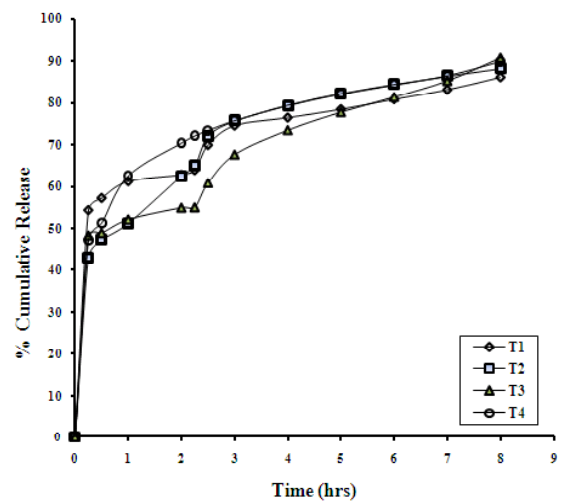


Figure 2. *In vitro* release of TS capsules containing drug: polymer ratio 1:4.

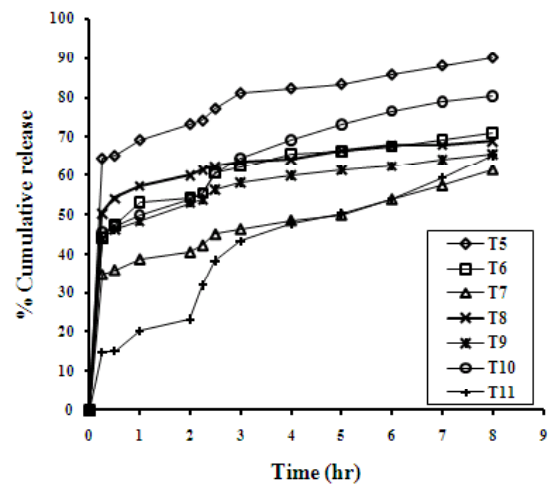


Figure 3. *In vitro* release of TS capsules containing drug: polymer ratio 1:6.

measuring the cumulative percent release. Figures 2-4 show the *in vitro* release of TS from capsules containing the drug and Eudragit in the ratios of 1:4, 1:6, and 1:8, respectively. The best formulae for *in vitro* release after a period of 8 h were observed to be T₁₁, T₇, T₁₂, T₉, and T₁₄. The investigated formulae containing different drug-polymer ratios (1:4, 1:6, and 1:8) were arranged, in ascending order, in terms of micromeritic properties and *in vitro* release. The best formulae in terms of both *in vitro* release and micromeritic properties were found to be T₁₁, T₁₂, T₉, T₂, and T₇.

3.5. Kinetic study of the *in vitro* release of TS capsules

The data of the *in-vitro* release from TS capsules were treated by different kinetic orders or systems to explain the release mechanism for each formula. The formulations were subjected to zero, first and second-order kinetic equations, as well as, to Higuchi's diffusion model, Hixson-Crowell cube root law and Baker-Lonsdale equation. Table 4 shows the kinetic

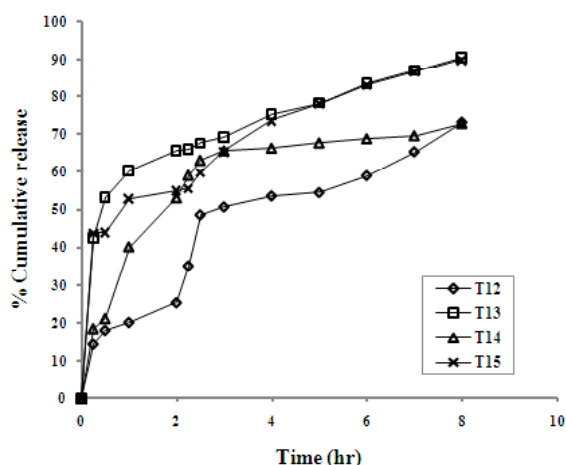


Figure 4. *In vitro* release of TS capsules containing drug: polymer ratio 1:8.

parameters for each formula according to the suitable order or system.

3.6. Data correlation with *in vitro* release and particle size

It was found that the particle size of the prepared microcapsules was an important factor affecting the *in vitro* release of the drug. Also the technique parameters had a great effect on *in vitro* release. So, the three levels of the Box-Behnken design studied were correlated with both *in vitro* release from TS capsules after 8 h on one side and particle size of TS microcapsules in the range 500-315 μm on the other side. These relationships are illustrated in Figure 5. It shows the factor range of the three levels (-1, 0, and +1) which indicate the minimum and maximum level of each item used. For example, -1 speed equals up to 500 rpm. Zero equals to 700 rpm and +1 equals to 900 rpm. It was found that increasing the speed of the apparatus would decrease and then increase the *in vitro* release after 8 h. The best speed for preparation of TS microspheres may be either 500 rpm or 900 rpm. The same effect was observed using the second level *i.e.* the drug-polymer ratio) but the increase of the *in vitro* release in the 1:4 ratio was found to be less than the 1:8 drug-polymer ratio. The best drug-polymer ratio was found to be 1:8, while, the effect of Span 80% was decreased gradually from 1% to 2%. The best percentage of Span 80 was found to be the lowest concentration, *i.e.* 1%.

Based on these figures it could be interpreted that the optimum *in vitro* release of TS after 8 h was obtained at a speed of 500 or 900 rpm using a 1:8 drug-polymer ratio and 1% of Span 80. On correlating the factor range versus the obtained particle size percent in the range from 500 μm to 315 μm of the prepared TS microspheres as seen in Figure 5B, the particle size percent studied would increase and then decrease by increasing the speed, drug-polymer ratio and the Span 80%.

Table 4. Kinetic parameters for *in vitro* release of TS capsules

Formula No.	Intercept	Slope	Correlation coefficient	Specific Rate constant (h^{-1})	$t_{1/2}$ (h)	Order of reaction
T ₁	1.662	0.065	0.985	0.150	4.608	First
T ₄	1.673	0.083	0.983	0.192	3.592	First
T ₂	0.012	0.008	0.995	0.008	1.132	Second
T ₁₀	0.014	0.004	0.991	0.004	2.237	Second
T ₁₄	0.015	0.002	0.924	0.002	3.403	Second
T ₅	58.37	11.33	0.989	11.33	19.46	Diffusion
T ₆	39.83	11.52	0.979	11.52	18.82	Diffusion
T ₈	48.88	7.668	0.979	7.668	42.50	Diffusion
T ₉	39.85	9.488	0.990	9.788	27.76	Diffusion
T ₃	0.768	0.209	0.989	0.209	4.561	H-C [†]
T ₇	0.606	0.077	0.993	0.077	12.22	H-C
T ₁₅	0.713	0.223	0.995	0.223	4.271	H-C
T ₁₁	0.004	0.012	0.985	0.012	4.294	B&L*
T ₁₂	0.005	0.016	0.969	0.016	3.248	B&L
T ₁₃	0.044	0.028	0.993	0.028	1.919	B&L

[†]Hixson Crowell cube root law; * Baker-Lonsdal equation

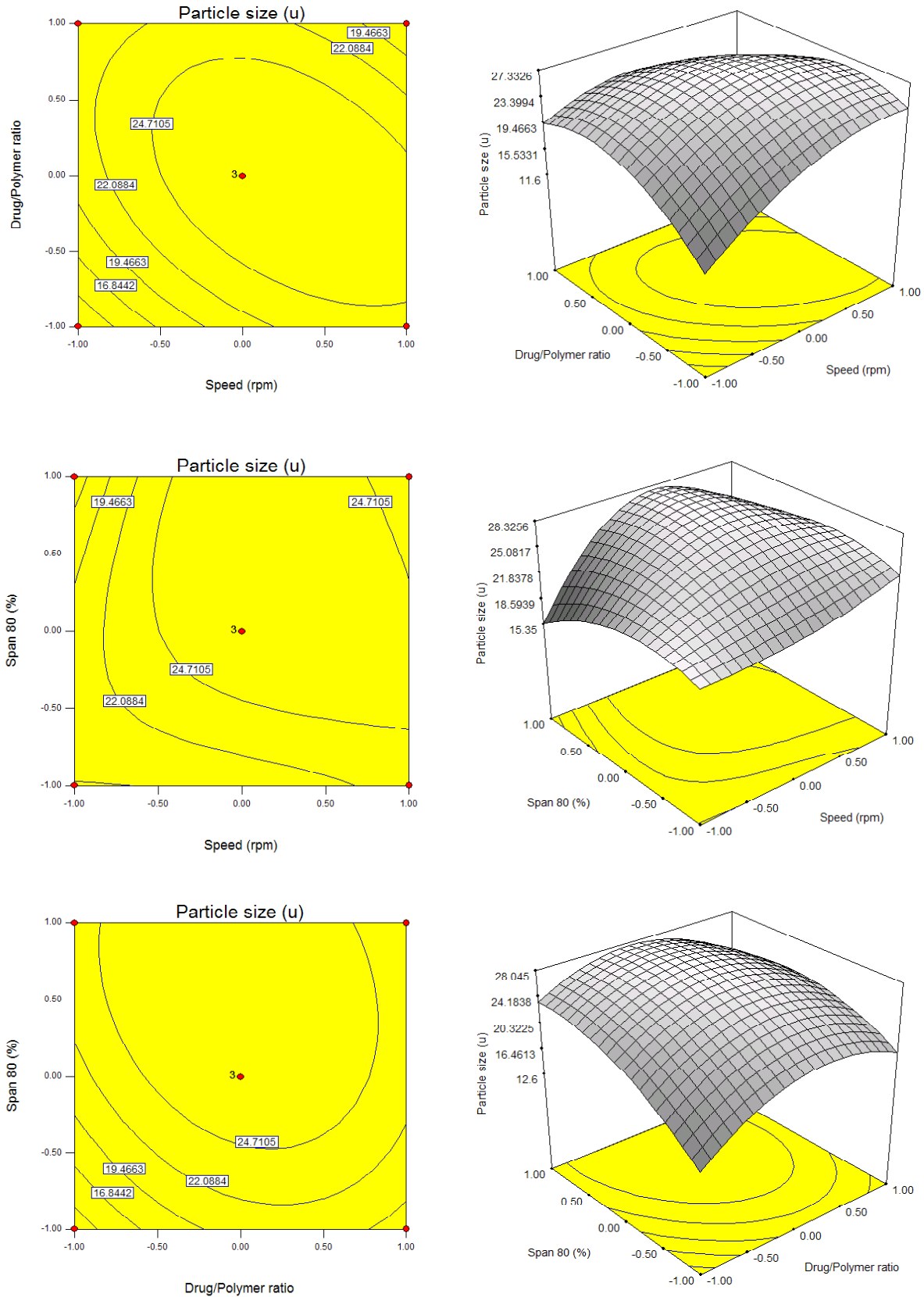


Figure 5. Response surface plots showing the effect of different levels of independent variable (X) on particle size (Y₁). X₁ = speed (rpm); X₂ = drug : polymer; X₃ = % span 80.

3.7. Characterization of TS microspheres and formulated capsules using response surface methodology

The dependent variables studied were Y_1 (percent particle size range between 500-315 μm) and Y_2 (cumulative percent released after 8 h). Based on the experimental design, the factor combination resulted in different TS release rates. The range of response for Y_1 was 29.60% in T_7 (maximum) and 11.6% in T_1 (minimum). The range of response for Y_2 was 90.7% in T_3 (maximum) and 61.3% in T_7 (minimum). The dependent and independent variables were related using mathematical relationships obtained from the statistical package. The polynomial equation obtained was:

$$Y_1 \text{ (Particle size)} = 26.95 + 1.58X_1 + 1.46X_2 + 1.09X_3 - 4.95X_1^2 - 5.82X_2^2 - 2.15X_3^2 - 1.96X_1X_2 + 0.55X_1X_3 - 1.79X_2X_3$$

$$Y_2 \text{ (Dissolution after 8 h)} = 62.33 - 0.55X_1 - 3.50X_2 - 7.38X_3 + 5.72X_1^2 + 16.87X_2^2 + 6.42X_3^2 + 3.27X_1X_2 - 1.13X_1X_3 - 5.02X_2X_3$$

The equations represent the quantitative effect of process variables (X_1 , X_2 , and X_3) and their interactions on the responses (Y_1 and Y_2). The values of X_1 , X_2 , and X_3 were substituted in the equation to obtain the theoretical values of Y_1 and Y_2 . The theoretical (predicted) values were compared with the observed values and were found to be in reasonably close agreement. Table 5 shows the observed, predicted and residual values for particle size, while Table 6 shows the observed, predicted and residual values for the *in vitro* release after 8 h.

The relationship between the dependent and independent variables were further elucidated using contour plots and response surface plots. In Figure 6 are the contour plots showing the effect of factors X_1 ,

X_2 , and X_3 on the response Y_1 , where the small circles indicate levels at which maximum response would be observed. Figure 7 shows the response surface plots for the independent variables and their influence on the response Y_1 (particle size). At low levels of X_3 (Span 80), Y_1 increased from 19.36 to 23.26% when the speed (X_1) was increased from 500 to 900 rpm. At high levels of X_3 , Y_1 was increased from 15.35 to 21.45% when the speed (X_1) was increased from 500-900 rpm. At low levels of X_1 (Speed), Y_1 increased from 15.3 to 19.36% when the span 80% (X_3) was decreased from 2 to 1%. At high levels of X_1 , Y_1 was increased from 21.45 to 23.26% when the span 80 (X_3) was decreased from 2 to 1%. At low levels of X_3 (Span 80), Y_1 was increased from 12.6 to 18.1% when the drug-polymer ratio (X_2) was increased from 1:4 to 1:8. At high levels of X_3 , Y_1 was decreased from 23.45 to 21.78% when the drug-polymer ratio (X_2) was increased from 1:4 to 1:8. At low levels of drug-polymer ratio (X_2) Y_1 was decreased from 23.4 to 12.6 when the span 80 (X_3) was decreased from 2 to 1%. At high levels of X_2 , Y_1 was decreased from 21.78 to 18.1% when the span 80 (X_3) was decreased from 2 to 1%. At low levels of X_1 (Speed), Y_1 was increased from 11.6 to 19.45% when the drug-polymer ratio (X_2) was increased from 1:4 to 1:8. At high levels of X_1 , Y_1 was decreased from 23.75 to 16.85% when the drug-polymer ratio (X_2) was increased from 1:4 to 1:8. At low levels of drug-polymer ratio (X_2) Y_1 was decreased from 23.75 to 11.6% when the speed (X_1) was decreased from 900 to 500 rpm. At high levels of X_2 , Y_1 was increased from 16.85 to 19.45% when the speed (X_1) was decreased from 900 to 500 rpm.

Figure 5 represents the contour plots showing the effects of factors X_1 , X_2 , and X_3 on the response Y_1 (particle size), where the small circles indicate levels at which maximum response would be observed. Figure 6 shows the response surface plots for the independent variables and their influence on the response Y_2

Table 5. Actual values, predicted values and residuals for particle size

Formula No.	Variable levels*			Particle size			Dissolution after 8 h		
	X_1	X_2	X_3	Actual	Pred.	Residual [†]	Actual	Pred.	Residual [†]
T_1	-1	-1	0	11.60	11.18	0.42	86.20	92.25	-6.05
T_4	0	-1	-1	12.60	14.64	-2.04	88.30	91.48	-3.93
T_2	0	-1	1	23.45	20.40	3.05	90.70	86.77	3.93
T_{10}	1	-1	0	23.75	20.27	3.48	89.90	84.60	5.30
T_{14}	-1	0	-1	19.36	17.74	1.62	90.50	81.27	9.23
T_5	-1	0	1	15.35	18.81	-3.46	70.90	68.78	2.13
T_6	0	0	0	29.60	26.95	2.65	61.30	62.33	-1.03
T_8	0	0	0	23.60	26.95	-3.35	69.00	62.33	6.67
T_9	0	0	0	27.65	26.95	0.70	65.70	62.33	3.37
T_3	1	0	-1	23.26	19.80	3.46	80.30	82.43	-2.12
T_7	1	0	1	21.45	23.08	-1.63	65.20	65.43	-0.23
T_{15}	-1	1	0	19.45	18.03	1.42	73.40	78.70	-5.30
T_{11}	0	1	-1	18.10	21.15	-3.05	90.60	94.52	-3.92
T_{12}	0	1	1	21.78	19.74	2.04	72.90	69.73	3.18
T_{13}	1	1	0	16.85	17.27	-0.42	90.20	84.15	6.05

* X_1 = speed (rpm); X_2 = drug: polymer; X_3 = % span 80; [†] Residual value = actual value - predicted value.

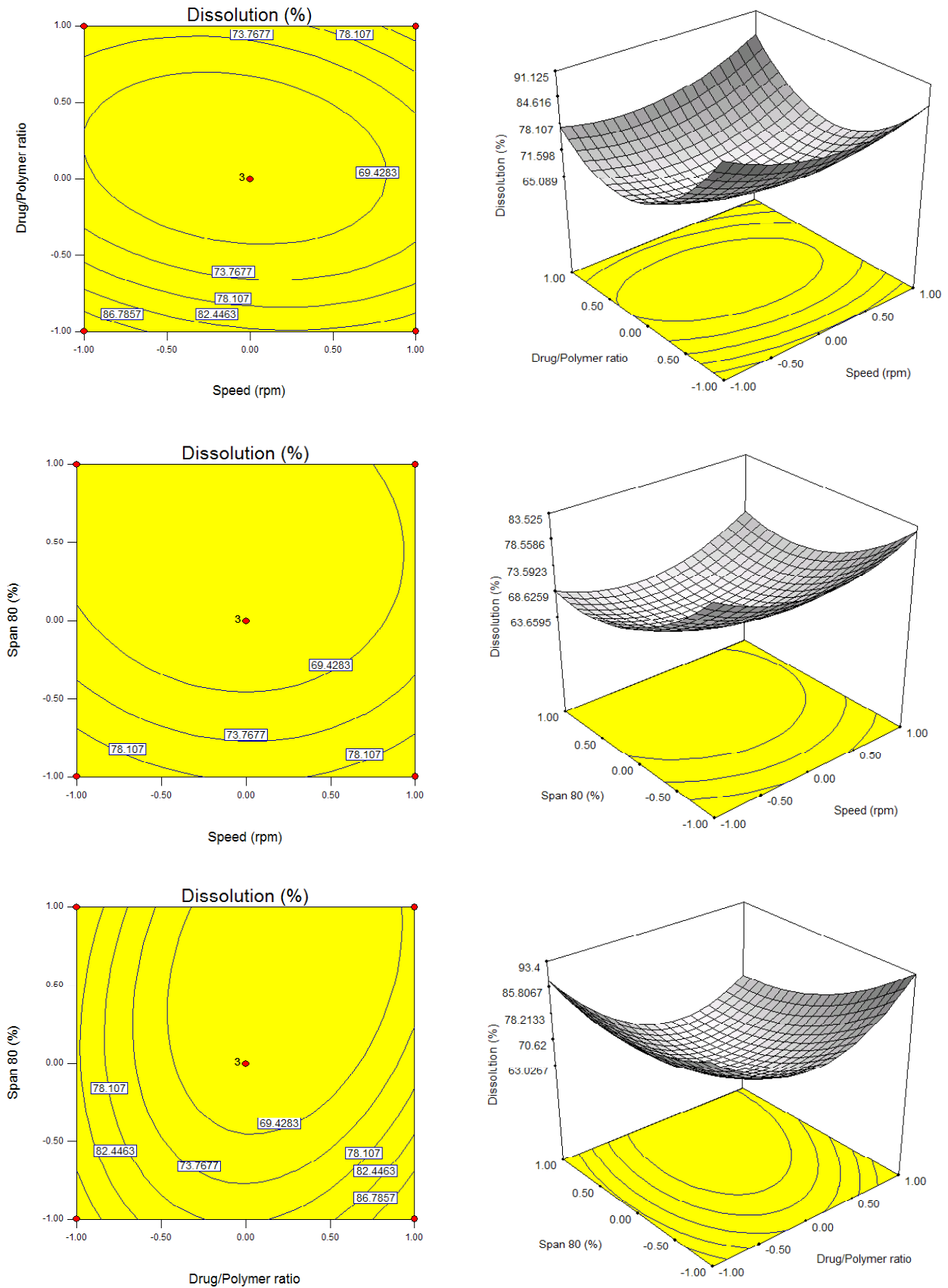


Figure 6. Response surface plots showing the effect of different levels of independent variable (X) on percent drug release from TS microspheres after 8 h (Y₂). X₁ = speed (rpm); X₂ = drug: polymer; X₃ = % span 80.

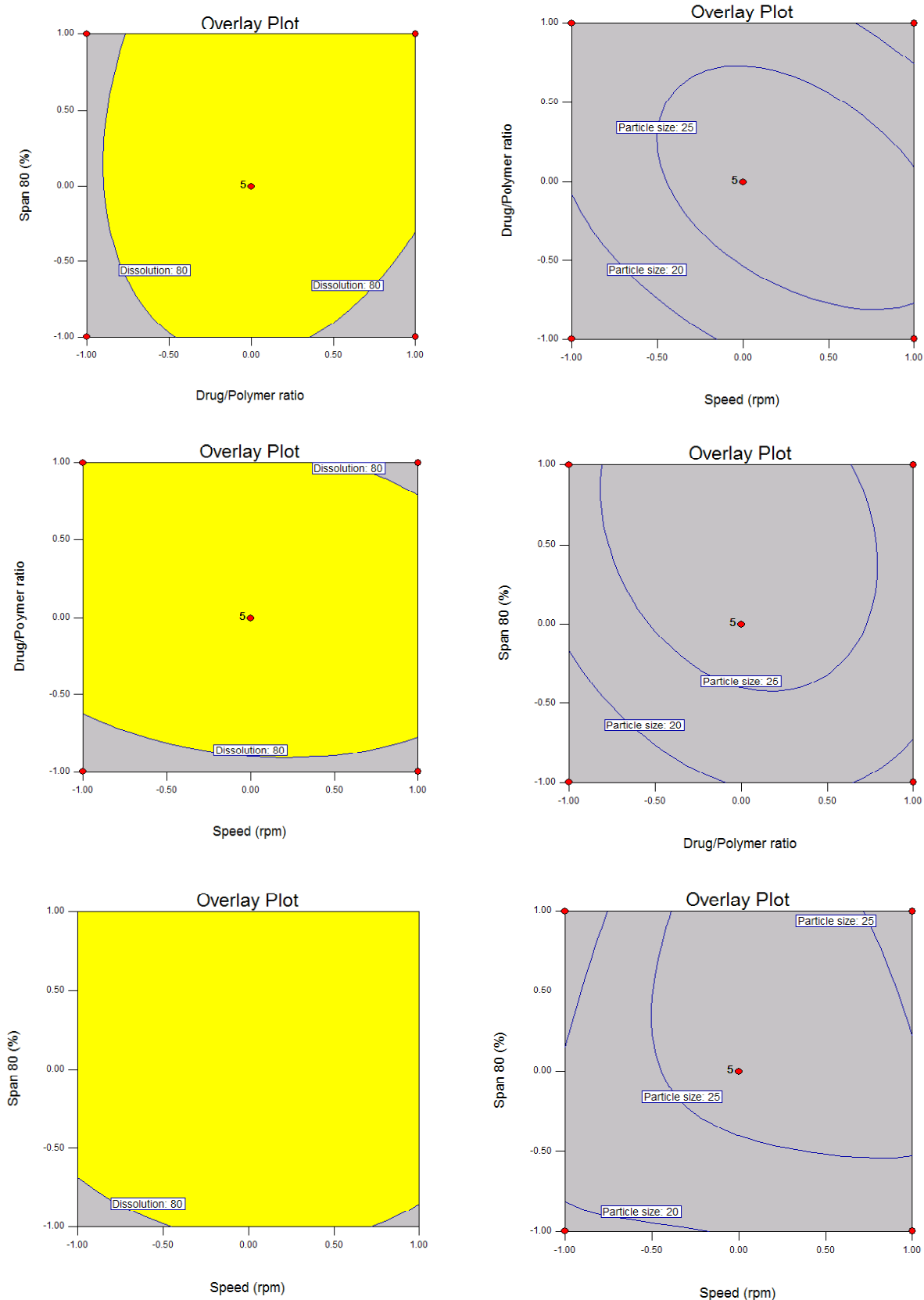


Figure 7. Overlay plots showing the effect of different levels of independent variable (X) on the dependent variable; Y_1 (right) particle size and Y_2 (left) % drug release. X_1 = speed (rpm); X_2 = drug: polymer; X_3 = % span 80.

(dissolution after 8 h). At low levels of X_3 (Span 80%), Y_2 was decreased from 90.5 to 80.3% when the speed (X_1) was increased from 500 to 900 rpm. At high levels of X_3 , Y_2 was decreased from 70.9 to 65.2% when the speed (X_1) was increased from 500-900 rpm. At low levels of X_1 (Speed), Y_2 was increased from 70.9 to 90.5% when the span 80% (X_3) was decreased from 2 to 1%. At high levels of X_1 , Y_2 was increased from 90.5 to 89.5% when the span 80 (X_3) was decreased from 2 to 1%. At low levels of X_3 (Span 80%), Y_2 was increased from 88.3 to 90.6 % when the drug-polymer ratio (X_2) was increased from 1:4 to 1:8. At high levels of X_3 , Y_2 was decreased from 90.7 to 72.9% when the drug-polymer ratio (X_2) was increased from 1:4 to 1:8. At low levels of drug-polymer ratio (X_2), Y_2 was decreased from 90.7 to 88.3% when the span 80% (X_3) was decreased from 2 to 1%. At high levels of X_2 , Y_2 was increased from 72.9 to 90.6% when the span 80 (X_3) was decreased from 2 to 1%. At low levels of X_1 (Speed), Y_2 was decreased from 86.2 to 73.4% when the drug-polymer ratio (X_2) was increased from 1:4 to 1:8. At high levels of X_1 , Y_2 was increased from 89.5 to 90.2% when the drug-polymer ratio (X_2) was increased from 1:4 to 1:8. At low levels of drug-polymer ratio (X_2), Y_2 was decreased from 89.9 to 86.2% when the speed (X_1) was decreased from 900 to 500 rpm. At high levels of X_2 , Y_2 was decreased from 90.2 to 73.4% when the speed (X_1) was decreased from 900 to 500 rpm. By superimposing the contour plots of both responses we can delimit the optimal zone (Figure 7). We consider that the average particle size is optimum 20 to 25 μ and a satisfactory drug release will be achieved with a value more than 80%. This zone has been verified with an experimental point (speed 700 rpm, drug/polymer ratio 1:5.6, span 0.85%) which leads to optimal particle size and maximum drug release.

4. Conclusions

From the present investigations it can be concluded that the emulsion solvent evaporation technique is an effective method for the preparation of terbutaline sulfate microspheres using Eudragit RSPM as a release retardant. The application of a factorial design approach helped in identifying the critical factors in the preparation and optimization of microcapsules. The results of the experimental study confirm that the polymer and emulsifier concentration as well as the speed of emulsification, significantly influence the dependent variables, *i.e.*, particle size and *in vitro* release. The total rank-order of terbutaline sulfate concerning the micromeritic parameters and the *in-vitro* dissolution could be arranged in a descending order as follow: $T_{12} > T_{11} > T_9$. An accelerated stability study of the TS microspheres will be a continuation of this work.

References

1. Cuna M, Vila Jato JL, Torres D. Controlled release liquid suspensions based on ion-exchange particles entrapped within acrylic microcapsules. *Int J Pharm.* 2000; 199:151-158.
2. Swarbrick J, Boylan J. Controlled and Modulated-Release Drug-Delivery Systems. In: *Encyclopedia of Pharmaceutical Technology* (Swarbrick J, Boylan J, eds.). Marcel Dekker, Inc., New York, 1990; pp. 802-851.
3. Bozdag S, Calys S, Kas HS, Ercan MT, Peksoy I, Hyncal AA. *In vitro* evaluation and intra-articular administration of biodegradable microspheres containing naproxen sodium. *J Microencapsul.* 2001; 18:443-456.
4. Tuncay M, Calys S, Kas HS, Ercan MT, Peksoy I, Hyncal AA. *In vitro* and *in vivo* evaluation of diclofenac sodium loaded albumin microspheres. *J Microencapsul.* 2000; 17:145-155.
5. Song M, Li N, Sun S, Tiedt LR, Liebenberg W, de Villiers MM. Effect of viscosity and concentration of wall former, emulsifier and pore inducer on the properties of amoxicillin microcapsules prepared by emulsion solvent evaporation. *Farmaco.* 2005; 60:261-267.
6. Eroglu H, Kas HS, Oner L, Turkoglu OF, Akalan N, Sargon MF, Ozer N, Hyncal AA. *In vitro/in vivo* characterisation of bovine serum albumin microspheres containing dexamethasone sodium phosphate. *STP Pharma Sci.* 2000; 10:303-308.
7. Patrick BD, James WG. Preparation of microspheres by the solvent evaporation technique. *J Control Release.* 2000; 69:445-454.
8. Soppimath KS, Kulkarni AR, Aminabhavi TM, Bhaskar C. Cellulose acetate microspheres prepared by o/w emulsification and solvent evaporation method. *J Microencapsul.* 2001; 18:811-817.
9. Perumal D. Microencapsulation of ibuprofen and Eudragit RS 100 by the emulsion solvent diffusion technique. *Int J Pharm.* 2001; 218:1-11.
10. Palmieri G, Bonacucina G, Martino P, Martelli S. Microencapsulation of semisolid ketoprofen/polymer microspheres. *Int J Pharm.* 2002; 242:175-178.
11. Mateovic T, Kriznar B, Bogataj M, Mrhar A. The influence of stirring rate on biopharmaceutical properties of Eudragit RS microspheres. *J Microencapsul.* 2002; 19:29-36.
12. Kim BK, Hwang JB, Park HJ. Preparation and characterization of drug-loaded polymethacrylate microspheres by an emulsion solvent evaporation method. *J Microencapsul.* 2002; 19:811-822.
13. Bhalerao SS, Lalla JK, Rane MS. Study of processing parameters influencing the properties of diltiazem hydrochloride microspheres. *J Microencapsul.* 2001; 18:299-307.
14. Obeidat WM, Price JC. Viscosity of polymer solution phase and other factors controlling the dissolution of theophylline microspheres prepared by the emulsion solvent evaporation method. *J Microencapsul.* 2003; 20:57-65.
15. Kang F, Singh J. Effect of additives on the release of a model protein from PLGA microspheres. *AAPS PharmSciTech.* 2001; 2:30.
16. Aulton ME. *Pharmaceutical Technology*. In:

- Pharmaceutics: The Science of Dosage Forms Design (Aulton ME, ed.). Churchill Livingstone, New York, 1998; pp. 600-615.
17. Palmieri GF, Grifantini R, Martino PD, Martelli S. Emulsion/solvent evaporation as an alternative technique in pellet preparation. *Drug Dev Ind Pharm.* 2000; 26:1151-1158.
 18. Yang C, Tsay S, Tsiang RC. Encapsulating aspirin into a surfactant free ethyl cellulose microspheres using non-toxic solvents by emulsion solvent evaporation technique. *J Microencapsul.* 2001; 18:223-236.
 19. Hariharan M, Price JC. Solvent emulsifier and drug concentration factors in poly-(D,L-lactic acid) microspheres containing hexamethylamine. *J Microencapsul.* 2002; 19:95-109.
 20. The United States Pharmacopoeia 25 and National Formulary 20. US Pharmacopoeial Convention Inc. 12th ed., 2002; pp. 1658.
 21. Ahuja S, Ashman J. Terbutaline sulfate. In: *Analytical Profiles of Drug Substances* (Florey K, ed.). Academic Press, New York, 1990; pp. 601-623.
 22. Udem BJ, Lichtenstein LM. Drugs used in the treatment of asthma. In: *Goodman and Gilman's-The pharmacological basis of therapeutics* (Hardman JG, Limbird LE, Gilman AG, eds.). McGraw-Hill Medical Publishing Division, New York, 2001; pp. 736-789.
 23. Manekar NC, Puranik PK, Joshi SB. Prolonged released terbutaline sulphate microcapsules. *J Microencapsul.* 1991; 8:521-523.
 24. Manekar NC, Puranik PK, Joshi SB. Microencapsulation of terbutaline sulphate by solvent evaporation technique. *J Microencapsul.* 1992; 9:481-487.
 25. Kim CK, Kim MH. Preparation and evaluation of sustained release microspheres of terbutaline sulfate. *Int J Pharm.* 1994; 106:213-219.
 26. Sahin S, Selek H, Ponchel G, Ercan MT, Sargon M, Hincal AA, Kas HS. Preparation, characterization and *in vivo* distribution of terbutaline sulfate loaded albumin microspheres. *J Control Release.* 2002; 82:345-358.
 27. Lehmann K, Dreher D. Mixtures of aqueous polymethacrylate dispersions for drug coating. *Drugs Made Ger.* 1988; 31:101-102.
 28. Vecchio C, Fabiani F, Gazzaniga A. Use of colloidal silica as a separating agent in film forming processes performed with aqueous dispersion of acrylic resins. *Drug Dev Ind Pharm.* 1995; 21:1781-1787.
 29. Jovanvic M, Jovicic G, Duvic Z, Agbaba D, Nikolic L. Effect of fillers and lubricants on acetylsalicylic acid release kinetics from Eudragit matrix tablets. *Drug Dev Ind Pharm.* 1997; 23:595-602.
 30. Kibbe AH. In: *Hand Book of Pharmaceutical Excipients* 3rd ed. American Pharmaceutical Association, London, UK, 2000; pp. 401-406.
 31. Box GEP, Behnken DW. Some new three level designs for the study of quantitative variables. *Technometrics.* 1960; 2:455-475.
 32. Krishna S, Manohar B, Divakar S, Prapulla SG, Karanth NG. Optimization of isoamyl acetate production by using immobilized lipase from *Mucor miehei* by response surface methodology. *Enzyme Microb Technol.* 2000; 26:131-136.
 33. El-Helow ER, Abdel-Fattah YR, Ghanem KM, Mohamad EA. Application of the response surface methodology for optimizing the activity of an aprE-driven gene expression system in *Bacillus subtilis*. *Appl Microbiol Biotechnol.* 2000; 54:515-520.
 34. Khan MA, Vaithiyalingam SR, Faltinek J, Reddy IK, Zaghoul AA. Response surface methodology to obtain naproxen controlled release tablets from its microspheres with Eudragit L100-55. *J Microencapsul.* 2001; 18:651-662.
 35. Annadurai G, Juang RS, Lee DJ. Factor optimization for phenol removal using activated carbon immobilized with *Pseudomonas putida*. *J Environ Sci Health Part A Tox Hazard Subst Environ Eng.* 2002; 37:149-161.
 36. Nazzal S, Nutan M, Palamakula A, Shah R, Zaghoul AA, Khan MA. Optimization of a self-nanoemulsified tablet dosage form of ubiquinone using response surface methodology: effect of formulation ingredients. *Int J Pharm.* 2002; 20:103-114.
 37. The United States Pharmacopoeia 25 and National Formulary 20, 12th ed. US Pharmacopoeial Convention Inc. 2002; pp.786, 204.
 38. Martin A. In: *Physical Pharmacy: Physical and Chemical Principles in the Pharmaceutical Sciences*, 4th Ed. Martin A, Lea, Febiger, London, UK, 1993; pp. 423-452.
 39. Carr RL. Evaluating flow properties of solids. *Chem Eng.* 1965; 18:163-168.

(Received March 15, 2009; Accepted May 9, 2009)

Original Article

Stability studies of the effect of crosslinking on hydrochlorothiazide release

Aliaa N. Elmeshad¹, Manal K. Darwish^{2,*}

¹ Department of Pharmaceutics, Faculty of Pharmacy; Cairo University, Cairo, Egypt;

² Department of Pharmaceutics, Faculty of Pharmacy (Girls), Al-Azhar University, Cairo, Egypt.

ABSTRACT: The aim of this study was to determine the changes in the *in vitro* drug release from cross-linked hard gelatin capsules containing a water-insoluble drug. An immediate release hydrochlorothiazide (HCTZ) capsule formulations containing drug, lactose, starch 1500 were prepared and exposed to accelerated stability study (40°C/ambient RH (relative humidity), 40°C/60% RH, 40°C/75% RH, and 40°C/90% RH) in closed dark bottles for 4 weeks. Notable decrease in drug dissolution was observed after 4 weeks in all humidity conditions as compared with freshly prepared capsules. In an attempt to overcome capsule cross-linking, glycine alone, citric acid alone and both glycine and citric acid were added to the prepared formulations. In all humidity conditions, addition of glycine alone or citric acid alone did not affect the decrease in dissolution profile. On the other hand, addition of both glycine and citric acid together was found to prevent capsule cross-linking completely. Fourier transfer infrared (FTIR) spectroscopy and differential scanning calorimetry (DSC) were performed on blank capsules (with no glycine or citric acid) and after storage for 4 weeks to identify the physicochemical changes in drug and other capsule components hence its effect on dissolution.

Keywords: Hard gelatin capsule, cross-linking, hydrochlorothiazide, relative humidity, starch

1. Introduction

Exposure of a dosage form to high temperature and relative humidity is an attempt to assess its long-

term stability in a relatively short period of time (1). While accelerated conditions at temperatures greater than 30°C and humidities outside the range of 40-60% are not recommended by gelatin capsule shell manufactures (2), storage conditions more stressful than these are routinely required by governmental agencies as evidence of the long-term stability of the dosage form and the drug entity itself (3). Gelatin capsule cross-linking is a well known phenomenon that results in reduced dissolution of capsule products by time and/or under accelerated conditions. Cross-linking is facilitated when the formulation in the capsule either contains a carbonyl compound as an impurity or decomposes into a carbonyl compound or derivative such as formaldehyde (4,5). Combination products of various antihypertensive drugs with hydrochlorothiazide (HCTZ) are routinely formulated to augment their pharmacological effects or to provide step-up therapy (6). HCTZ when incorporated in hard gelatin capsules can undergo hydrolysis with the formation of formaldehyde and 4-amino-6-chloro-1,3-benzenedisulfonamide (free amine) (7,8). The degradation of HCTZ in a dosage form is undesirable since the US Pharmacopeia (USP) sets a tight limit for the free amine content of not more than 1% of the HCTZ potency due to toxicological reasons. On the other hand, by time and/or under the accelerated conditions, formaldehyde reacts with the amino acid groups within the gelatin shell to generate a cross-linked structure. This leads to the formation of a very thin, tough, and water insoluble film noted around the capsule contents during dissolution testing, this water-insoluble thin film acts as a barrier, restricting drug release (9). The purpose of the present study is to evaluate the effect of storage conditions on the disintegration and dissolution of HCTZ from hard gelatin capsule. In addition, the study aimed to indicate that cross-linking has a great impact on the results of the *in vitro* dissolution testing which is commonly employed as a method to assess the stability of drug products (10). Besides, the study aims to overcome this capsule cross-linking problem throughout all humidity conditions.

*Address correspondence to:

Dr. Manal K. Darwish, Pharmaceutics Department, Faculty of Pharmacy (Girls), Al-Azhar University, Cairo, Egypt.

e-mail: maboushady2000@yahoo.com

2. Materials and Methods

2.1. Materials

Hydrochlorothiazide was a kind gift from Hikma-Egypt Pharmaceuticals, 6th October City, Egypt. Lactose monohydrate powder was purchased from Cooper (Melun, France), pre-gelatinized starch (Starch[®] 1500) from Colorcon (Shizuoka, Japan), glycine from Winlab Laboratory Chemicals (Leicestershire, UK), citric acid and hydrochloric acid (34%) from Adwic (Cairo, Egypt). Magnesium stearate was supplied by SEDICO Pharmaceutical Co., 6th October City, Egypt. Capsules (size 1) were Coni-Snap[®] type (Capsugel, Colmar, France). All chemicals were of commercial analytical grade.

2.2. Preparation of capsules

The composition of the HCTZ capsules is shown in Table 1 as follows: Formulation (A) is the blank formula with neither glycine nor citric acid. Formulation (B) contains citric acid alone. Formulation (C) contains glycine alone, while formulation (D) contains both glycine and citric acid. All ingredients were passed through sieve #40, properly mixed together, and carefully filled into gelatin capsule.

2.3. In vitro dissolution study

Dissolution was performed using USP Apparatus 2 (Vankel Industries, Cary, NC, USA) at 100 ± 1 rpm in 900 mL of SGF (pH 1.2) at $37 \pm 0.5^\circ\text{C}$. To avoid floating, the capsules were ballasted by using a wire. Samples were filtered through a $0.45 \mu\text{m}$ pore size membrane filter (Millipore Co., Bedford, MA, USA) and analyzed spectrophotometrically (Shimadzu, model-UV-1601 PC, Kyoto, Japan) at 271 nm. The dissolution medium was replenished with fresh SGF (pH 7.4) maintained at 37°C . A cumulative correction factor was exploited to compensate for the withdrawn samples. Data were computed with reference to a standard calibration curve of the drug ($r = 0.999$) and the values obtained were the mean of three determinations. For dissolution stability evaluation, the capsules were packed in amber-colored glass containers and were exposed to $40^\circ\text{C}/\text{ambient RH}$, $40^\circ\text{C}/60\% \text{RH}$,

$40^\circ\text{C}/75\% \text{RH}$, and $40^\circ\text{C}/90\% \text{RH}$ in a stability cabinet (Climacell, Medcenter, Einrichtungen GmbH, MMM group, Germany) for 4 weeks after which dissolution of all stored formulations was performed under the same conditions previously mentioned.

2.4. Fourier transfer infra-red spectroscopy (FTIR)

Samples (2-3 mg) of the fresh and stored capsules were mixed each with about 100 mg of dry potassium bromide, and were compressed into discs under pressure of 10-15 pounds/inch². The FTIR spectra were recorded.

2.5. Differential scanning calorimetry (DSC)

The instrument was calibrated using indium. Samples (3.49-5.8 mg) of the fresh and stored capsules were weighed directly into platinum pans and scanned between $80-140^\circ\text{C}$ at a rate of $10^\circ\text{C}/\text{min}$. Dry nitrogen was used as a carrier gas with a flow rate of 30 mL/min.

2.6. Data analysis

A two factors three variables factorial is used which requires 9 experiments. The two factors X_1 , humidity percent and X_2 , addition of citric/glycine are represented by -1, 0, and +1, analogous to the low, middle and high values respectively (Table 2).

The following quadratic model was built to describe the response:

$$Y_i = b_0 + b_1X_1 + b_2X_2 + b_{11}X_1^2 + b_{12}X_2^2 + b_{13}X_1X_2$$

where y is the response, x the factors, and b the coefficients of each term calculated by multiple regression analysis. The responses studied for the drugs were the disintegration time (Y_1), amount dissolved or dissolution after 10 min (Y_2) and after 20 min (Y_3).

3. Results and Discussion

3.1. In vitro dissolution study

Complete drug release was observed from the prepared HCTZ capsules after 20 min as shown in Figure 1. This

Table 1. Composition of different HCTZ formulations

Ingredients	Formulations (%w/w)			
	A	B	C	D
Hydrochlorothiazide	50	50	50	50
Lactose	244	242.2	235.25	233.5
Citric acid	-	1.75	-	1.75
Glycine	-	-	8.75	8.75
Starch 1500	52.5	52.5	52.5	52.5
Magnesium stearate	3.5	3.5	3.5	3.5

Table 2. Experimental domains and coding of the variables

Variables	Levels		
	-1	0	+1
Citric/glycine (X_1)	Citric	Glycine	Both
Humidity (X_2)	60	75	90
Responses			
Y_1	disintegration time of capsule		
Y_2	dissolution after 10 min		
Y_3	dissolution after 20 min		

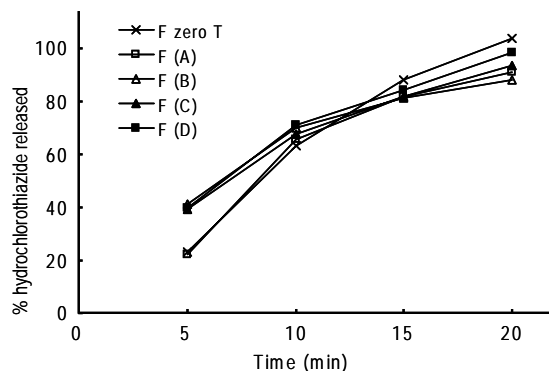


Figure 1. Percent HCTZ released (F zero time) and after 4 weeks at 40°C/ambient humidity.

is due to the presence of the super-disintegrant starch 1500 which acts by absorbing water, swelling, and producing the fast disintegration effect. After 4 weeks, there was a slight drop in the dissolution profiles for formulations A, B, and C at 40°C/ambient humidity, while formulation (D) showed no significant change in drug release ($p > 0.05$) (Figure 1). After 4 weeks, storage at 40°C/60, 75, or 90% RH, there was a significant drop in the dissolution profiles for formulations A, B, and C ($p < 0.05$), while formulation (D) exhibited no change in drug release. This is illustrated in Figure 2 and Table 3 in which formulation (D) gave maximum $DP_5\%$ (percent drug dissolved in 5 min), maximum $DP_{20}\%$ (percent drug dissolved in 20 min), and maximum DE_{20} (Dissolution efficiency at $t = 20$ min). At all accelerated conditions, the remarkable decrease in dissolution was attributed to the formation of trace amounts of formaldehyde due to hydrolysis of HCTZ in humid environment, which interact with the amino acid groups within gelatin shell to generate a cross-linked structure and it becomes less soluble in aqueous media and thus decreasing the drug release from the capsule (11). In addition, formaldehyde which is a highly reactive substance, reacts with starch 1500 leading to the loss of its swelling capacity (12), hence retarding its disintegration effect. Addition of citric acid (formulation B) was found to improve the dissolution slightly. This is due to the fact that the hydrolysis process of HCTZ is a pH dependent, so through manipulation of pH by adjusting the pH of the capsule content with citric acid to nearly 5.0 (optimums pH for HCTZ), hydrolysis of drug and subsequent formaldehyde formation will be reduced, thereby reducing gelatin crosslinking (13). Addition of glycine (formulation C) also improves the dissolution profiles as it functions as a carbonyl scavenger in gelatin capsule formulations, preventing the interaction of the aldehyde with the gelatin shell, thereby preventing gelatin cross-linking (14). It is even reported that if the formaldehyde, initially present in the capsule fill, is scavenged by the use of glycine, it prevents or reduces the further introduction of aldehyde. Formulations containing both citric acid and glycine exhibited no decrease in dissolution profiles. It appeared that citric acid

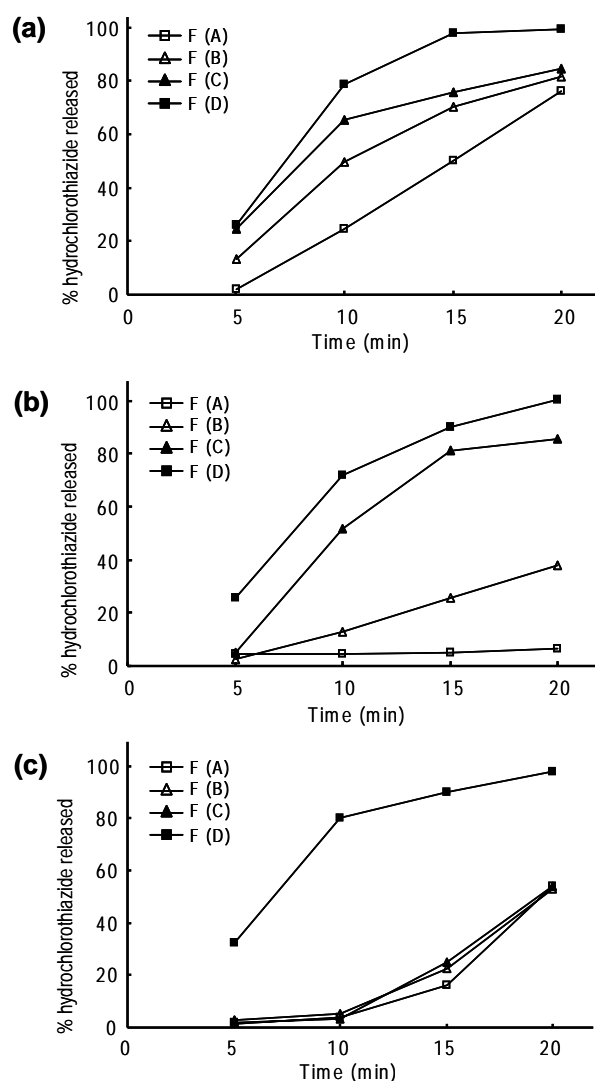


Figure 2. Percent HCTZ released after 4 weeks at (a) 40°C/60% RH, (b) 40°C/75% RH, and (c) 40°C/90% RH.

Table 3. Dissolution parameters of HCTZ formulations

Formulation	DP_5 (%)	DP_{20} (%)	DE_{20} (%)
F zero T	35.9	100	82.1
F (A)i	1.8	76.1	47.7
F (B)i	13.3	81.7	64.2
F (C)i	24.7	84.6	73.2
F (D)i	25.9	99	87.7
F (A)ii	3.8	5.9	5.4
F (B)ii	2.1	37.4	23.8
F (C)ii	4.6	85	65.9
F (D)ii	25.1	100	83.9
F (A)iii	0.91	53.4	24.9
F (B)iii	2.5	52.5	27.1
F (C)iii	1.6	53.7	27.5
F (D)iii	31.8	97.3	86.8

DP_5 : Percent drug dissolved in 5 min. DP_{20} : Percent drug dissolved in 20 min. DE_{20} : Dissolution efficiency at $t = 20$ min (calculated from the area under the dissolution curve at $t = 20$ min and expressed as % of the area of the rectangle described by 100% dissolution in the same time). Each value is the average of three determinations. (i): 40°C/60 RH, (ii): 40°C/75 RH, and (iii): 40°C/90 RH.

facilitated solubilization of glycine in humid conditions, thus becoming more evenly distributed throughout the capsule content and preventing cross-linking. FTIR and

DSC spectrum were carried out on all stored capsules in different conditions but only three formulations were chosen in this study to show the effect of storage on them. These formulations were F_1 which contains citric acid only, F_2 with glycine only, and F_5 with both glycine and citric acid, all stored at $40^\circ\text{C}/90\%$ RH and were compared with blank formulation F_{blank} (containing no glycine and citric acid).

3.2. Fourier transfer infra-red spectroscopy

The FTIR spectrum of plain HCTZ (Figure 3) illustrates peaks at 3362 , 3267 , and 3170 cm^{-1} assigned to NH and NH_2 stretching. It also shows peaks at 1602 and 1520 cm^{-1} corresponding to the heterocyclic ring system, and peaks at 2361 and 2339 cm^{-1} assigned to C-H stretching of the thiazide ring. In addition, it shows a peak at 1321 cm^{-1} corresponding to SO_2 asymmetric stretching and at 1174 and 1152 cm^{-1} corresponding to SO_2 symmetric stretching.

All fresh and stored formulations at different relative humidities showed a peak at 3526 cm^{-1} which characterized the stretching vibrations of O-H bonds of lactose alcohol group (corresponding to lactose used as filler), which could be free or bonded (15).

By comparing FTIR spectra of formulations F_{blank} , F_1 , and F_2 stored at $40^\circ\text{C}/90\%$ RH for 4 weeks, the peak at 3170 cm^{-1} assigned to NH stretching of secondary amine of the intact drug disappeared, which might indicate the cleavage of the heterocyclic ring in the above formulations, while it was still present in formula F_5 (Figure 3).

The intensity of the peaks at 1165 , 1143 , 1068 , and 1030 cm^{-1} corresponding to C-H stretching of formaldehyde was increased in spectra of formulae F_1 , F_2 , and F_{blank} indicating the presence of formaldehyde in large amount. On the other hand, the same peaks were found in the spectrum of formula F_5 , but with much less intensity indicating the presence of trace amounts of formaldehyde (15).

By examining the FTIR spectra of the formulations,

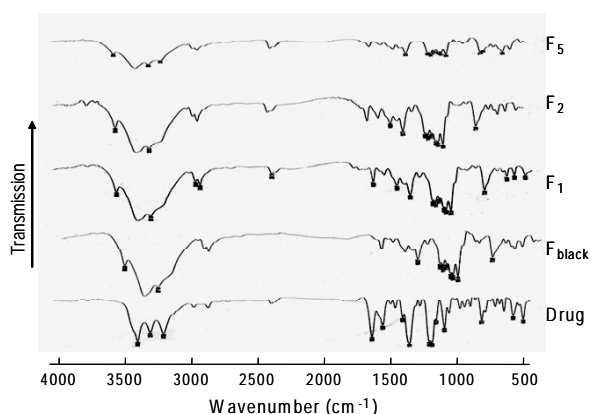


Figure 3. FTIR spectra of drug, F_{blank} , F_1 , F_2 , and F_5 stored at $40^\circ\text{C}/90\%$ RH for 4 weeks.

the peak at 2300 cm^{-1} assigned to the thiazide ring of the drug was absent in the spectrum of blank formulation which may be attributed to the absence of both glycine and citric acid. Conversely, this peak was found in the spectra of F_1 , F_2 , and F_5 indicating the presence of the thiazide ring intact in these formulations (16). This result was correlated with that obtained from the dissolution studies where the blank formulation showed the least $\text{DP}_{5\%}$, $\text{DP}_{20\%}$, and DE_{20} .

3.3. Differential scanning calorimetry

The DSC of plain HCTZ (Figure 4) shows an endothermic peak corresponding to its melting point at 271.13°C with an apparent heat of fusion of -123.41 mJ which agrees with the melting point reported in Analytical Profiles (13). The disappearance of the peak of the drug in the thermograms of formulation F_5 proved that the drug was completely miscible in the excipients used. On the other hand, the same peak of the drug appeared in the thermograms of F_{blank} , F_1 , and F_2 with relatively small intensity. This may be due to the absence of glycine in F_1 , absence of citric acid in F_2 and absence of both in F_{blank} which caused the drug to be less soluble in the mentioned formulations resulting in the appearance of its peak.

3.4. Data analysis

The causal factor and response variables were related using polynomial equation with statistical analysis through Design-Expert® software (17).

The contour plots illustrating the simultaneous effect of the causal factors on individual and combined response variable are represented in Figures 5-7. This expression gives an insight into the effect of the different independent variables (response). A positive sign of coefficient indicates a synergistic effect while a negative term indicates an antagonistic effect upon the response (Tables 4-7).

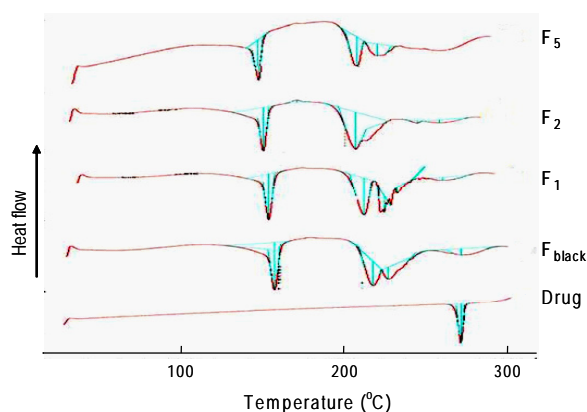


Figure 4. DSC spectra of drug, F_{blank} , F_1 , F_2 , and F_5 stored at $40^\circ\text{C}/90\%$ RH for 4 weeks.

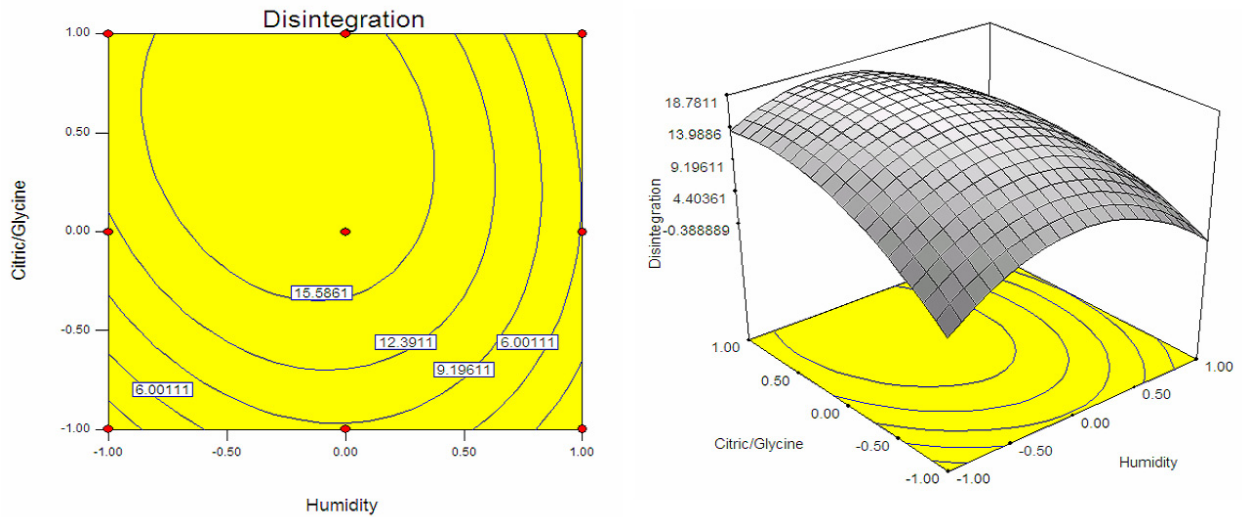


Figure 5. Contours of disintegration time (Y_1) as a function of humidity % (X_1) and addition of citric/glycine (X_2).

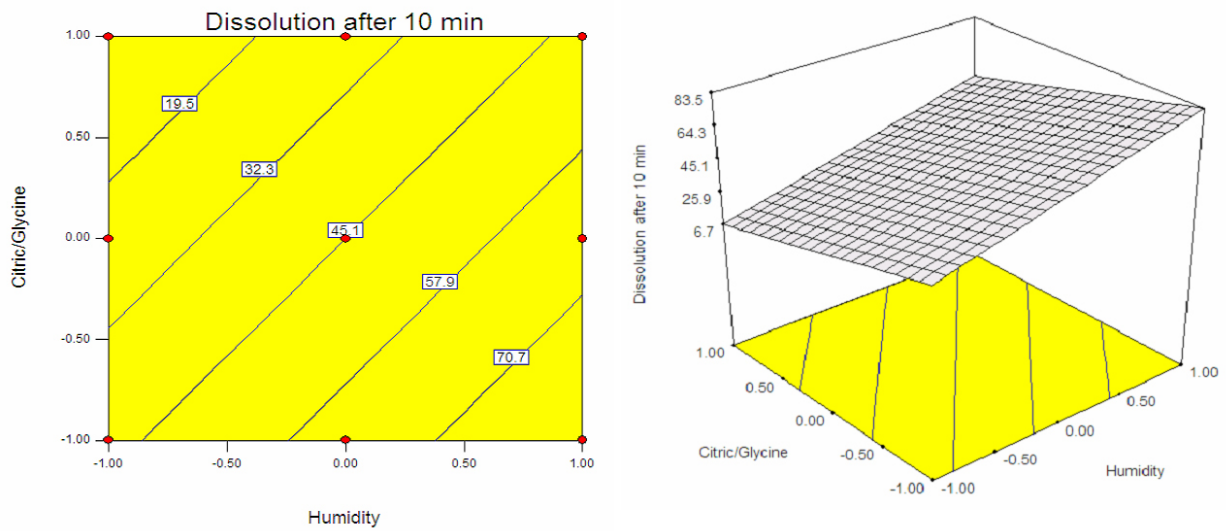


Figure 6. Contours of dissolution after 10 min (Y_2) as a function of humidity % (X_1) and addition of citric/glycine (X_2).

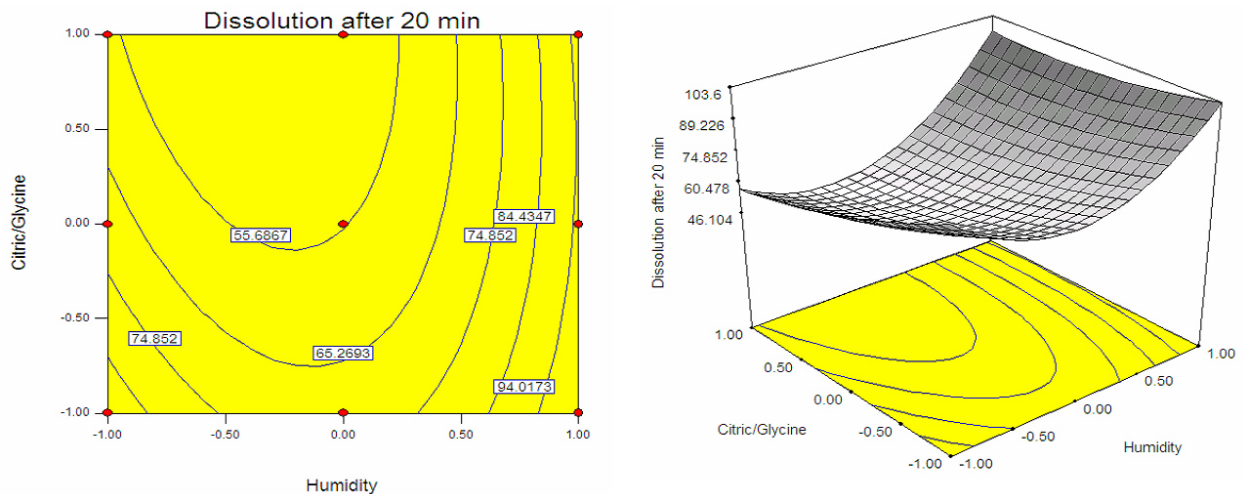


Figure 7. Contours of dissolution after 20 min (Y_3) as a function of humidity % (X_1) and addition of citric/glycine (X_2).

Table 4. Actual, predicted, residual values for disintegration time of capsules in minutes as a function of humidity % (X_1) and addition of citric/glycine (X_2)

Standard order	X_1	X_2	Actual value	Predicted value	Residual	Run order
1	-1	1	3.00	5.78	-2.78	7
2	0	0	2.00	-0.39	2.39	8
3	0	-1	3.00	8.78	-5.78	3
4	-1	0	7.00	11.78	-4.78	4
5	1	1	25.0	17.44	7.56	2
6	-1	-1	3.00	2.61	0.39	5
7	1	0	4.00	0.61	3.39	6
8	1	-1	15.0	16.78	-1.78	9
9	0	1	15.0	13.61	1.39	1

Table 5. Actual, predicted, residual values for percent drug released from capsules after 10 min as a function of humidity % (X_1) and addition of citric/glycine (X_2)

Standard order	X_1	X_2	Actual value	Predicted value	Residual	Run order
1	-1	1	71.00	72.83	-1.83	7
2	0	0	78.70	84.50	-5.80	8
3	0	-1	65.50	43.27	22.23	3
4	-1	0	51.00	31.57	19.43	4
5	1	1	2.50	20.10	-17.60	2
6	-1	-1	79.60	71.97	7.63	5
7	1	0	49.80	66.23	-16.43	6
8	1	-1	3.10	7.73	-4.63	9
9	0	1	4.70	7.70	-3.00	1

Table 6. Actual, predicted, residual values for percent drug released from capsules after 20 min as a function of humidity % (X_1) and addition of citric/glycine (X_2)

Standard order	X_1	X_2	Actual value	Predicted value	Residual	Run order
1	-1	1	99.00	95.53	3.47	7
2	0	0	99.30	103.6	-4.30	8
3	0	-1	84.60	70.27	14.33	3
4	-1	0	85.00	70.07	14.93	4
5	1	1	37.00	55.40	-18.40	2
6	-1	-1	97.30	96.47	0.83	5
7	1	0	81.70	91.73	-10.03	6
8	1	-1	53.60	49.53	4.07	9
9	0	1	52.50	57.40	-4.90	1

Table 7. Optimal regression equation for each response variable a function of humidity % (X_1) and addition of citric/glycine (X_2)

Model	Coefficient	Y_1	Y_2	Y_3
	B_0	79.67	91.11	19.67
	$b_1(X_1)$	14	0.5	-9
	$b_2(X_2)$	-27	-11	13
	$b_{11}(X_1^2)$	-14.5	-10.67	0.5
	$b_{12}(X_2^2)$	-11.5	-1.17	13.5
	$b_{13}(X_1X_2)$	3.75	3.75	-11.75
Quadratic	CV	80.82	50.85	23.08
	R^2	0.7200	0.8181	0.7807
	Adjusted R^2	0.2532	0.5150	0.4152
	PRESS	1,138	1,5919	7,832

4. Conclusion

In the environment of high humidity, the decrease in the dissolution of HCTZ capsules was attributed to the formation of formaldehyde due to the hydrolysis of HCTZ in the presence of moisture and excipients.

The liberated formaldehyde reacted with the gelatin in the capsule shell and starch 1500 in the formulation to form an insoluble compound that led to a decrease in the dissolution profile and a decrease in the capsule disintegration capacity. This capsule cross-linking was overcome by using a combination of an amino acid (glycine) and a buffer (citric acid) which prevent the formaldehyde formation inside the capsule and thus attain its dissolution profile.

References

1. Mike D, Robin E, Mike K, David G, Doug S, Richard W. The dissolution and bioavailability of etodolac from capsules exposed to conditions of high relative humidity and temperature. *Pharm Res.* 1993; 10:1295-1300.
2. Elanco Qualicaps. Technical Service Reference Manual, 1991.
3. Guideline for submitting Documentation for the Stability of Human Drugs and Biologics, Centre for Drugs and Biologics, Food and Drug Administration, 1987; pp.

- 11-43.
4. Adesunloye TA, Stach PE. Effect of glycine/citric acid on the dissolution of hard gelatin capsules. *Drug Dev Ind Pharm.* 1998; 24:493-500.
 5. Ofner CM, Zhang YE, Jobeck VC, Bowman BJ. Cross-linking studies in gelatin capsules treated with formaldehyde and in capsules exposed to elevated temperature and humidity. *J Pharm Sci.* 2001; 90:79-88.
 6. Desai DS, Rubitski BA, Varia SA, Jain NB. Povidone- and poloxamer-mediated degradation of hydrochlorothiazide in an antihypertensive combination tablet product. *Int J Pharm.* 1996; 142:61-66.
 7. Mollica JA, Rehm CR, Smith JB. Hydrolysis of hydrochlorothiazide. *J Pharm Sci.* 1969; 58:635-636.
 8. Deventer K, Pozo O, Van Eenoo P, Delbeke F. Detection of urinary markers for thiazide diuretics after oral administration of hydrochlorothiazide and altizide-relevance to doping control analysis. *J Chromat A.* 2009; 1216:2466-2473.
 9. Carstensen JT, Rhode CT. Pellicle formation in gelatin capsule. *Drug Dev Ind Pharm.* 1993; 19:2709-2712.
 10. Digenis GA, Gold TB, Shah VB. Cross-linking of gelatin capsules and its relevance to their *in-vitro in-vivo* performance. *J Pharm Sci.* 1994; 83:915-921.
 11. Singh S, Rao KVR Venugopal K, Manikandan R. Alteration in dissolution characteristics of gelatin-containing formulations. A review of the problem, test methods, and solutions. *Pharm Technol.* 2002; 26:36-58.
 12. Desai DS, Rubitski BA, Bergum JS, Varia SA. Effect of different types of lactose and disintegrant on dissolution stability of hydrochlorothiazide capsule formulations. *Int J Pharm.* 1994; 110:257-265.
 13. Deppeler H. Hydrochlorothiazide. In: *Analytical Profiles of Drug Substances, Vol. 10* (Florey K, ed.). Academic Press, New York, NY, USA, 1981; pp. 405-441.
 14. Murthy KS, Enders NA, Fawzi MB. Dissolution stability of hard-shell capsule products. Part 1: The effect of exaggerated storage conditions. *Pharm Technol.* 1989; 13:72-85.
 15. *Spectrometric Identification of Organic Compounds, seventh edition* (Silverstein RM, Webster FX, Kiemle DJ, eds.). John Wiley & Sons, NJ, USA, 2005; pp. 72-126.
 16. Juan M, Aceves-Hernández J, Agacino E, Paz M, Hinojosa J. Experimental and theoretical study of the conformational analysis of hydrochlorothiazide. *J Mol Struct.* 2006; 786:1-8.
 17. Vaughn N, Polnaszek C, Smith B, Helseth T. Program DESIGN-EXPERT, Stat-Ease Inc., 2000.

(Received April 12, 2009; Accepted May 2, 2009)

Drug Discoveries & Therapeutics

Guide for Authors

1. Scope of Articles

Drug Discoveries & Therapeutics mainly publishes articles related to basic and clinical pharmaceutical research such as pharmaceutical and therapeutical chemistry, pharmacology, pharmacy, pharmacokinetics, industrial pharmacy, pharmaceutical manufacturing, pharmaceutical technology, drug delivery, toxicology, and traditional herb medicine. Studies on drug-related fields such as biology, biochemistry, physiology, microbiology, and immunology are also within the scope of this journal.

2. Submission Types

Original Articles should be reports new, significant, innovative, and original findings. An Article should contain the following sections: Title page, Abstract, Introduction, Materials and Methods, Results, Discussion, Acknowledgments, References, Figure legends, and Tables. There are no specific length restrictions for the overall manuscript or individual sections. However, we expect authors to present and discuss their findings concisely.

Brief Reports should be short and clear reports on new original findings and not exceed 4000 words with no more than two display items. *Drug Discoveries & Therapeutics* encourages younger researchers and doctors to report their research findings. Case reports are included in this category. A Brief Report contains the same sections as an Original Article, but Results and Discussion sections must be combined.

Reviews should include educational overviews for general researchers and doctors, and review articles for more specialized readers.

Policy Forum presents issues in science policy, including public health, the medical care system, and social science. Policy Forum essays should not exceed 2,000 words.

News articles should not exceed 500 words including one display item. These articles should function as an international news source with regard to topics in the life and social sciences and medicine. Submissions are not restricted to journal staff - anyone can submit news articles on subjects that would be of interest to *Drug Discoveries & Therapeutics'* readers.

Letters discuss material published in *Drug Discoveries & Therapeutics* in the last 6 months or issues of general interest. Letters should not exceed 800 words and 6 references.

3. Manuscript Preparation

Preparation of text. Manuscripts should be written in correct American English and submitted as a Microsoft Word (.doc) file in a single-column format. Manuscripts must be paginated and double-spaced throughout. Use Symbol font for all Greek characters. Do not import the figures into the text file but indicate their approximate locations directly on the manuscript. The manuscript file should be smaller than 5 MB in size.

Title page. The title page must include 1) the title of the paper, 2) name(s) and affiliation(s) of the author(s), 3) a statement indicating to whom correspondence and proofs should be sent along with a complete mailing address, telephone/fax numbers, and e-mail address, and 4) up to five key words or phrases.

Abstract. A one-paragraph abstract consisting of no more than 250 words must be included. It should state the purpose of the study, basic procedures used, main findings, and conclusions.

Abbreviations. All nonstandard abbreviations must be listed in alphabetical order, giving each abbreviation followed by its spelled-out version. Spell out the term upon first mention and follow it with the abbreviated form in parentheses. Thereafter, use the abbreviated form.

Introduction. The introduction should be a concise statement of the basis for the study and its scientific context.

Materials and Methods. Subsections under this heading should include sufficient instruction to replicate experiments, but well-established protocols may be simply referenced. *Drug Discoveries & Therapeutics* endorses the principles of the Declaration of Helsinki and expects that all research involving humans will have been conducted in accordance with these principles. All laboratory animal studies must be approved by the authors' Institutional Review Board(s).

Results. The results section should provide details of all of the experiments that are required to support the conclusions of the paper. If necessary, subheadings may be used for an orderly presentation. All figures, tables, and photographs must be referred in the text.

Discussion. The discussion should include conclusions derived from the study and supported by the data. Consideration should be given to the impact that these conclusions have on the body of knowledge in which context the experiments were conducted. In Brief Reports, Results and Discussion sections must be combined.

Acknowledgments. All funding sources should be credited in the Acknowledgments section. In addition, people who contributed to the work but who do not fit the criteria for authors should be listed along with their contributions.

References. References should be numbered in the order in which they appear in the text. Cite references in text using a number in parentheses. Citing of unpublished results and personal communications in the reference list is not recommended but these sources may be mentioned in the text. For all references, list all authors, but if there are more than fifteen authors, list the first three authors and add "et al." Abbreviate journal names as they appear in PubMed. Web references can be included in the reference list.

Example 1:

Hamamoto H, Akimitsu N, Arimitsu N, Sekimizu K. Roles of the Duffy antigen and glycoprotein A in malaria infection and erythrocyte. *Drug Discov Ther.* 2008; 2:58-63.

Example 2:

Zhao X, Jing ZP, Xiong J, Jiang SJ. Suppression of experimental abdominal aortic aneurysm by tetracycline: a preliminary study. *Chin J Gen Surg*. 2002; 17:663-665. (in Chinese)

Example 3:

Mizuochi T. Microscale sequencing of N-linked oligosaccharides of glycoproteins using hydrazinolysis, Bio-Gel P-4, and sequential exoglycosidase digestion. In: *Methods in Molecular Biology: Vol. 14 Glycoprotein analysis in biomedicine* (Hounsell T, ed.). Humana Press, Totowa, NJ, USA, 1993; pp. 55-68.

Example 4:

Drug Discoveries & Therapeutics. Hot topics & news: China-Japan Medical Workshop on Drug Discoveries and Therapeutics 2007. <http://www.ddtjournal.com/hotnews.php> (accessed July 1, 2007).

Figure legends. Include a short title and a short explanation. Methods described in detail in the Materials and methods section should not be repeated in the legend. Symbols used in the figure must be explained. The number of data points represented in a graph must be indicated.

Tables. All tables should have a concise title and be typed double-spaced on pages separate from the text. Do not use vertical rules. Tables should be numbered with Arabic numerals consecutively in accordance with their appearance in the text. Place footnotes to tables below the table body and indicate them with lowercase superscript letters.

Language editing. Manuscripts submitted by authors whose primary language is not English should have their work proofread by a native English speaker before submission. The Editing Support Organization can provide English proofreading, Japanese-English translation, and Chinese-English translation services to authors who want to publish in *Drug Discoveries & Therapeutics* and need assistance before submitting an article. Authors can contact this organization directly at <http://www.iacmhr.com/iac-eso>.

IAC-ESO was established in order to facilitate manuscript preparation by researchers whose native language is not English and to help edit work intended for international academic journals. Quality revision, translation, and editing services are offered by our staff, who are native speakers of particular languages and who are familiar with academic writing and journal editing in English.

4. Figure Preparation

All figures should be clear and cited in numerical order in the text. Figures must fit a one- or two-column format on the journal page: 8.3 cm (3.3 in.) wide for a single column; 17.3 cm (6.8 in.) wide for a double column; maximum height: 24.0 cm (9.5 in.). Only use the following fonts in the figure: Arial and Helvetica. Provide all figures as separate files. Acceptable file formats are JPEG and TIFF. Please note that files saved in JPEG or TIFF format in PowerPoint lack sufficient resolution for publication. Each Figure file should be smaller than 10 MB in size. Do not compress files. A fee is charged for a color illustration or photograph.

5. Online Submission

Manuscripts should be submitted to *Drug Discoveries & Therapeutics* online at <http://www.ddtjournal.com>. The manuscript file should be smaller than 10 MB in size. If for any reason you are unable to submit a file online, please contact the Editorial Office by e-mail: office@ddtjournal.com

Editorial and Head Office

Wei TANG, MD PhD

Executive Editor

Drug Discoveries & Therapeutics

TSUIN-IKIZAKA 410,

2-17-5 Hongo, Bunkyo-ku,

Tokyo 113-0033, Japan.

Tel: 03-5840-9697

Fax: 03-5840-9698

E-mail: office@ddtjournal.com

Cover letter. A cover letter from the corresponding author including the following information must accompany the submission: name, address, phone and fax numbers, and e-mail address of the corresponding author. This should include a statement affirming that all authors concur with the

submission and that the material submitted for publication has not been previously published and is not under consideration for publication elsewhere and a statement regarding conflicting financial interests.

Authors may recommend up to three qualified reviewers other than members of Editorial board. Authors may also request that certain (but not more than three) reviewers not be chosen.

The cover letter should be submitted as a Microsoft Word (.doc) file (smaller than 1 MB) at the same time the work is submitted online.

6. Accepted Manuscripts

Proofs. Rough galley proofs in PDF format are supplied to the corresponding author via e-mail. Corrections must be returned within 4 working days of receipt of the proofs. Subsequent corrections will not be possible, so please ensure all desired corrections are indicated. Note that we may proceed with publication of the article if no response is received.

Transfer of copyrights. Upon acceptance of an article, authors will be asked to agree to a transfer of copyright. This transfer will ensure the widest possible dissemination of information. A letter will be sent to the corresponding author confirming receipt of the manuscript. A form facilitating transfer of copyright will be provided. If excerpts from other copyrighted works are included, the author(s) must obtain written permission from the copyright owners and credit the source(s) in the article.

Cover submissions. Authors whose manuscripts are accepted for publication in *Drug Discoveries & Therapeutics* may submit cover images. Color submission is welcome. A brief cover legend should be submitted with the image.

Revised April 20, 2009



Editorial Office

TSUIN-IKIZAKA 410,
2-17-5 Hongo, Bunkyo-ku,
Tokyo 113-0033, Japan

Tel: 03-5840-9697

Fax: 03-5840-9698

E-mail: office@ddtjournal.com

URL: www.ddtjournal.com

JOURNAL PUBLISHING AGREEMENT

Ms No:

Article entitled:

Corresponding author:

To be published in Drug Discoveries & Therapeutics

Assignment of publishing rights:

I hereby assign to International Advancement Center for Medicine & Health Research Co., Ltd. (IACMHR Co., Ltd.) publishing Drug Discoveries & Therapeutics the copyright in the manuscript identified above and any supplemental tables and illustrations (the articles) in all forms and media, throughout the world, in all languages, for the full term of copyright, effective when and if the article is accepted for publication. This transfer includes the rights to provide the article in electronic and online forms and systems.

I understand that I retain or am hereby granted (without the need to obtain further permission) rights to use certain versions of the article for certain scholarly purpose and that no rights in patent, trademarks or other intellectual property rights are transferred to the journal. Rights to use the articles for personal use, internal institutional use and scholarly posting are retained.

Author warranties:

I affirm the author warranties noted below.

- 1) The article I have submitted to the journal is original and has not been published elsewhere.
- 2) The article is not currently being considered for publication by any other journal. If accepted, it will not be submitted elsewhere.
- 3) The article contains no libelous or other unlawful statements and does not contain any materials that invade individual privacy or proprietary rights or any statutory copyright.
- 4) I have obtained written permission from copyright owners for any excerpts from copyrighted works that are included and have credited the sources in my article.
- 5) I confirm that all commercial affiliations, stock or equity interests, or patent-licensing arrangements that could be considered to pose a financial conflict of interest regarding the article have been disclosed.
- 6) If the article was prepared jointly with other authors, I have informed the co-authors(s) of the terms of this publishing agreement and that I am signing on their behalf as their agents.

Your Status:

I am the sole author of the manuscript.

I am one author signing on behalf of all co-authors of the manuscript.

Please tick one of the above boxes (as appropriate) and then sign and date the document in black ink.

Signature:

Date:

Name printed:

Please return the completed and signed original of this form by express mail or fax, or by e-mailing a scanned copy of the signed original to:

Drug Discoveries & Therapeutics office
TSUIN-IKIZAKA 410, 2-17-5 Hongo,
Bunkyo-ku, Tokyo 113-0033, Japan
e-mail: proof-editing@ddtjournal.com
Fax: +81-3-5840-9698

